Primary Corrector with Atmospheric Dispersion Corrector for Subaru Telescope

Kunio Takeshi

Doctor of Philosophy

Department of Astronomical Science
School of Mathematical and Physical Science
The Graduate University for Advanced Studies

2000

Contents

Photographs

Photo 1. Primary Corrector for Subaru before Installation

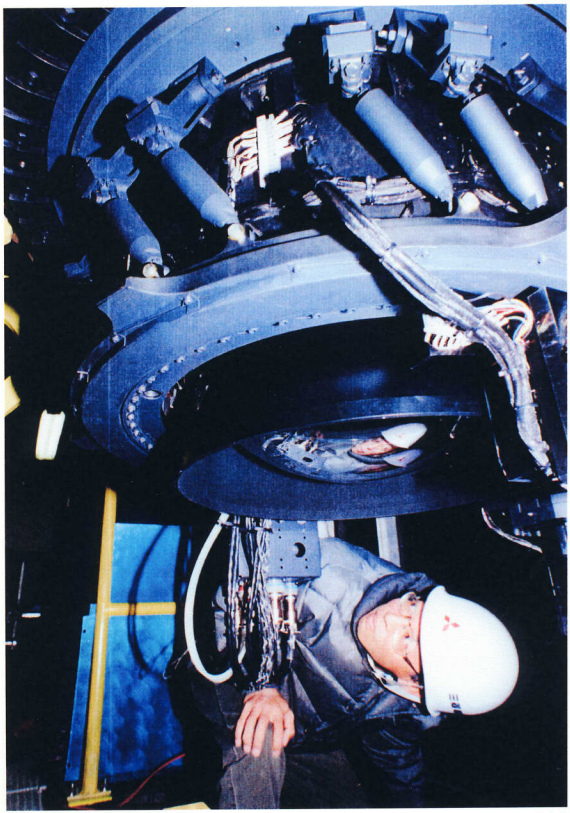

Photo 2. Primary Corrector installed in the Prime Focus Unit of Subaru

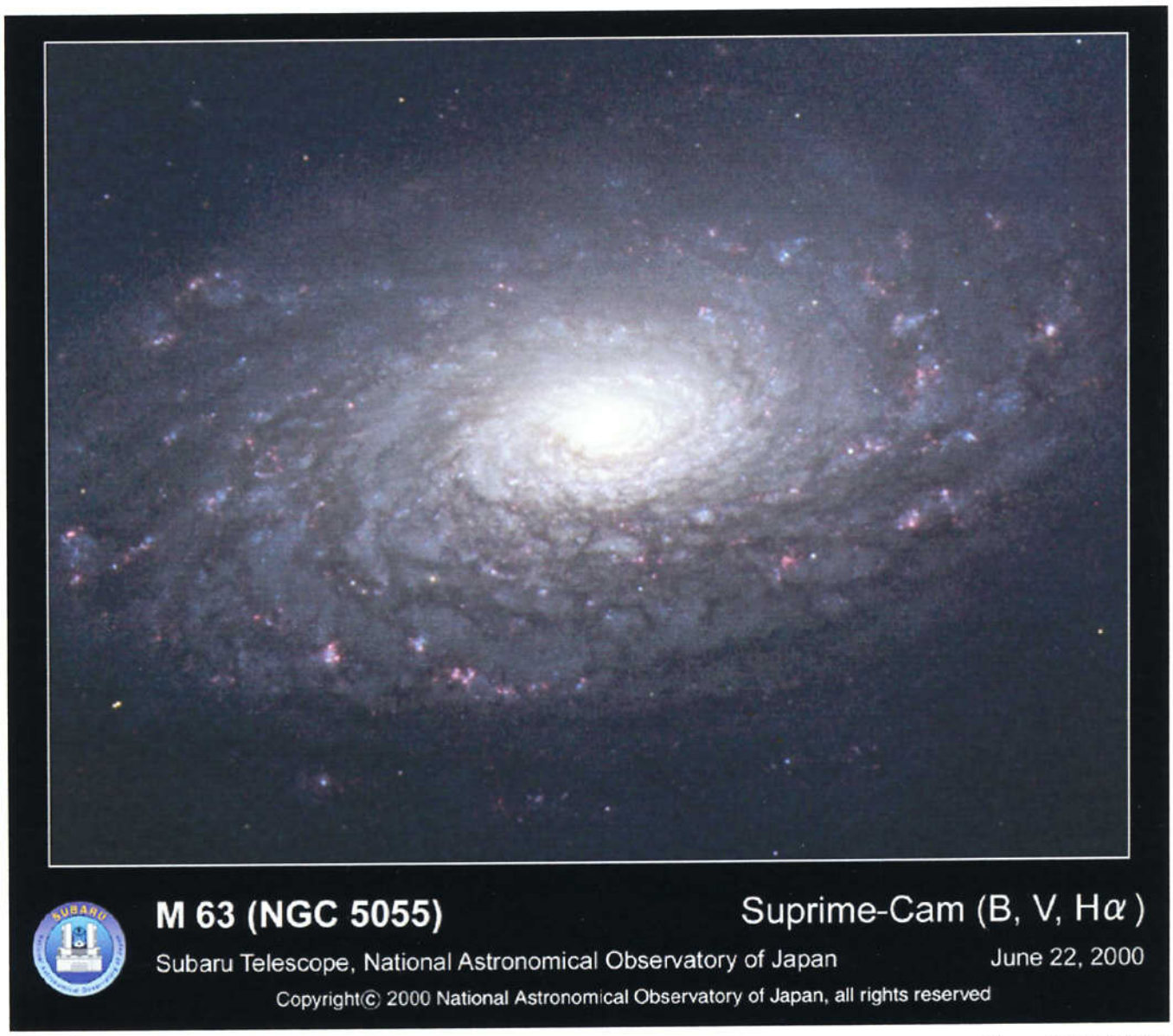

Photo 3. Spiral Galaxy M63 taken with the Suprime-Cam

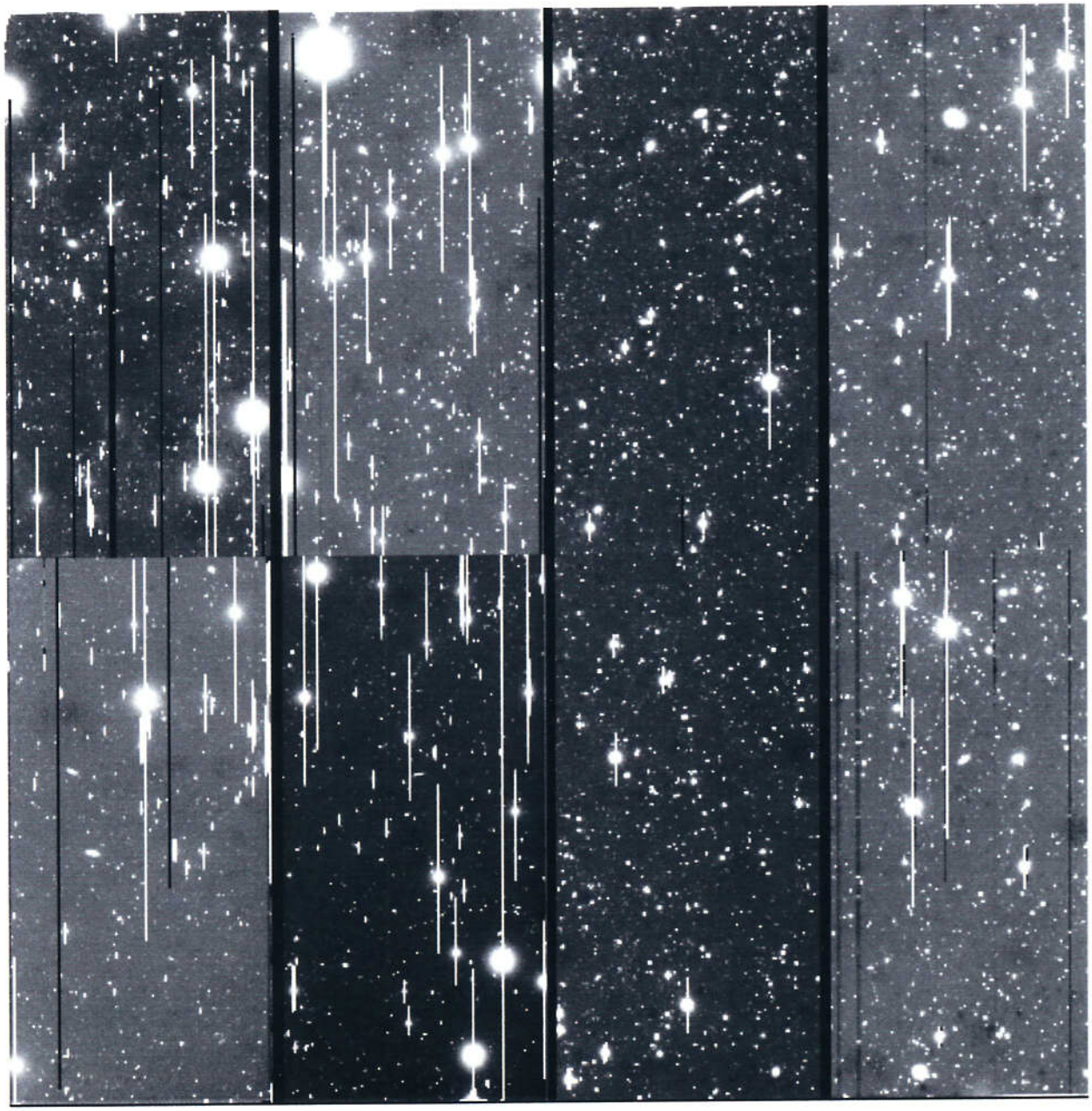

Photo 4. Raw CCD images during the test observation

Abstract

Modern large telescopes have small aperture ratios to meet the two requirements from the astronomical observation, namely large aperture and precise movement. This causes large coma at the primary focal plane. In order to get good imaging within 15 minutes of arc from the center of the field of the primary focal plane of the Subaru telescope, we designed and fabricated a primary focus corrector.

Ross designed and fabricated a two-lens coma corrector for the Hale telescope (D=5m, F/3.3, operating since 1948). Wynne designed and fabricated three-lens correctors for the four-meter class telescopes constructed in 1970's. In 1980's, Epps designed a primary corrector with two direct vision prisms to correct atmospheric dispersion for the Keck telescope, but this was not manufactured.

This paper reports the design and fabrication of the primary corrector for the Ritchey-Chr tien main mirror(D=8.2 m, F/1.83) of the Subaru telescope with a new type Atmospheric Dispersion Corrector(=ADC). ADC consists of a plane parallel plate made of a plano-convex lens and a plano-concave lens whose glass material has about the same refractive indices but different dispersion. Translation of this ADC acts as a variable prism, thus enabling us to correct the atmospheric dispersion.

This ADC as a part of the primary corrector gives one degree of freedom among the secondary spectrum, chromatic difference of aberrations (spherical aberration and coma), longitudinal chromatic aberration, chromatic aberration of magnification, and the power distribution of lenses. Because of this fact, it was possible to make the primary corrector small without losing the high overall performance. In designing the primary corrector, I adopted the three-lens corrector system as the basis, included the ADC, and used two aspheric surfaces.

In astronomy, there are two series of cameras, namely astrographic cameras for wide field such as Schmidt cameras, the telescope at Las Campanas, and Sloan Digital Sky Survey(SDSS), and cameras attached to large telescopes for deep survey with small field of view. Subaru as a successor of Hale telescope is looking for deep survey of the sky, therefore it is indispensable to have a good primary corrector. Test observation has already proved that the corrector is made to comply with the specification from the Japanese astronomers prior to the fabrication.

Cross sections of optical systems in this paper are given in the scale of 1/10 so that various systems can be compared easily to each other.

1. Introduction

Light emanating from an object, passing through a light gathering device, makes an image of the object at the focal plane of the device. This device is called a telescope, and it is called either a refractor or a reflector according to whether the light gathering device is a convex mirror or a concave mirror. A single lens has chromatic aberration because of the dispersion of refractive index of glass. A refractor uses a composite lens whose components are made of different glass material so that the chromatic aberration vanishes. High degree of homogeneity of glass is required for a large lens. Because of difficulty of making a large glass blank that matches the requirement for a refractor, the largest size of refractor ever made is 1 meter. A reflector usually uses glass as the mirror material. As the light is reflected at the mirror surface, requirement for homogeneity of glass is not serious and a large telescope can be achieved.

Elementary geometry teaches that a paraboloidal mirror makes a pin-point image at its focal point when the incident light is parallel to its optical axis. This corresponds to zero spherical aberration. When the incident light is not parallel to the optical axis, the image is blurred by off-axis aberration such as coma and astigmatism. In the case of a reflector, coma is usually the largest blurring source. Before reaching a telescope, a stellar image is already blurred by inhomogeneity of the air that is called seeing. The region where the blurring by coma is less than the atmospheric seeing (coma free region) is used for astronomical observation.

Modern telescopes have large apertures to make the available light large. If large focal length is chosen, the telescope tube and then the dome size become large. Corresponding mechanical parts become large and heavy. So, focal length is kept at a reasonable size. This makes the F ratio (= focal length / aperture) of a large telescope small. As coma is inversely proportional to the square of F ratio, coma free region of a large telescope is small. At a good sight like Mauna Kea where the seeing size is small, coma free region becomes smaller. Subaru telescope uses a hyperboloidal main mirror so that Ritchey-Chrétien system is formed when used with the secondary mirror. Coma free region of a paraboloidal mirror of the size of Subaru is, however, 14 seconds of arc corresponding to 1mm on the focal plane when the seeing size is assumed to be 0.4 second of arc.

The preceding calculation shows that a correcting lens system is required so that a field of 30 minutes of arc (=130mm on the focal plane) of good imaging characteristics is obtained for a paraboloidal mirror. As Subaru uses a hyperboloidal mirror that has spherical aberration, it cannot do without a correcting lens system.

Light coming from other than the zenith enters the earth's atmosphere obliquely and refracts. When seen from the earth's surface, an object is observed a little above the true position. As the atmosphere has dispersion of refractive index, a stellar image is prolonged in the altitude direction and is colored. This is called atmospheric dispersion and it amounts to 1.9 seconds of arc at the zenith angle of 60 degrees (= 30 degrees of altitude) for the wavelength region of 0.4μm-1.0μm. In the SDSS band system, it is 1 second of arc for g' band(0.4-0.55μm), 0.42 second of arc for r' band(0.55-0.69μm), 0.25 second of arc for i' band(0.69-0.84μm), and 0.15 second of arc for z' band(0.84-0.98μm) of the Sloan Digital Sky Survey(SDSS) system.

Hale telescope of Mt. Palomar (200"= 5m, F/3.3, completed 1948) has a 2 lens corrector designed by Ross(1935). In 1970's, Wynne designed 3 lens correctors for 4 meter class telescopes with F/3. In 1980's, Epps designed a primary focus corrector with atmospheric dispersion corrector using two direct-vision prisms for Keck telescope that was the first-runner among the 8-10 meter class telescope, but this corrector was not fabricated.

This paper describes the design and fabrication of the primary focus corrector that incorporates a new type atmospheric dispersion corrector (ADC) for the Ritchey-Chrétien main mirror of Subaru telescope (8.2 m, F/1.83). The ADC consists of two lenses (plano-convex and plano-concave) whose radii of curvature are the same. The glasses are so chosen that the refractive indices are approximately equal to each other but the dispersions are different. These two lenses are put together with the curved surfaces inside to make a plano-parallel plate. When this plate is shifted perpendicular to the optical axis, it behaves as an ADC. This ADC act also as an element of the correction of chromatic aberration of the entire system giving one degree of freedom among the secondary spectrum, chromatic differences of aberrations, longitudinal chromatic aberration, lateral chromatic aberration, and the power distribution. Because of this additional one degree of freedom coming

from ADC, it was possible to make the primary corrector small keeping high performance. The basic structure of primary corrector is the three lens system with ADC. Two aspheric surfaces are used to achieve its high performance.

Astronomy uses two lines of tools; astrographic camera for wide field photographs and large telescopes that aim at faint and distant astronomical object. In the first line are Schmidt camera, the telescope at Las Campanas, and the telescope of Sloan Digital Sky Survey (SDSS) (Gunn et al. 1998). The field of SDSS is 3 degrees and the limiting magnitude is 23 magnitude. Subaru telescope belongs to the latter line destined to be the successor of the Hale telescope. Its limiting magnitude is 29 magnitude. The role of SDSS is large when searching astronomical objects of interest, but it is not sufficient when Subaru tries to look through the edge of the universe. In such cases the primary corrector reported in this paper is the indispensable tool. The corrector was already used in the test observation and was reported with good performance. We may expect brilliant results in the twenty first century.

2. Atmospheric Dispersion

Atmospheric refraction was known since the time of Ptolemy (Tanaka 1991). Light from a star is refracted by the earth's atmosphere. Therefore, a star is observed a little higher than its true position. See Figure 2-1.

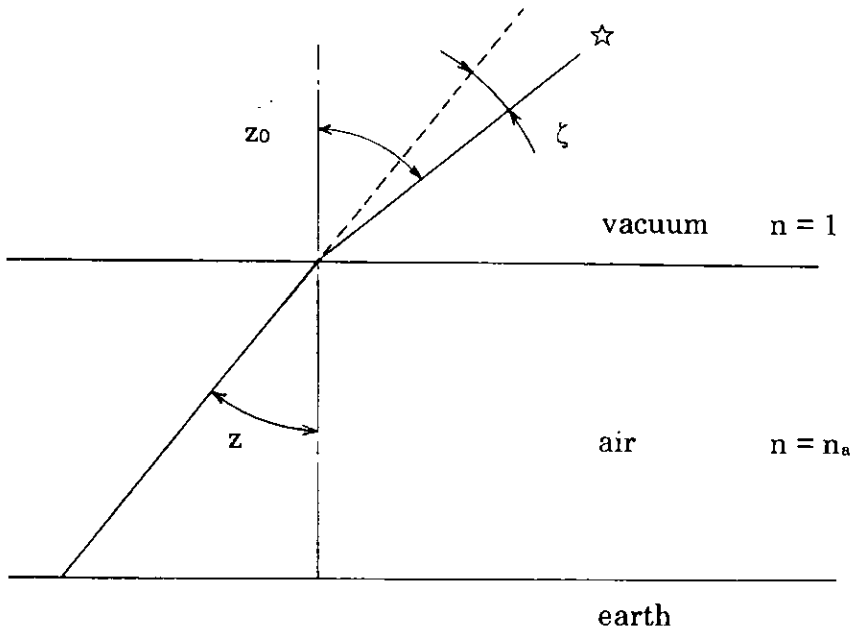

Figure 2-1. Model for atmospheric refraction

The amount of this difference ζ is calculated with one layer atmosphere model as follows;

Above the atmosphere, it is vacuum, therefore the refractive index equals 1. Let n_a represent the refractive index of the atmosphere, z_0 and z the true and apparent zenith distance. From the Snell's law we have

$$n_a \sin z = \sin z_0 \qquad (1)$$

Then we have

$$\zeta \equiv z - z_0 \cong (1 - n_a) \tan z_0 \qquad (2)$$

With a more detailed model, we have (Tanaka 1991) ζ as

$$\zeta = \zeta_0 \tan z - \zeta_1 \tan^3 z + \zeta_2 \tan^5 z \qquad (3)$$

The coefficients ζ_0, ζ_1, ζ_2 depend on the atmospheric condition. For average

condition on Mauna Kea (atmospheric pressure p= 450mmHg, gravitational constant g=978.627gal, temperature T= 0℃, absolute humidity f=1mmHg), and at $\lambda = 0.575\,\mu$m, ζ_0, ζ_1, and ζ_2 are calculated as 35."746, 0."0431,and 0."000164, respectively (Tanaka 1991). In the following discussion, we use one layer model that uses only ζ_0.

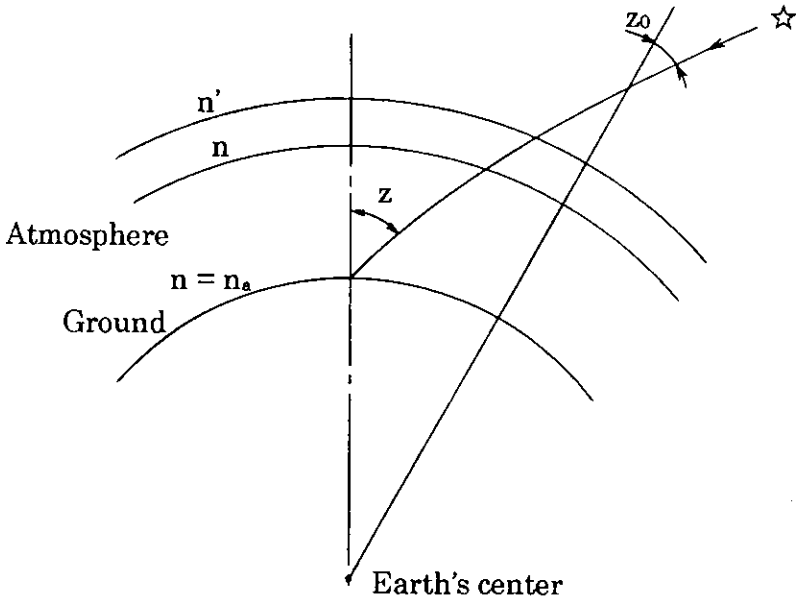

Figure 2-2. Precision model for atmospheric refraction

Figure 2-3 shows the atmospheric refraction as function of wavelength relative to the value at $\lambda = 0.575\,\mu$m, for zenith distance z = 45° and z = 60° on the Mauna Kea summit.

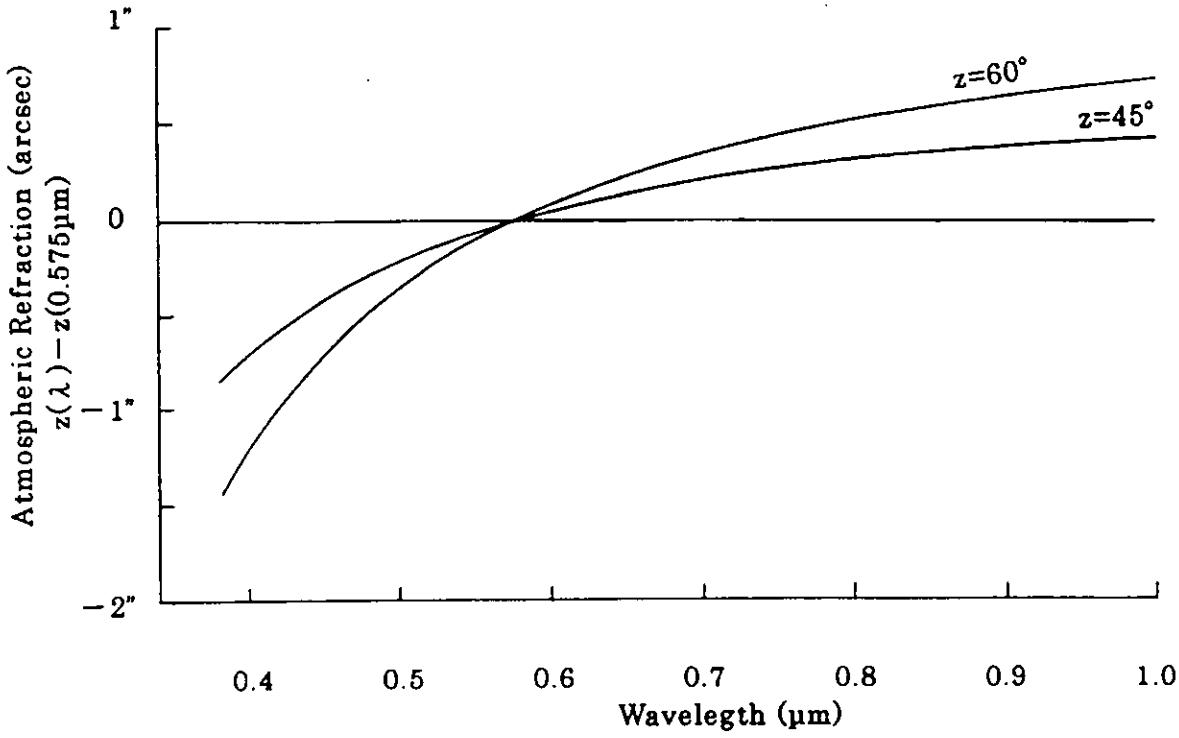

Figure 2-3. Atmospheric refraction as function of wavelength relative to the value at λ = 0.575 μm, for zenith distance z = 45º and z = 60º on the Mauna Kea summit (Courtesy, Wataru Tanaka. See also Tanaka 1991)

3. Correction of Atmospheric Dispersion

Atmospheric dispersion on the summit of Mauna Kea at the zenith distance 60° amounts to 1.9 seconds of arc for the full wavelength range of the primary corrector of Subaru Telescope (0.4-1.0 μm). The dispersion for the g', r', i', z' filters of SDSS system are calculated as 1.0", 0.42", 0.25", 0.15", respectively. These filters of SDSS system will also be used at the primary focus of the Subaru telescope. Figure 3-1 and Figure 3-2 show these filters of SDSS system and atmospheric dispersion as function of zenith distance for these filters.

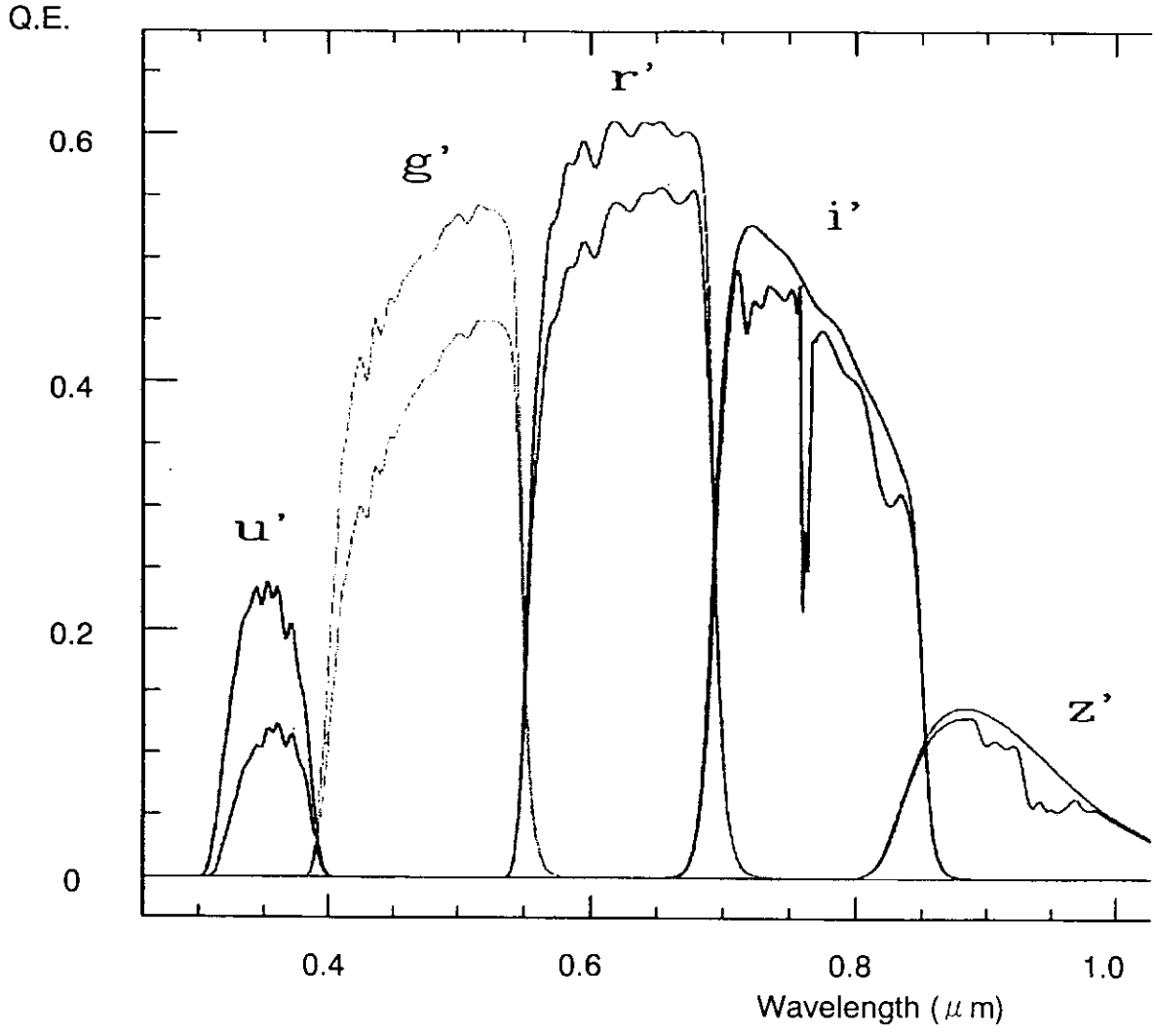

Figure 3-1. SDSS Bandpass System (Gunn et al. 1998)

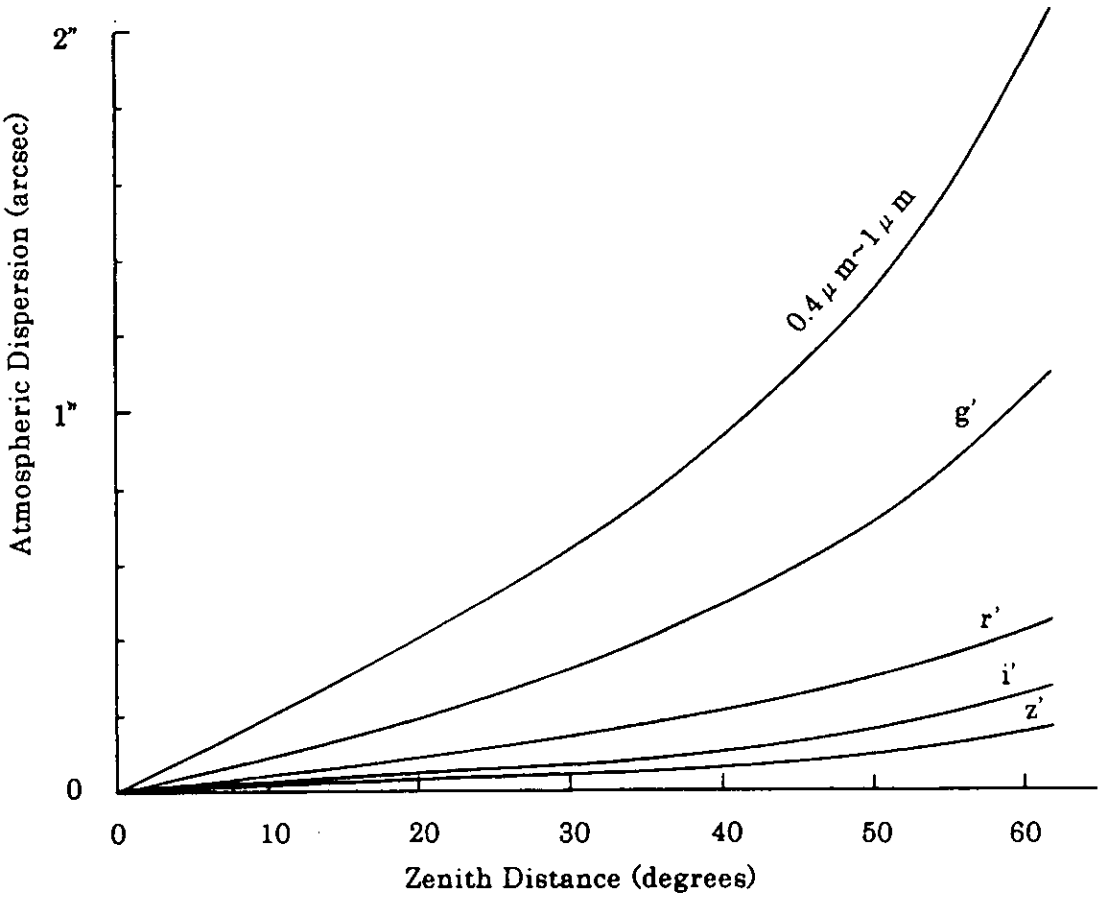

Figure 3-2. Atmospheric dispersion at the Mauna Kea Subaru Observatory for full wavelength range and SDSS filters as a function of zenith distance

As the seeing size on Mauna Kea is usually less than 1" and sometimes reaches 0.3", this atmospheric dispersion must be corrected. Various atmospheric dispersion corrector (ADC) designs were proposed. Some of them are used in the primary corrector and others are used at the Cassegrain focus. They are explained in this chapter. But our ADC design will be shown in chapter 5 where we will introduce our optical design of the entire primary corrector for the Subaru Telescope.

3.1. Atmospheric dispersion corrector of Epps (Epps et al. 1984)

Two direct-vision prisms are used for this ADC. In this type of design, one can adjust the quantity of correction by rotating two prisms in the opposite direction to each other. When the direction of dispersion of two prisms are both vertical, ADC has maximum prism effect, and when they are horizontal and in the opposite directions ADC has no prism effect. Epps' original design was for Keck telescope but this was not manufactured. See Figure 3-3. Subaru telescope used this type of ADC at the Cassegrain and Nasmith foci.

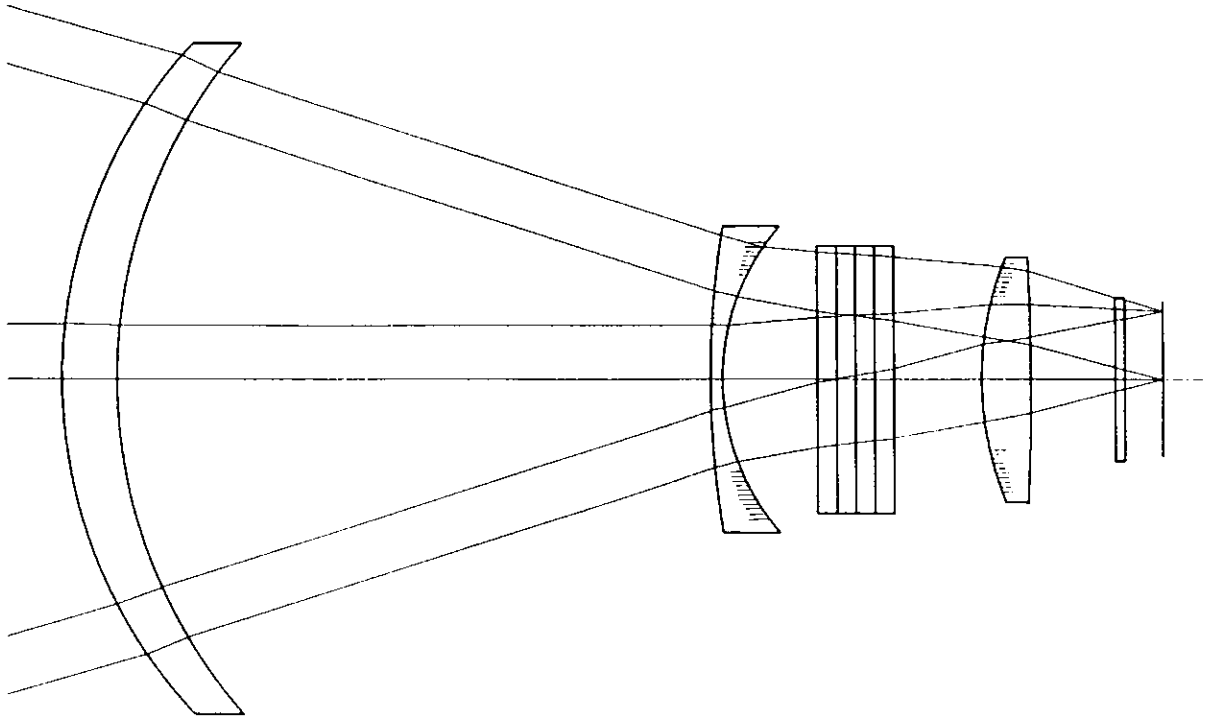

EFL=20.32m(800inch), Fno.=2.0, FOV=30 arcmin

Figure 3-3. Epps' Primary Corrector with direct-vision prism ADC (Epps et al. 1984)

3.2. Su Ding-qiang's "Lensm" (Su Ding-qiang 1986)

Lensm (lens-prism) incorporates a direct-vision prism into the lens element of a primary corrector. A lensm is composed of two glasses and the surface between them is a sphere whose center of curvature is displaced from the optical axis of the corrector. See Figure 3-4.

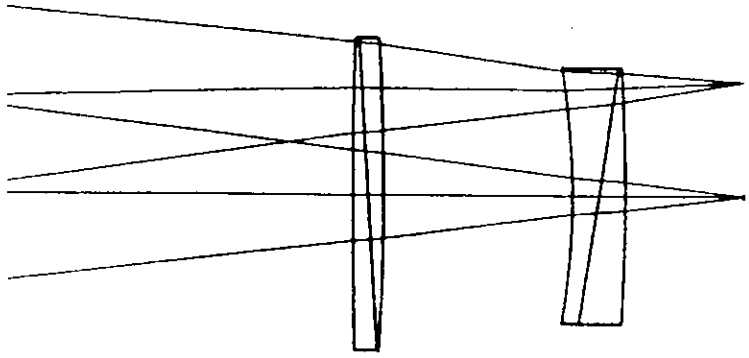

Figure 3-4. Su Ding-qiang's Field Corrector of "lensm"(Su Ding-qiang 1986)

Two lensms moving like the direct-vision prisms in the Epps's design work as an ADC. The merit of this design lies in decreasing the number of surfaces in a corrector.

3.3. Shift of Prism (Avila et al. 1997)

This type of ADC uses two prisms directing opposite to each other. The first prism corrects the atmospheric dispersion, and the second prism corrects the direction of the pupil of the telescope. Resulting image shift laterally. Coma is also observed when the distance between two prisms becomes large. This ADC can be used only at Cassegrain focus. This is not adequate to be included in a primary corrector. See Figure 3-5.

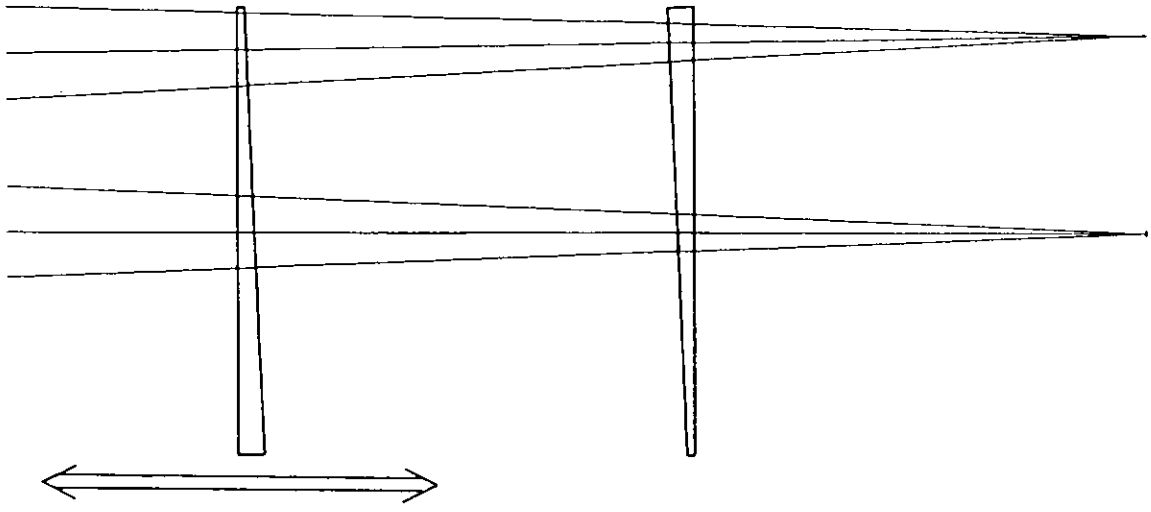

Figure 3-5. Linear ADC of Avila et al.(Avila et al. 1997)

4. History of Primary Correctors

The surface of the main mirror of a Cassegrain telescope is a paraboloid. Therefore, imaging at the center of the field is perfect, but large coma limits the field size. F. E. Ross made a research to correct this large coma of a paraboloid with two simple lenses near the focal plane (Ross 1935). He designed correctors for several telescopes including the Palomar 200-inch telescope. His design allowed the spherical aberration and distortion to remain.

Wynne designed three-lens corrector for R-C hyperboloid mirror (Wynne, 1968). This may be interpreted as the modification of Ross type corrector with an additional third convex lens. His corrector was 'anastigmat' that corrected spherical aberration, coma, astigmatism, field distortion, and longitudinal and lateral (axial and oblique) chromatic aberrations for a wide field.

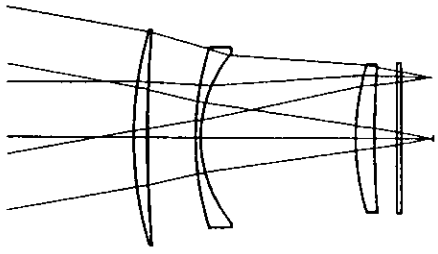

EFL=10.93m, Fno.=2.87, FOV=50 arcmin

Figure 4-1. Wynne's three lens Primary Corrector (Wynne 1968)

Epps et. al. included ADC in a primary corrector for the first time. They designed a three-lens corrector including direct-vision prism ADC for the primary focus of F/1.75 R-C main mirror with two aspheric surfaces and obtained 80 percent encircled energy of 1/4 arcsec for a field of 30 arcmin and for the wavelength range of $0.33\mu m$-$1\mu m$ (Epps et al. 1984). This design was made for Keck telescope, but a primary corrector was put out of scope of the project at an early stage. See Figure 3-3.

Nariai et al designed a corrector for the F/2 R-C mirror of the Subaru telescope with the field of view of 30 arcmin and RMS image diameter of 0.2 arcsec. They determined the positions of the three lenses balancing the chromatic aberration of the spherical aberration and the imaging at the edge of the field, and eliminating higher order curvature of field. They also studied the effect of aspheric surfaces and concluded that the rear surface of the second lens and the front surface of the third lens are the most effective positions for aspheric surfaces (Nariai et al. 1985). See Figure 4-2.

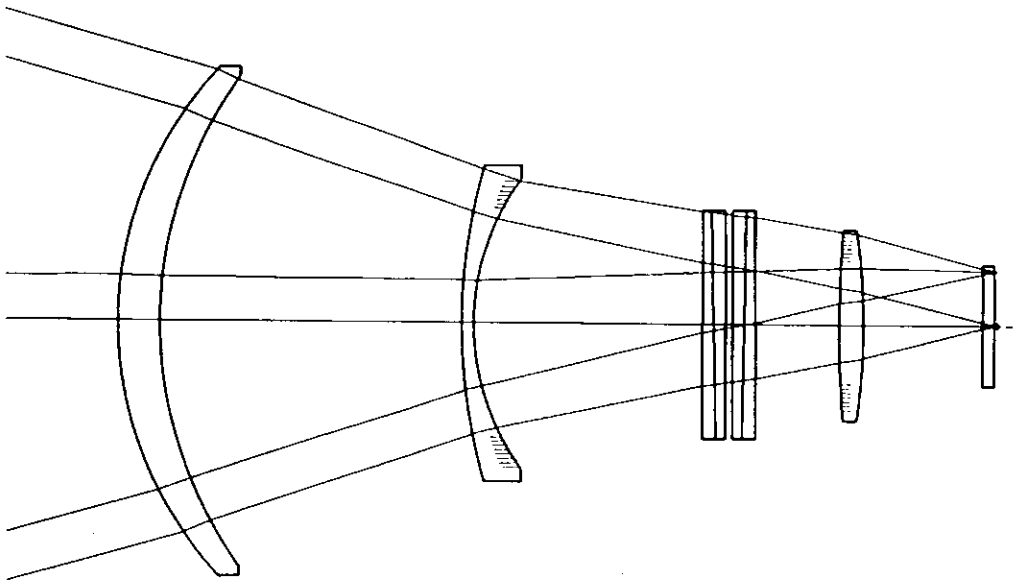

Figure 4-2. Nariai's Primary Corrector with direct-vision prism ADC (Nariai et al. 1985)

Su Ding-qiang made each of the two lenses of a field corrector for R-C system to be a composite lens whose component glasses have similar refractive index with different dispersion and made the boundary of the two glasses inclined. He called this a lensm (lens-prism). (Su Ding-qiang 1986). See Figure 3-4. Many designs of primary correctors with lensm for various cases were published (Wang Ya-nan et al. 1990). See Figure 4-3.

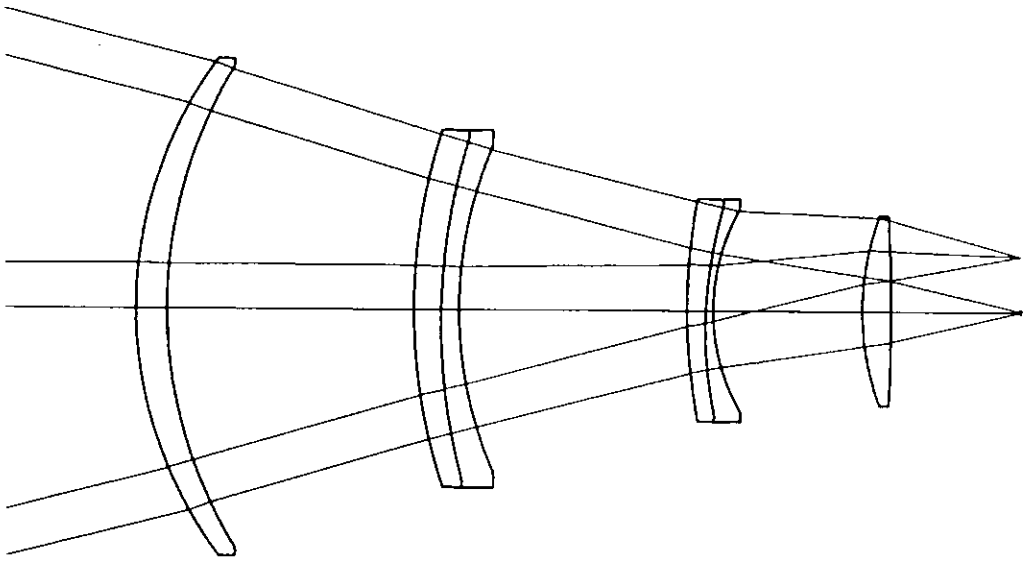

EFL=16.45m, Fno.=2.19, FOV= 30arcmin

Figure 4-3. Wang Ya-nan and Su Ding-qiang's Primary Corrector with "lensm" (Wang Ya-nan et al. 1990)

5. Optical Design

5.1. Design Requirements

There are already ten 8-10m class telescope under construction or already in operation at the time of writing this thesis; two 10m Keck Telescopes built by University of California and its consortium on Mauna Kea, 8m Hobby-Everly Telescope, 8.2m Subaru Telescope built by National Astronomical Observatory of Japan on Mauna Kea, four 8.1m VLTs built by European Southern Observatory at Cerrp Paranal in Chile, two 8m Gemini telescopes under construction on Mauna Kea, Hawaii and at Cerro Pachon in Chile. Among these 8-10m class telescopes none but Subaru Telescope has implemented a wide field primary focus. All other major new telescope abandoned to implement the wide field primary focus. This was mainly because of its anticipated engineering difficulties in designing and manufacturing an enormous corrector lens system for such a fast focus with a capability to compensate aberrations over the wide field and at the same time the atmospheric dispersion depending on the zenith distance. The scientific needs for the wide field capability for 8-10m class telescopes were evident and astounding. For instance, 1m class Schmidt telescopes provided wide field survey capability to search for new interesting objects to be studied closely by 4m class telescopes. In this sense, 1m class Schmidt telescopes were good match to 4m class telescopes. However, situation for 8-10m class telescopes has not been satisfactory because that there was no adequate telescopes allowing deep wide field survey type observations to isolate interesting new faint objects that are worth for observation with 8-10m class telescopes.

Realizing such a strong need and importance to enable wide field survey capability for Subaru telescope, NAOJ astronomers decided to implement the primary corrector. The requested unvignetted field of view was 30 arcmin in diameter. A huge mosaic CCD camera, named Suprime-Cam, was proposed to cover 30 x 24 arcmin field with 10 large format CCDs each having 8M pixels of 15 micron square providing a sampling rate at 0.2 arcsec/pixel. The specifications for the primary corrector with ADC capability to realize such a wide field observation are shown in Table 5-1. The specifications laid down by NAOJ were extremely challenging for optical designers and manufacturers.

Table 5-1. Specifications for Subaru Primary Corrector

Primary Mirror	diameter 8.2m, radius of curvature 30m, RC for F12.2
FOV for primary focus	30 arcmin, unvignetted
Wavelength	0.4 μ-1.0 μ for optimization
Pixel Scale	0.2 arcsec/pixel
FWHM Image size	0.2 arcsec or smaller
Zenith Distance	0-60 degree

Apart from the difficulty in realizing the optimum optical design, there were other practical constraints as well. For instance, the originally assumed weight of the prime focus assembly, including the primary corrector, prime focus CCD camera Suprime-Cam, and their associated supporting structure, electronics and cables, was 500kg. The telescope main truss structure was designed assuming this load at the prime focus to balance the moment and stiffness. In fact, as the detailed designing work proceeded for the prime focus structure, including the hexapod platform for aligning the prime focus unit correctly relative to the primary mirror, it turned out that the mass budget assignable for the primary corrector was not as generous as was originally assumed and it became desirable though not mandatory to reduce the mass of the primary corrector unit as far as possible to retain the imaging and tracking performance of the telescope.

Also, considering the need to implement a primary baffle structure to reduce unwanted light entering into the prime focus unit, the size of the primary corrector should be confined as small as possible. The backfocus from the last surface of the detector dewar window was another concern for the Suprime-Cam group in optimizing the mechanical and thermal design of the instrument.

5.2. Nariai's Design and My Efforts to Overcome its Difficulties

As was shown in chapter 4, Nariai's design of the primary corrector (1994) using a pair of classical direct prism was the starting point of the present work. Several difficulties were anticipated in the fabrication of the primary corrector according to the optical design of Nariai (1992). Following is the description of my efforts to overcome these difficulties.

(a) Easing the manufacturing difficulty of glass materials.

The glass material FPL51 (OHARA. Equivalent to FK52 of Schott) belongs to fluorine phosphor glass family. The coefficient of thermal expansion of this kind of glass is large. Besides, the coefficient for thermal conductivity is low. It is, therefore, very difficult to handle this glass safely because it will break easily at a small thermal shock. It is also difficult to get glass blanks of this size (diameters of 649mm, 392mm, and 220mm). A glass company, OHARA, kindly offered a proposal to challenge to make these glass blanks. However, only a glass blank of 200mm had been fabricated and used, and an experimental glass blank of 400mm had been fabricated. The Nariai design required a blank with diameter larger than 660mm. As a blank of FPL51 (or its equivalent) of this size had never been fabricated in the world by that time, great difficulty was anticipated in its fabrication. However, 200mm size lenses of this glass had already been fabricated by OHARA and had been processed by CANON at a rate of several par month. Therefore, it can be done although it needs careful handling. It appeared too risky to rely on the developmental processing of a 660mm diameter blank of FPL51 to realize the Subaru primary corrector.

I tried, therefore, to replace the glass material of the first and the second lenses with BSL7 (OHARA's equivalent to BK7 of Schott) because it is much easier to make large size blanks of this glass and its quality is stable. I found, however, that it is impossible to make the longitudinal and lateral chromatic aberrations zero simultaneously without FPL51. Chromatic differences of aberrations are usually difficult to suppress with this type of lens design. Therefore, the adoption of the ultra low dispersion glass FPL51 in Nariai design was effective. Since a smaller size FPL51 blank was available, I decided to use FPL51 as the third lens to compensate the chromatic aberrations.

(b) Smaller First Lens to reduce chromatic aberrations

With the three lens correctors hitherto published, the largest remaining aberrations are the chromatic differences of aberrations, specially those of spherical aberration and of coma. In Nariai design, ultra low dispersion glass is used so that these chromatic differences of aberrations become small. Replacement of FPL51(OHARA) with BSL7(OHARA) made these chromatic differences larger because of the larger dispersion of the glass besides the chromatic aberrations.

I modified the lens design in the following way. Making the position of the first lens closer to the focal plane (making the distance between the main mirror and the first lens larger) makes the chromatic difference of the spherical aberration smaller. This also makes the size of the first lens smaller. Moving the first lens in this way keeping the back focal distance constant means smaller length between the first and the last lenses of the corrector. Therefore, the three-lens design with small chromatic difference of the spherical aberration has the first lens with smaller power as a convex lens but with higher curvatures and the second and the third lenses with higher powers. If we use the same glass for three lenses, the chromatic aberration of magnification becomes large because of the higher powers of the second and the third lenses. Therefore, it is necessary to use lower dispersion glass in order to correct the chromatic aberration of magnification.

(c) New type atmospheric dispersion corrector (Nariai et al. 1994, Takeshi et al. 1994)

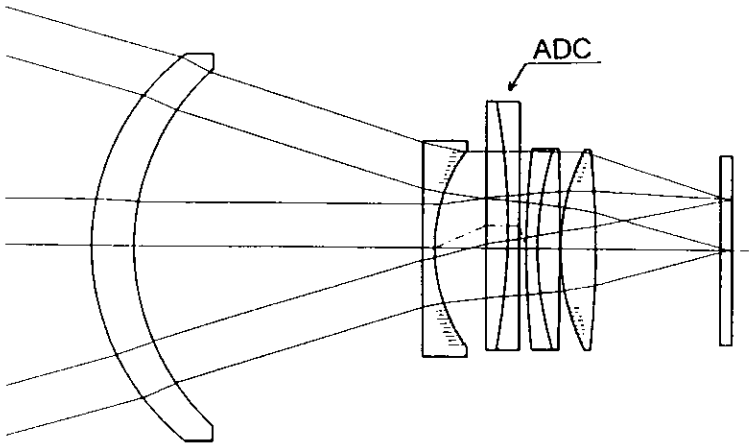

EFL=15.31m, Fno.=1.87, FOV=30 arcmin

Figure 5-1. Temporary model for the Primary Corrector with Lateral shift type ADC, Aspheric surface are indicated with hatches.

This ADC consists of two lens elements and has three surfaces. The first and third surfaces are flat and the second surface is spherical. Shift of this component perpendicularly to the optical axis causes nothing to the first and the third surfaces

and the de-centered spherical surface between two elements behaves as an ADC. Let us take the x-axis as the optical axis and the position of the spherical surface in the ADC the zero-point of the coordinate. Then, the surface is written for R as the radius of curvature of the surface, as

$$x = 1 - \sqrt{1 - \frac{y^2 + z^2}{R^2}} = \frac{1}{2}\frac{y^2 + z^2}{R^2} + \cdots\cdots, \qquad (R > 0) \tag{4}$$

We will discuss only the case $R>0$. The result for the case $R<0$ can be easily obtained with appropriate changes of signs. Let us shift ADC by d in the y-direction, then we have

$$x = 1 - \sqrt{1 - \frac{(y-d)^2 + z^2}{R^2}} = \frac{1}{2}\frac{(y-d)^2}{R^2} + \cdots\cdots = \frac{1}{2}\frac{y^2 + z^2}{R^2} - \frac{dy}{R^2} + \cdots \tag{5}$$

The first term represents the spherical surface while the second term is interpreted as a prism because it is proportional to y. Thus, the difference between the shifted spherical surface and the original surface can be interpreted as a variable prism.

Nariai's original design uses two direct-vision prisms in order to correct atmospheric dispersion. Using two components with a total of four elements only to correct atmospheric dispersion is somewhat extravagant. Reducing the number of elements has a great benefit in terms of transmission efficiency and so on, if the optical imaging performance is acceptable.

So, I replaced two direct-vision prisms with a pair of lenses each consisting of two elements in order to achieve two targets, namely, to correct atmospheric dispersion by lateral shift of this lens and to correct two chromatic aberrations (Nariai et al. 1994, Takeshi et al. 1994). The replacement of direct vision prisms with a pair of lenses consisting of two matched elements each introduced additional possibility to optimize the radius of curvature of these matched surfaces. I used this freedom to reduce the remaining chromatic aberrations and found it very effective in improving the optical performance.

Replacement of direct vision prisms with a pair of compound lenses opened an entirely new way to correct the atmospheric dispersion as was mentioned before. Since the matched surfaces of these compound lenses are curved, they produce a

chromatic dispersion when displaced diagonally from its optical axis, although this was not the case for a pair of direct vision prisms. The glass materials of the two pair of compound lenses were chosen so that the chromatic dispersion, that is produced when one of the pair of lenses is displaced diagonally from the optical axis, matches with that of the atmospheric dispersion. Since the Subaru Telescope is an alt-azimuth type telescope, and the atmospheric dispersion depends only to the elevation of the telescope, the required motion for operating the atmospheric dispersion corrector is a simple lateral motion of one of the pair of lenses diagonally to the optical axis synchronized with the telescope elevation. This also helped to simplify the driving mechanism as compared to the classical ADCs that required driving two direct vision prisms in opposite direction.

In fact the optical design was carried out in an iterative process taking the above two features (a) (b) and (c) into consideration. Figure 5-1 shows a temporary design in which glass materials are selected so that the following values become small; the second spectra of the longitudinal chromatic aberration and the chromatic aberration of magnification, chromatic difference of the spherical aberration, and chromatic difference of field curvature. It consists of three single lenses and two compound lenses and its field of view is 30 minutes of arc. The total number of surfaces is the same as for the three-lens design with two direct vision prisms.

(d) Shifting the aspheric surfaces for easier processing

The aspheric surface polishing machine developed by Canon Inc. was to be used for processing of aspheric surface. Those who developed and used this machine expressed their concern about the radii of curvature of aspheric surfaces of the optical design shown in Figure 5-1 and in Table B-1 (in Appendix) because the machine does not guarantee accuracy at the peripheral region of the lens when the curvature of the surface is large.

We have therefore changed the configuration as shown in Figure 5-2 and Table 5-1, where the aspheric surfaces are assigned to surfaces with smaller curvature. We avoided to assign the aspheric surface to the FPL51 glass to reduce the risk of processing the surface. Also, an odd order term is used so that rays passing through peripheral region behave gently. Figures 5-3 and 5-4 show the aberration diagrams of this new design at the zenith and at the zenith distance 60 degrees. Figure 5-5 shows the aberration diagrams at the zenith distance 60 degrees when

ADC is not working. Lateral shift of images for 0.4 μm and 1 μm exceeds 0.05 mm in these diagrams while the shift due to color is well corrected in Figure 5-4. Figures 5-6-1, 5-6-2, 5-6-3 and 5-7-1, 5-7-2, 5-7-3 are spot diagrams at the three wavelengths 0.5461 μm (e-line), 0.4 μm and 1 μm respectively for the zenith and zenith distance 60 degrees.

This design was chosen as the final design for processing the primary corrector of 8.2m Subaru Telescope.

k	ea	r	d	glass	maker	n_d	ν_d
1*	8200.046	30000.00000	14208.00000				
2	506.980	327.93795	56.00000	bsl7	ohara	1.516330	64.15
3	467.115	320.56994	399.05825			1.	
4*	274.917	-5178.61747	16.00000	bsl7	ohara	1.516330	64.15
5	251.457	214.49423	64.17665			1.	
6	340.000	0.00000	26.00000	pbm5	ohara	1.603420	38.01
7	340.000	-900.00000	14.00000	bsm14	ohara	1.603112	60.70
8	340.000	0.00000	6.00000			1.	
9	258.162	846.05620	15.00000	pbm2	ohara	1.620041	36.26
10	256.721	399.12770	29.70371	bsl7	ohara	1.516330	64.15
11*	256.606	5532.59291	1.00000			1.	
12	256.636	272.65658	47.43897	fpl51	ohara	1.496999	81.61
13	253.987	-1057.72498	140.00000			1.	
14	250.000	0.00000	30.00000	sio2	xxxxx	1.458670	67.90
15	250.000	0.00000	9.99590			1.	

Aspheric constant

k	*r*	e^2	*B*	*C*	*D*	*D'*	*E*
1	30000	1.00835					
4	-5178.61747		3.19417E-9	-8.00839E-14	1.81720E-18	-1.07649E-20	2.53189E-23
11	5532.59291		1.37929E-9	-5.17433E-14	-6.78490E-18	7.08040E-20	-2.33789E-22

$$x = \frac{h^2/r}{1+\sqrt{1-(1-e^2)(h/r)^2}} + Bh^4 + Ch^6 + Dh^8 + D'h^9 + Eh^{10}, \quad h = \sqrt{y^2+z^2}$$

f_e = 15315.397

Table 5-1. Optical data of final design of Primary Corrector of Subaru Telescope

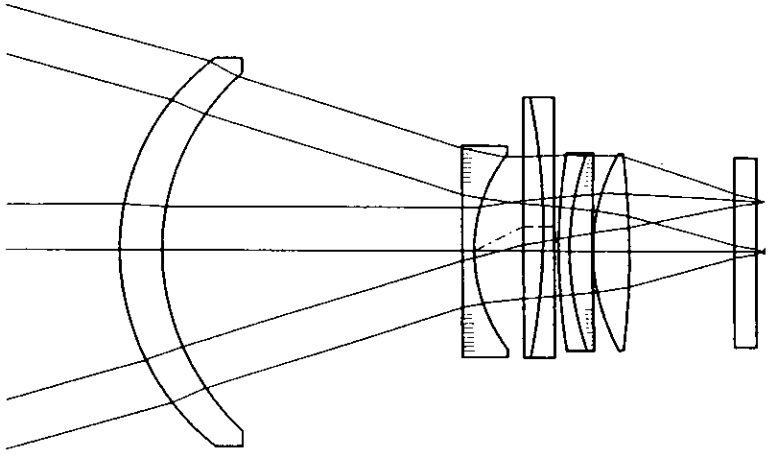

EFL=15.32m, Fno.=1.87, FOV=30 arcsec

Figure 5-2. Cross section of final design of Primary Corrector of Subaru Telescope

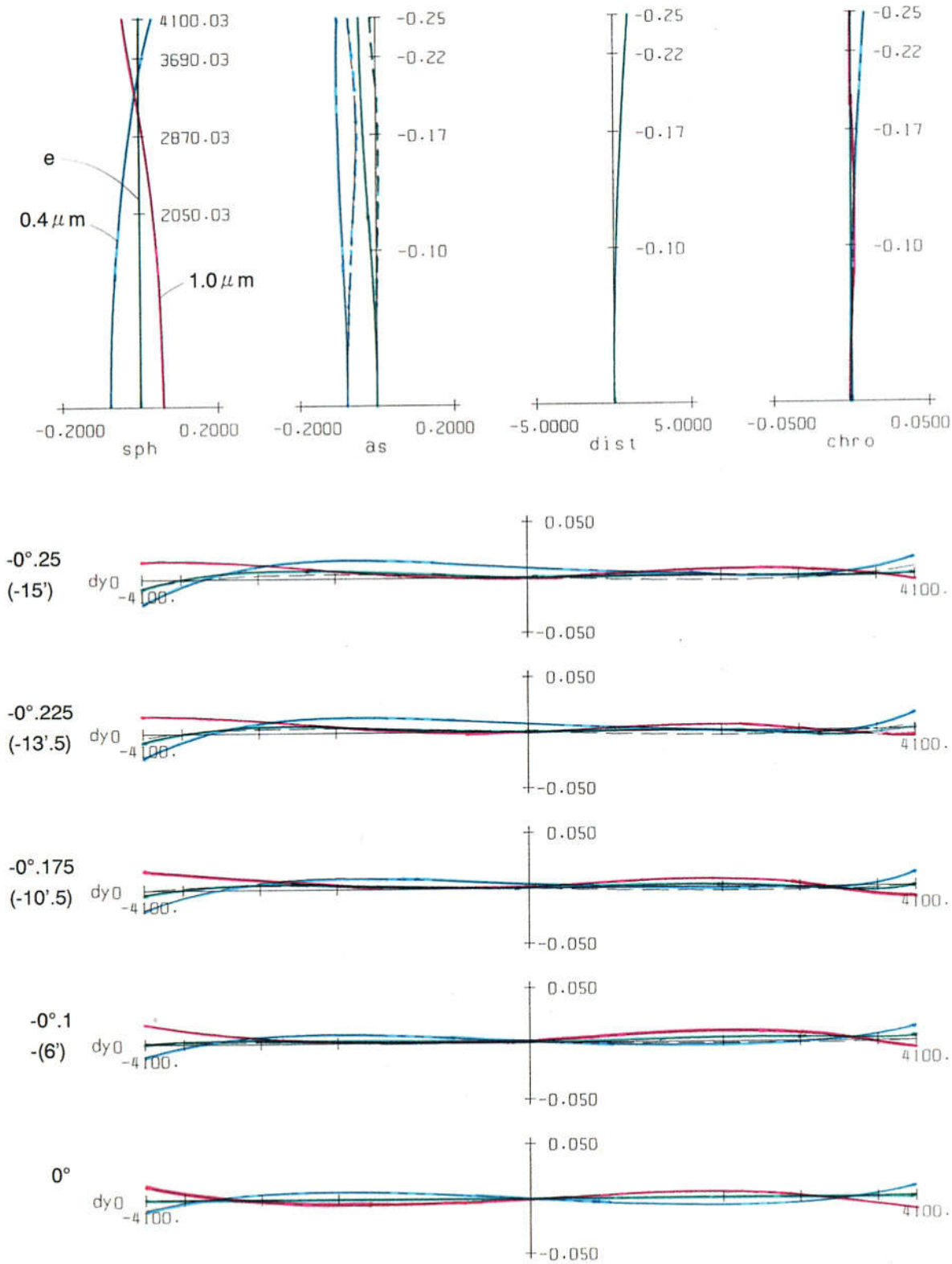

Figure 5-3. Aberration diagrams of Primary Corrector for Subaru Telescope, zenith distance 0°. The ordinates and abscissa are in millimeter except for the ordinate of three upper right diagrams where the ordinate is the field angle in degree.

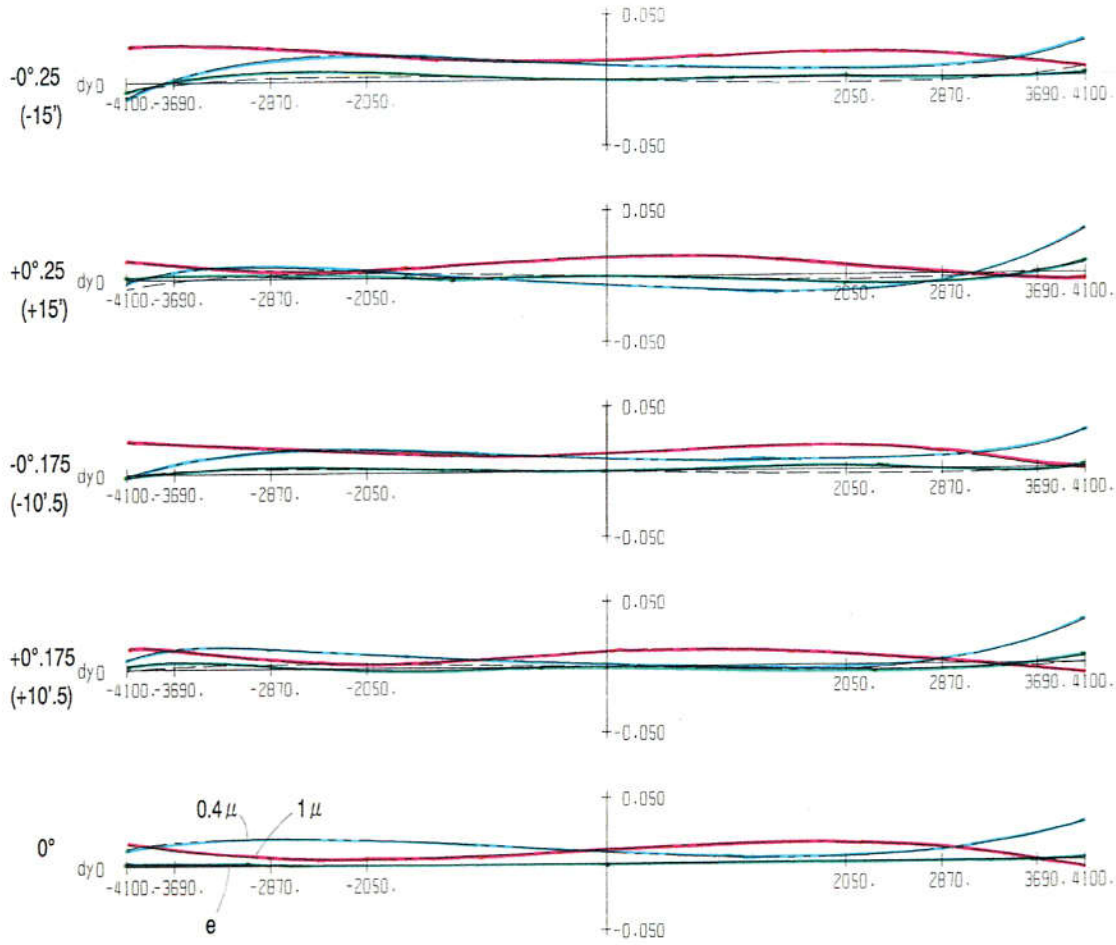

Figure 5-4. Aberration diagrams of Primary Corrector for Subaru Telescope where ADC is set at proper position. Zenith distance 60°

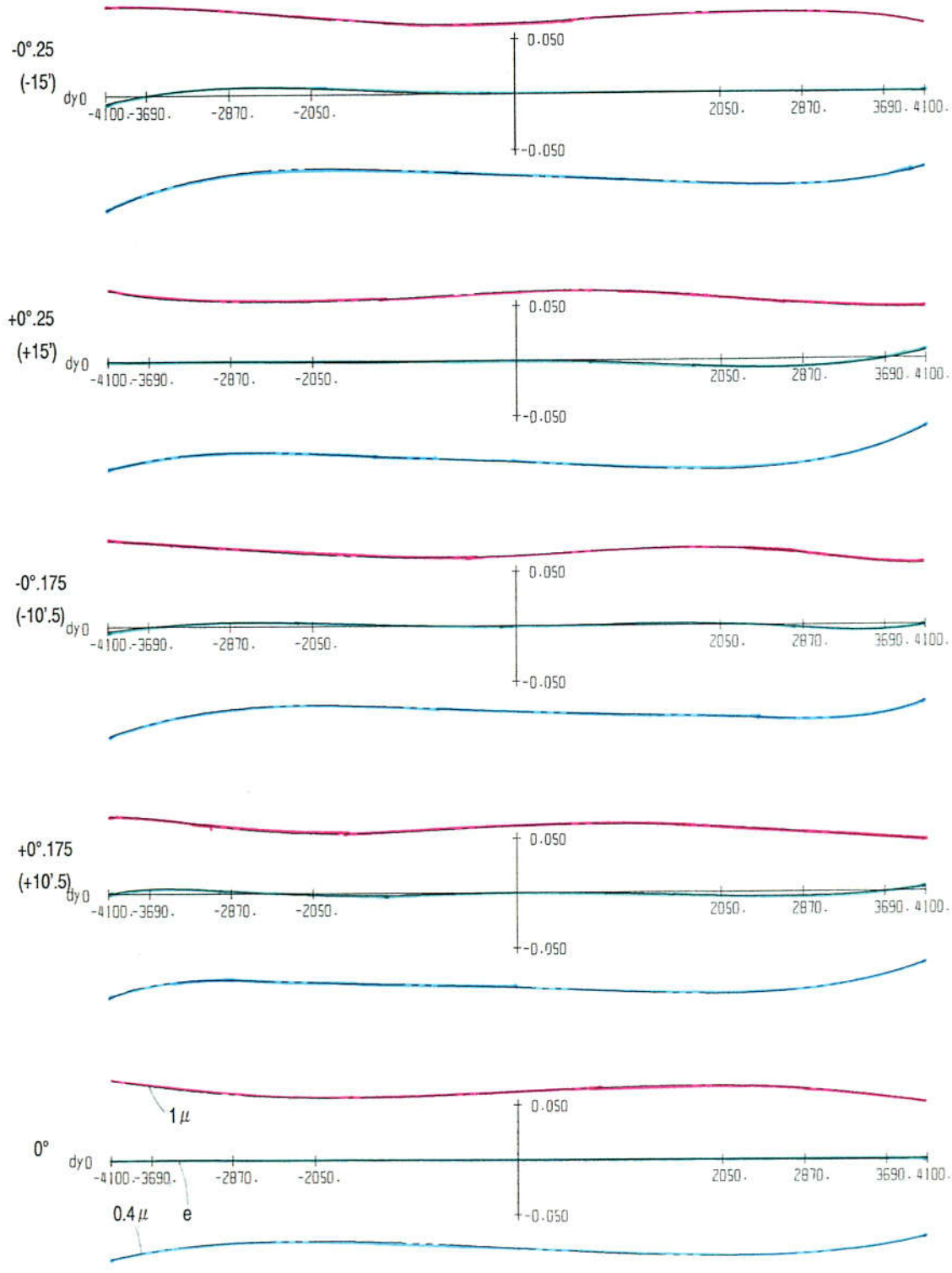

Figure 5-5. Aberration diagrams of Primary Corrector for Subaru Telescope when ADC is not working. Zenith distance 60°,

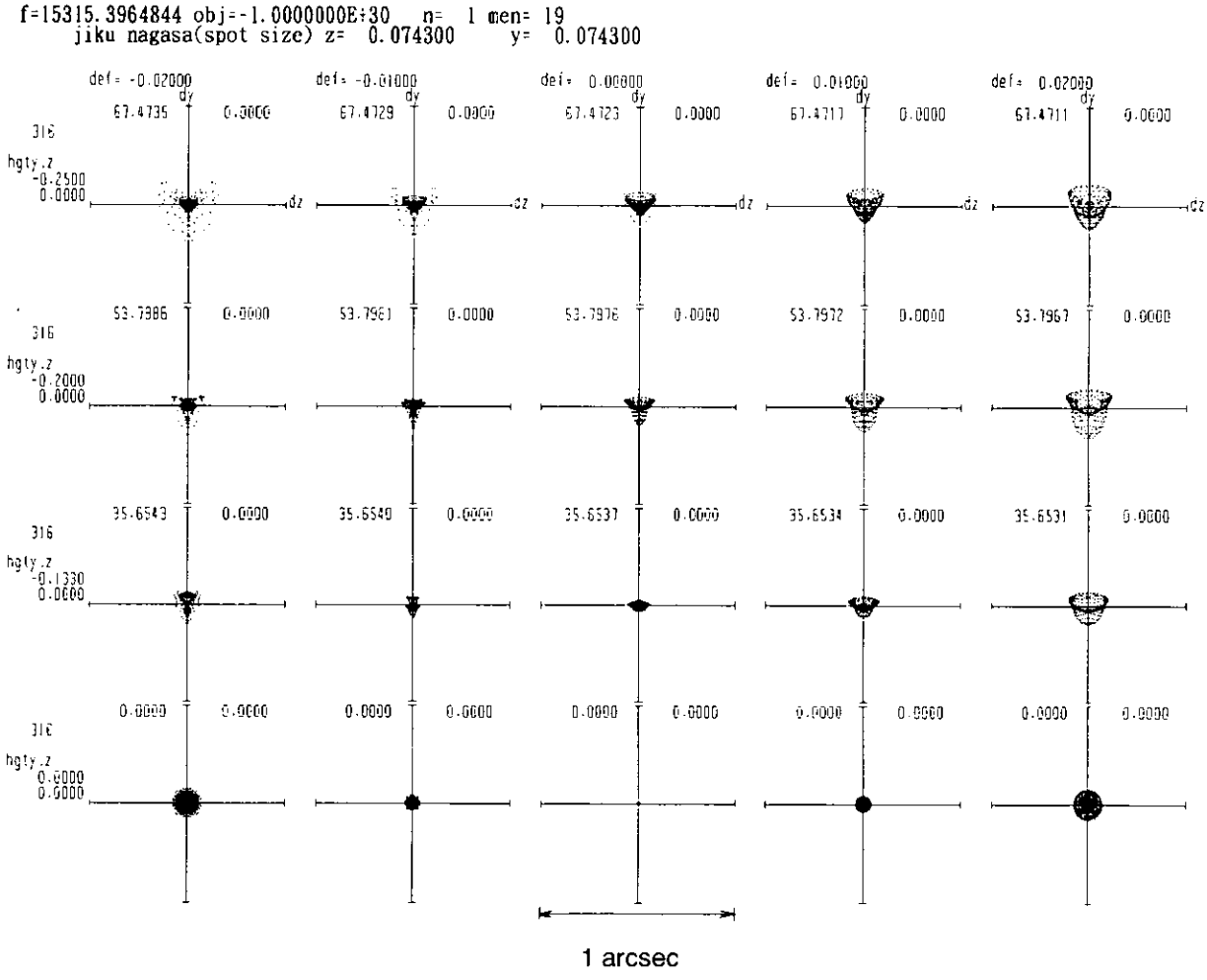

Figure 5-6-1. Spot diagrams of Primary Corrector for Subaru Telescope, zenith distance 0°, λ = 0.5461 μm. Four rows correspond to the field angle in degrees and five columns correspond to position of the focusing plane (defocusing amount shown in millimeter). Unit length for each spot is 0.0743mm.

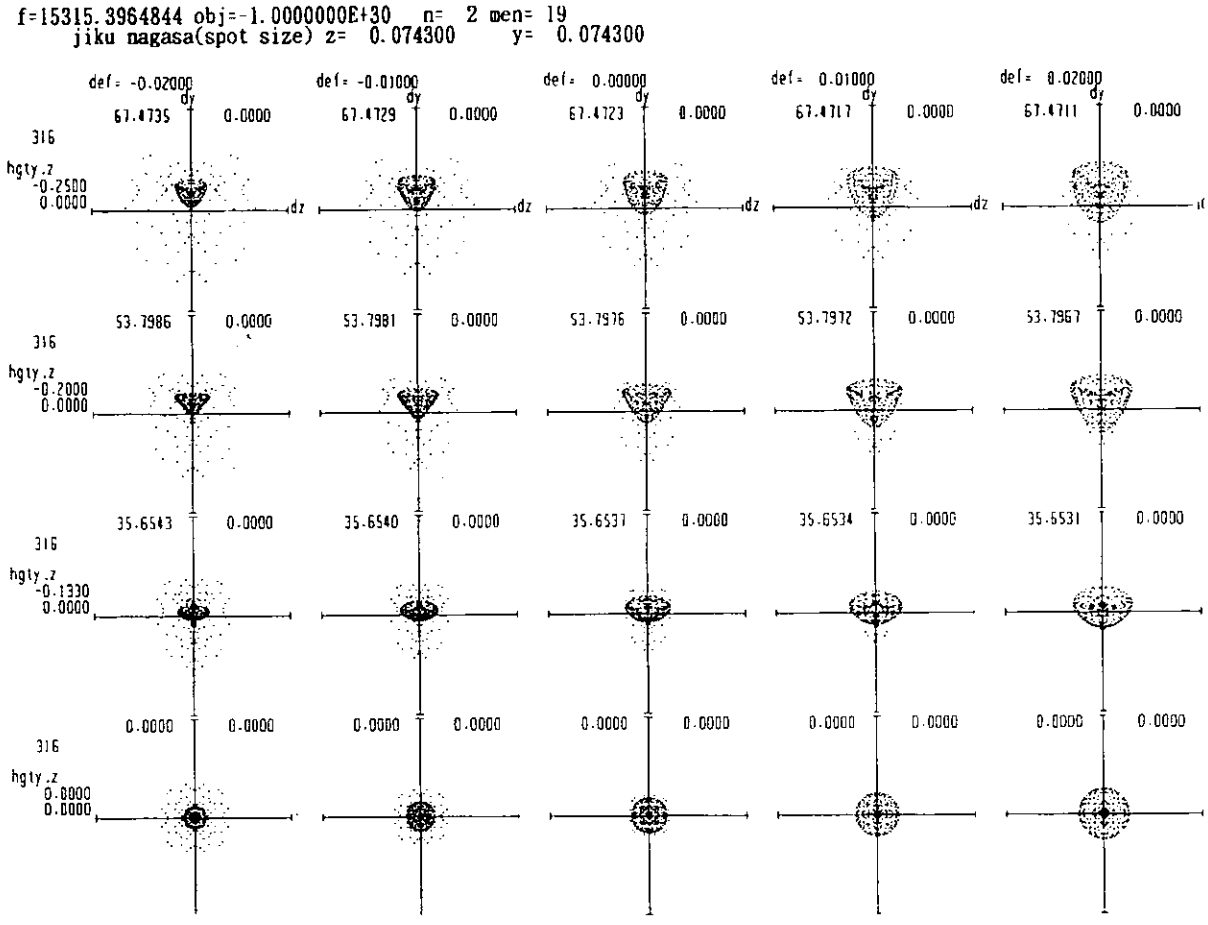

Figure 5-6-2. Spot diagrams of Primary Corrector for Subaru Telescope, zenith distance 0°, $\lambda = 0.4\,\mu$m

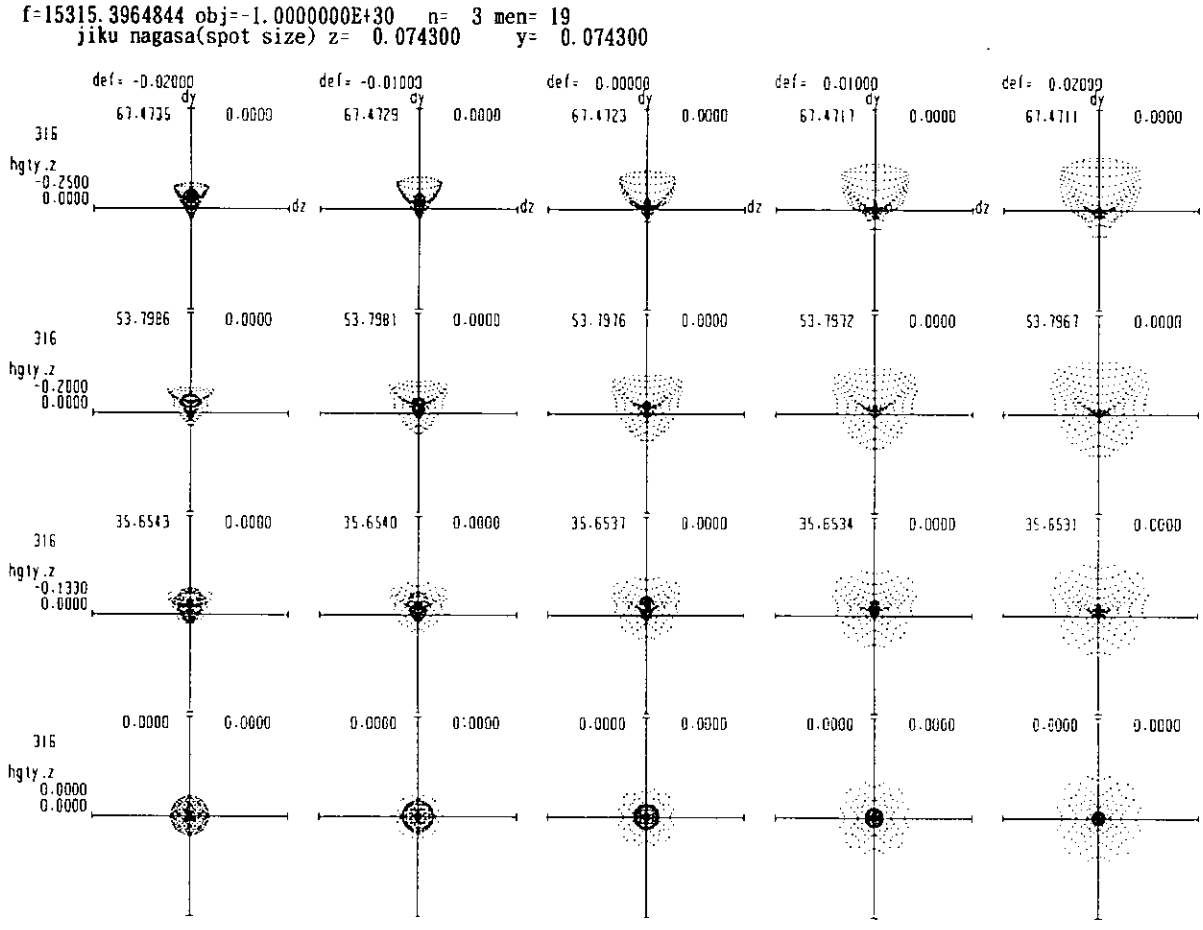

Figure 5-6-3. Spot diagrams of Primary Corrector for Subaru Telescope, zenith distance 0°, λ = 1.0 μm

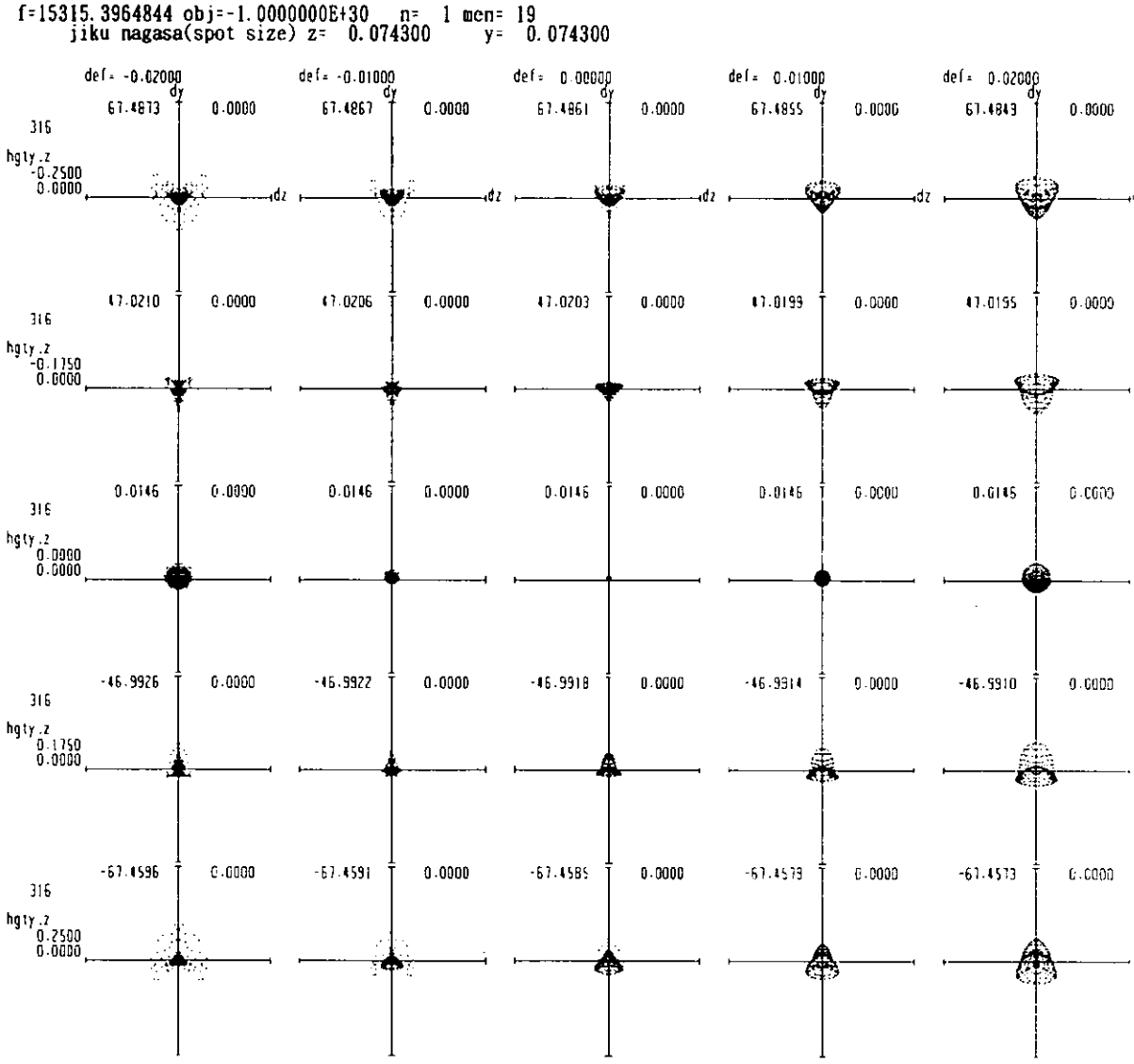

Figure 5-7-1. Spot diagrams of Primary Corrector for Subaru Telescope, zenith distance 60°, λ = 0.5461 μ m

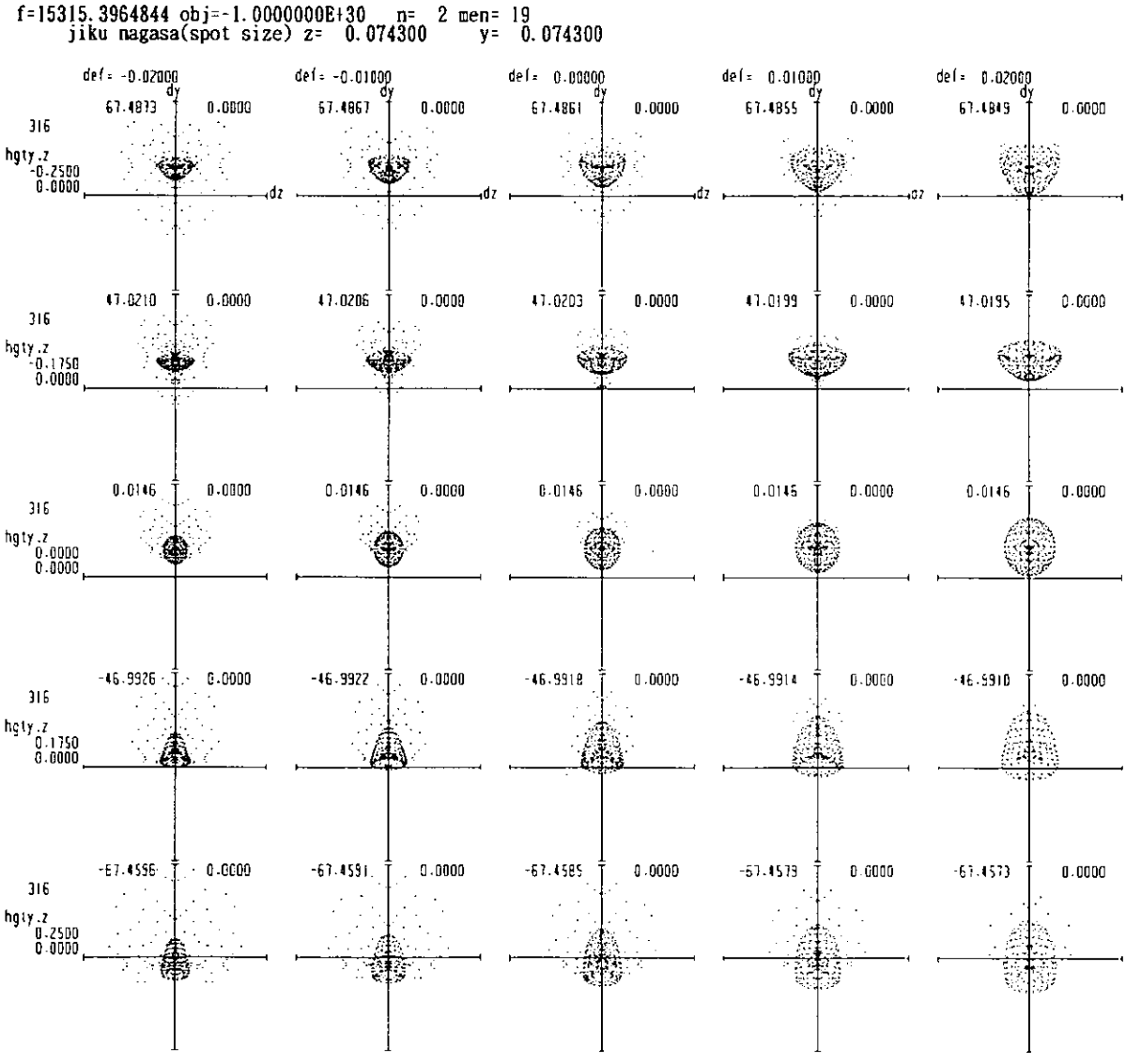

Figure 5-7-2. Spot diagrams of Primary Corrector for Subaru Telescope, zenith distance 60°, λ = 0.4 μ m

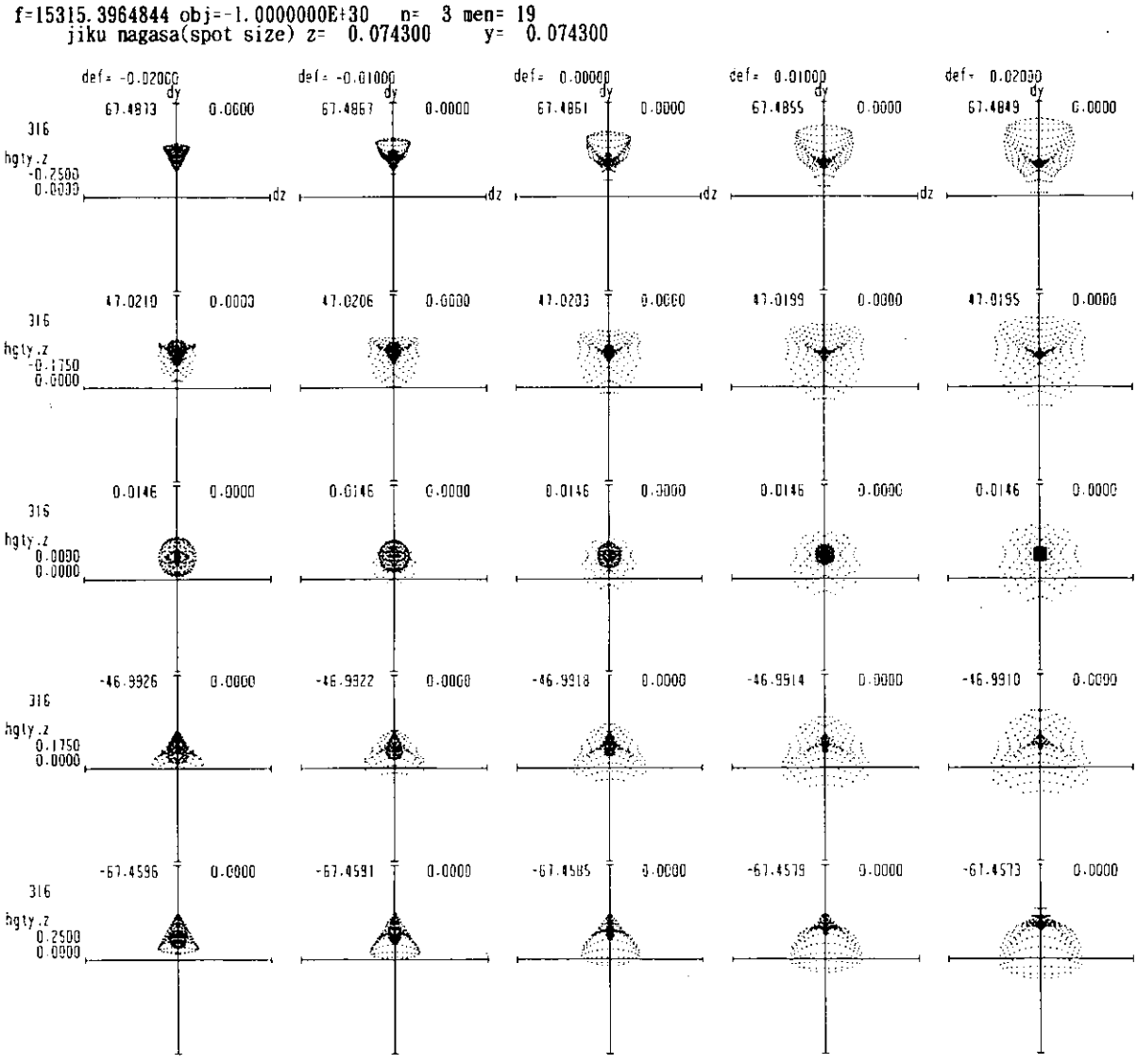

Figure 5-7-3. Spot diagrams of Primary Corrector for Subaru Telescope, zenith distance 60°, λ = 1.0 μ m

5.3. Throughput and ghost analysis

The throughput of the entire lens system of the primary corrector is calculated based on the basic data of the glass materials and is shown in Figure 5-8.

For the final design, ghost simulation was carried out. First, the imaging positions with two surface reflections in the corrector were obtained by paraxial calculation. We chose those whose imaging positions is close to the true imaging plane and traced rays. Examples are shown in Figures 5-9, 5-10, and 5-11. We also estimated the intensity of the ghost images. Assuming the size of the ordinary image of 0.5 arcsec, reflectivity of the filter at 10 percent, reflectivity of the surfaces with anti-reflection coating at 1 percent, and reflectivity of the glued surfaces at 0.1 percent, we obtained 1.2 x 10-7 as the largest ratio of intensity.

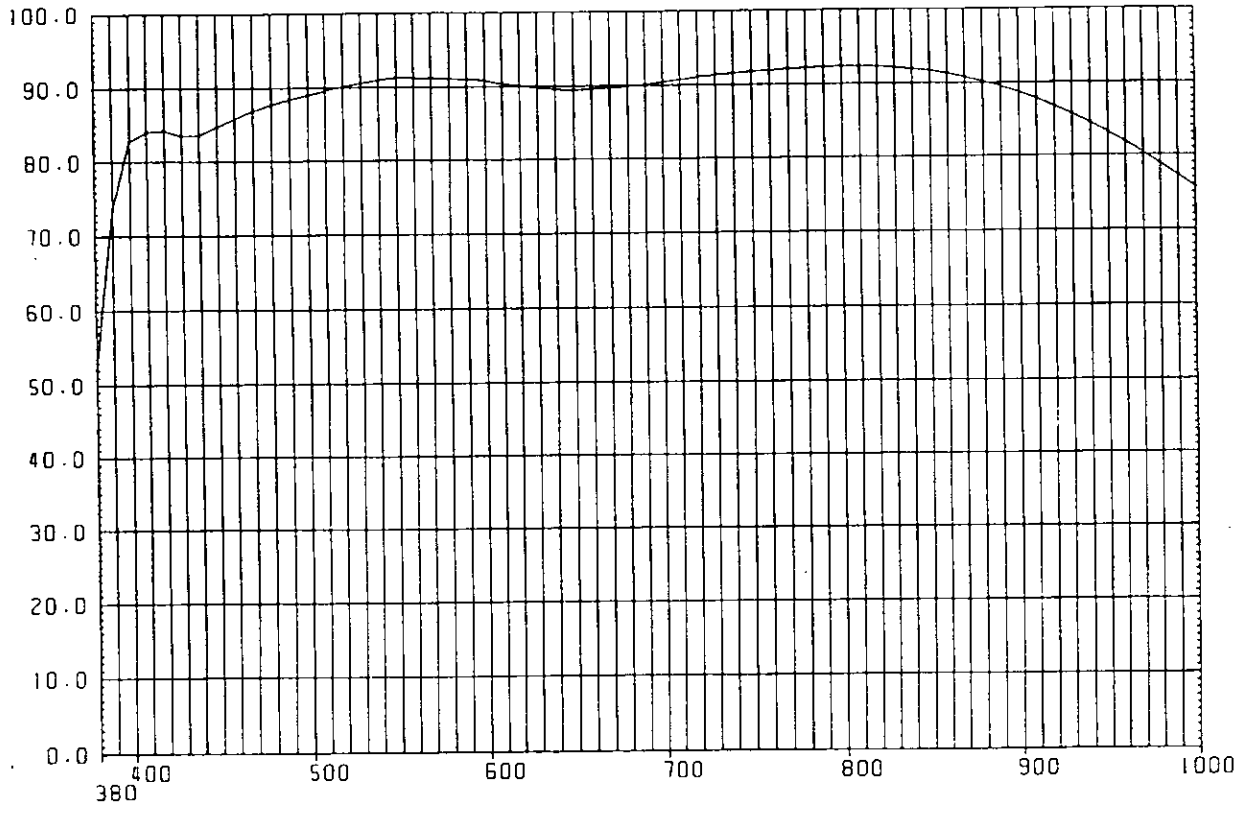

Figure 5-8. Transmittance of the entire corrector (calculated)

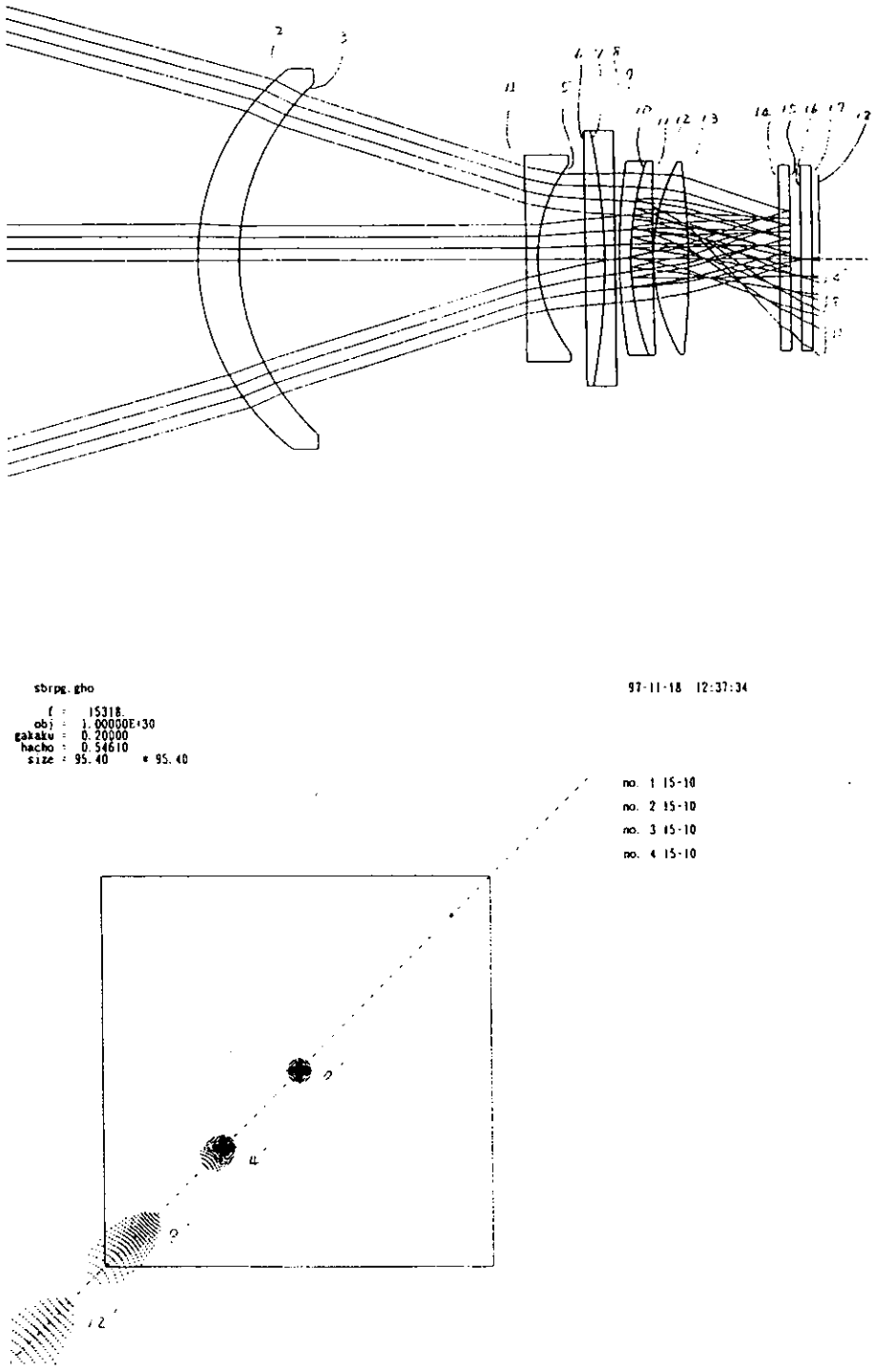

Figure 5-9. Ghost ray trace and spot diagrams of ghost image (1)

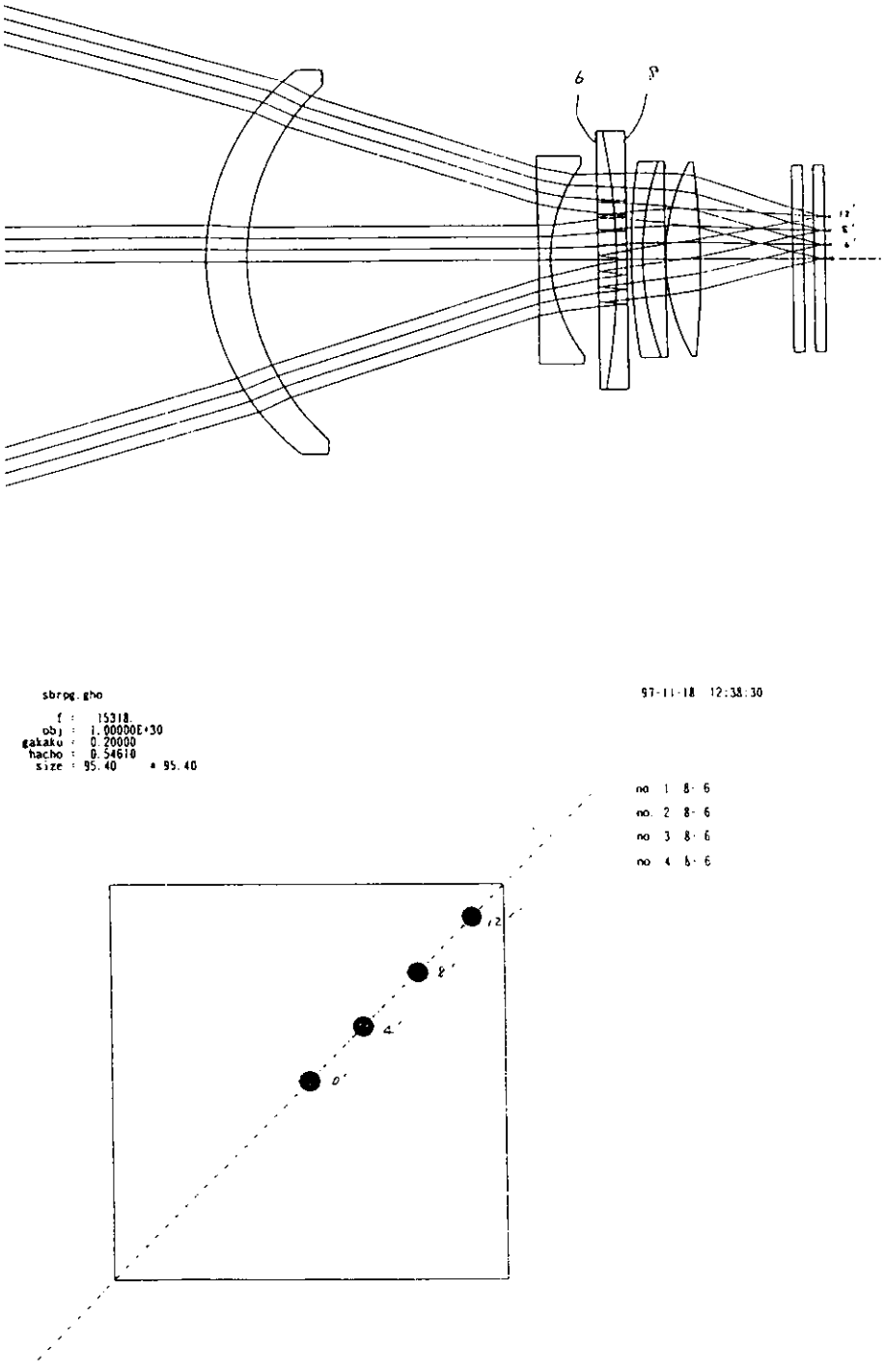

Figure 5-10. Ghost ray trace and spot diagrams of ghost image (2)

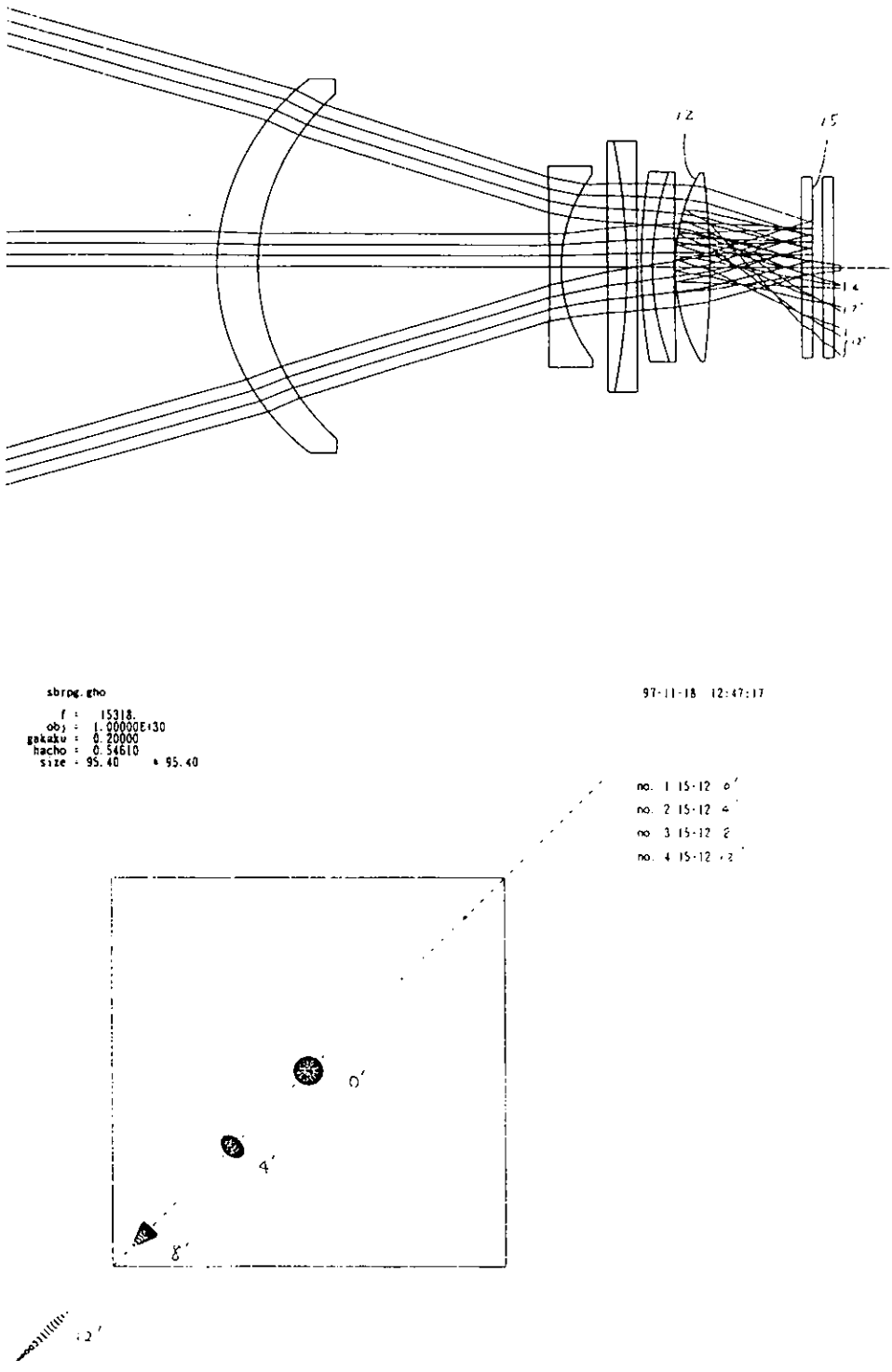

Figure 5-11. Ghost ray trace and spot diagrams of ghost image (3)

6. Fabrication

A lens manufacturing company has usually a series of standard spheres whose radii are precisely measured. When a lens system is going to be manufactured in quantity, the original lens design is usually modified so that the radius of each surface in the system is replaced by a value of the radius of a standard sphere closest to the original value. It is difficult to make a standard sphere with a desired radius and with sufficiently accurate surface. Therefore, if a standard sphere is to be manufactured for a particular lens design, the tolerance of the final radius is 1/2000 of the target value. So, by using standard sphere of known radii, we can make a lens closer to the original design rather than by making new standard sphere for a particular lens design.

For a lens produced in large quantities, error budgets are calculated for radius of curvature, departure from the ideal sphere, thickness, distance, refractive index, dispersion, so that the targeted performance is achieved, then manufacturing process starts with tolerances for each elements thus calculated.

The standard procedure for a precise lens system is follows; secure glass material, modify the design with the melt-data, modify the design again with the standard sphere system, polish, measure thickness of polished lenses, assemble into one system with distances modified on the basis of the measured lens thickness.

In the case of the Subaru primary corrector, however, we modified the design with the standard sphere system skipping the step of modifying the design with the melt-data. We estimated that the dependence of the imaging characteristics on the refractive index was relatively small and that the targeted performance could be achieved by adjusting thickness and distance if differences of melt-data and catalogue data fall within n_d: ± 0.0005 or ν_d: $\pm 0.8\%$. Thus, in order to save time, we decided radii of surfaces and ordered jigs.

As to glasses BSL7, BSM14, and PBM2, we decided to use BSL7Y, BSM51Y, and PBM2Y after having consulted with OHARA, the glass company. These new series of glasses were developed for the optical systems of stepper, printing machine of semi-conductor, for the use in the i-line(0.356 μm), and have the same refractive index and dispersion as the corresponding ordinary optical glasses but the transparency in

the ultraviolet and the homogeneity are better than those of latter. PBM5 did not have a counterpart in the new series. FPL51 is now replaced by S-FPL51, an Eco Optical Glass that does not contain toxic substances such as plumb or arsenic.

We might have had to re-order jigs if the optical constants of the glasses were outside of the range of our estimation, that leads to re-determination of radii of surfaces. But such worrying circumstance never happened. Table 6-1 shows Optical data after modifying with the standard sphere system.

k	ea	r	d	glass	maker	n_d	ν_d
1*	8200.000	30000.00000	14208.00000				
2	506.800	326.76000	56.00000	bs17	ohara	1.516330	64.15
3	467.000	319.65000	398.32431			1.	
4*	275.000	-4475.19983	16.00000	bs17	ohara	1.516330	64.15
5	251.400	213.36000	64.46860			1.	
6	340.000	0.00000	26.00000	pbm5	ohara	1.603420	38.01
7	340.000	-897.65000	14.00000	bsm14	ohara	1.603112	60.70
8	340.000	0.00000	6.00000			1.	
9	258.600	825.93000	15.00000	pbm2	ohara	1.620041	36.26
10	257.200	391.19500	30.29257	bs17	ohara	1.516330	64.15
11*	257.200	5355.97529	1.00000			1.	
12	257.200	268.24000	48.01604	fp151	ohara	1.496999	81.61
13	254.500	-1098.30000	125.50259			1.	
14	250.000	0.00000	15.00000	sio2	xxxxx	1.458670	67.90
15	250.000	0.00000	14.50000			1.	
16	250.000	0.00000	15.00000	sio2	xxxxx	1.458670	67.90
17	250.000	0.00000	10.00000			1.	

Aspheric constant

k	r	e^2	B	C	D	D'	E
1	30000	1.00835					
4	-4475.19983		3.38267E-9	-8.36303E-14	2.03782E-18	-1.33838E-20	3.49307E-23
11	5355.97529		1.30769E-9	-5.38888E-14	-6.67037E-18	6.94170E-20	-2.28747E-22

$$x = \frac{h^2/r}{1+\sqrt{1-(1-e^2)(h/r)^2}} + Bh^4 + Ch^6 + Dh^8 + D'h^9 + Eh^{10}, \quad h = \sqrt{y^2+z^2}$$

f_e = 15318.052

Table 6-1. Optical data after modifying with the standard sphere system

At the planning phase, we estimated delivery time to be between three to five months from the placement of order. However, it took more than our estimation because of accidents during the fabrication. So, we had to process lenses as glass came in, that means we did not have melt-data for all glass material. As we got individual melt-data, we replaced it with the corresponding catalogue data and made

ray-tracing in order to evaluate the effect of the difference between the melt-data and the catalogue data. It was not necessary to change the radii of surfaces or thickness of lenses, and adjustment of distances between lenses were the only things we had to do to get the targeted performance of the corrector. Table 6-2 shows the melt-data of glasses.

Melt Data

approved (承認) | issued (担当)

Year Month Day

,

OHARA Ohara Inc.
15-30, Oyama 1-chome, Sagamihara-shi
Kanagawa-ken 229 JAPAN

~~Mold No.~~	Part No.
7090982	

Ann. No.	Melt No.	Glass Type	~~n_c~~ nt	~~n_d~~ nC	n_c nd	n_F	n_g	nh	ν_d
AN5501	J0A7X31	BSL 7Y	1.50744 + 64	1.51449 + 64	1.51696 + 63	1.52253 + 63	1.52683 + 62	1.53037 + 61	64.3 + 2

Melt Data

キヤノン(株)
下丸子本社

approved (承認) | issued (担当)

Year Month Day

,

OHARA Ohara Inc.
15-30, Oyama 1-chome, Sagamihara-shi
Kanagawa-ken 229 JAPAN

~~Mold No.~~	Part No.
7070544	G2002

Ann. No.	Melt No.	Glass Type	~~n_C~~ nt	~~n_d~~ nC	~~n_c~~ nd	~~n_F~~ nF	~~n_g~~ ng	nh	ν_d
AN2501	J2A6427	BSL 7Y	1.50710 + 30	1.51415 + 30	1.51662 + 29	1.52218 + 28	1.52647 + 26	1.53002 + 26	64.3 + 2

Melt Data

キヤノン(株)
下丸子本社

approved (承認) | issued (担当)

Year Month Day

,

OHARA Ohara Inc.
15-30, Oyama 1-chome, Sagamihara-shi
Kanagawa-ken 229 JAPAN

~~Mold No.~~	Part No.
	ケース03

Ann. No.	Melt No.	Glass Type	~~$n_{e'}$~~ nt	~~n_d~~ nC	~~n_e~~ nd	n_F	n_g	nh	ν_d
AN3501	J7A7Y16	PBM 5	1.58748 + 23	1.59900 + 25	1.60367 + 25	1.61487 + 25	1.62407 + 25	1.63202 + 25	38.0 + 0

PRECISION MEASUREMENT
MELT DATA

(承 認)

Year Month Day

,

Ohara Inc.
15-30, Oyama 1-chome, Sagamihara-shi
Kanagawa-ken 229 JAPAN

Mold No.	Part No.
	4 2004

Ann. No.	Melt No.	Glass Type	~~nc~~ nt	~~nd~~ nC	~~ne~~ nd	n_F	n_g	nh	ν_d
AN. 3501	J0A7719	BSM51Y	1.59212	1.60041	1.60344	1.61035	1.61573	1.62018	60.7
			+ 33	+ 33	+ 33	+ 33	+ 33	+ 33	+ 0

Melt Data

approved (承 認)	issued (担 当)
開沼	

キヤノン(株)
下丸子本社

Year Month Day

,

Ohara Inc.
15-30. Oyama 1-chome, Sagamihara-shi
Kanagawa-ken 229 JAPAN

~~Mold No.~~	Part No.
7090957	G2005

Ann. No.	Melt No.	Glass Type	~~nc~~ nt	~~nd~~ nC	~~ne~~ nd	n_F	n_g	nh	ν_d
AN. 3504	J2D6112	PBM 2Y	1.60289	1.61513	1.62016	1.63223	1.64220	1.65084	36.3
			+ 14	+ 11	+ 12	+ 11	+ 12	+ 11	+ 0

Melt Data

approved (承 認)	issued (担 当)

キヤノン(株)
下丸子本社

Year Month Day

,

Ohara Inc.
15-30. Oyama 1-chome, Sagamihara-shi
Kanagawa-ken 229 JAPAN

Mold No.	Part No.
7070545	G2006

Ann. No.	Melt No.	Glass Type	~~nc~~ nt	~~nd~~ nC	~~ne~~ nd	~~nF~~ nF	~~ng~~ ng	nh	ν_d
AN2501	J2A6501	BSL 7Y	1.50710	1.51415	1.51663	1.52219	1.52648	1.53002	64.3
			+ 30	+ 30	+ 30	+ 29	+ 27	+ 26	+ 2

Melt Data

approved (承 認)	issued (担 当)
開沼	井上

キヤノン(株)
下丸子本社

Year Month Day

, 97 12 9

Ohara Inc.
15-30. Oyama 1-chome, Sagamihara-shi
Kanagawa-ken 229 JAPAN

Mold No.	Part No.
7090980	4 2007

Ann. No.	Melt No.	Glass Type	~~nc~~ nt	~~nd~~ nC	~~ne~~ nd	n_F	n_g	nh	ν_d
AN3502	002A607	S-FPL51	1.49017	1.49519	1.49706	1.50129	1.50457	1.50726	81.5
			+ 5	+ 5	+ 6	+ 6	+ 6	+ 6	- 1

Table 6-2. The melt-data of glasses

The dependence of the final performance of the corrector depends very much on the first lens. As fabrication process of the glass material for the first lens is quite complicated, it is explained in the following. Required volume of glass material of the first lens is first secured from thin cylindrical column raw material. They are placed vertically in the furnace. The temperature of the furnace is raised up to the softening point, then, we get a glass block. Finally, we put it into furnace again, using mold, to get a disc shaped glass. Figures 6-1 and 6-2 show the results of test of homogeneity of this disc after having polished both surfaces. Then, we put it into furnace again, using concave mold, to get meniscus shaped glass. This process is called slumping. After annealing, we measured for stain inside the meniscus block.

整理番号 98-1085

均質性測定結果報告書

1998年 4 月 15日
(株) オ ハ ラ

得意先	( )キヤノン一下丸子御中	注文番号	8020984
部番	G2001	硝種	BSL7Y
納入寸法(mm)	φ 710 × 76.0	熔解番号	J0A7X31
Δn規格	± 2.5 × 10^{-6}	アニール番号	2501
備考			

測定者	係長	課長
	98.4.15	98.4.15

品質管理部
測定課
物理測定係

測定結果

ID. No.	Δn (×10^{-6})	測定有効径 (mm)	測定時の実寸 (mm)	ピースNo.
55691	± 0.79	φ 450	φ 689 × 114.3	ナシ
92	± 0.79	φ	φ ×	
93	± 0.74	φ	φ ×	
94	± 0.84	φ	φ ×	
	±	φ	φ ×	
	±	φ	φ ×	
	±	φ	φ ×	
	±	φ	φ ×	
	±	φ	φ ×	
	±	φ	φ ×	
	±	φ	φ ×	
	±	φ	φ ×	
	±	φ	φ ×	
	±	φ	φ ×	
	±	φ	φ ×	
	±	φ	φ ×	
	±	φ	φ ×	
	±	φ	φ ×	
	±	φ	φ ×	
	±	φ	φ ×	

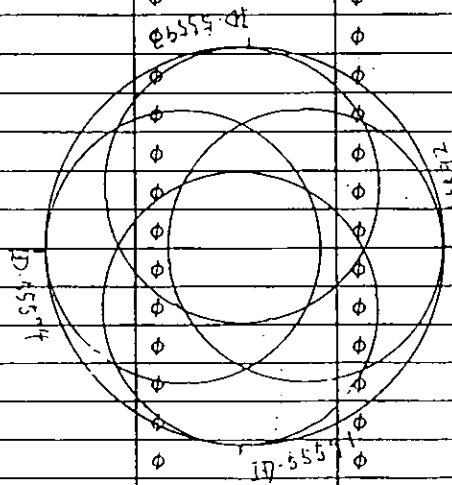

備考

56

Figure 6-1. The test results of homogeneity of disc shaped glass material for the first lens after having polished both surfaces (1)

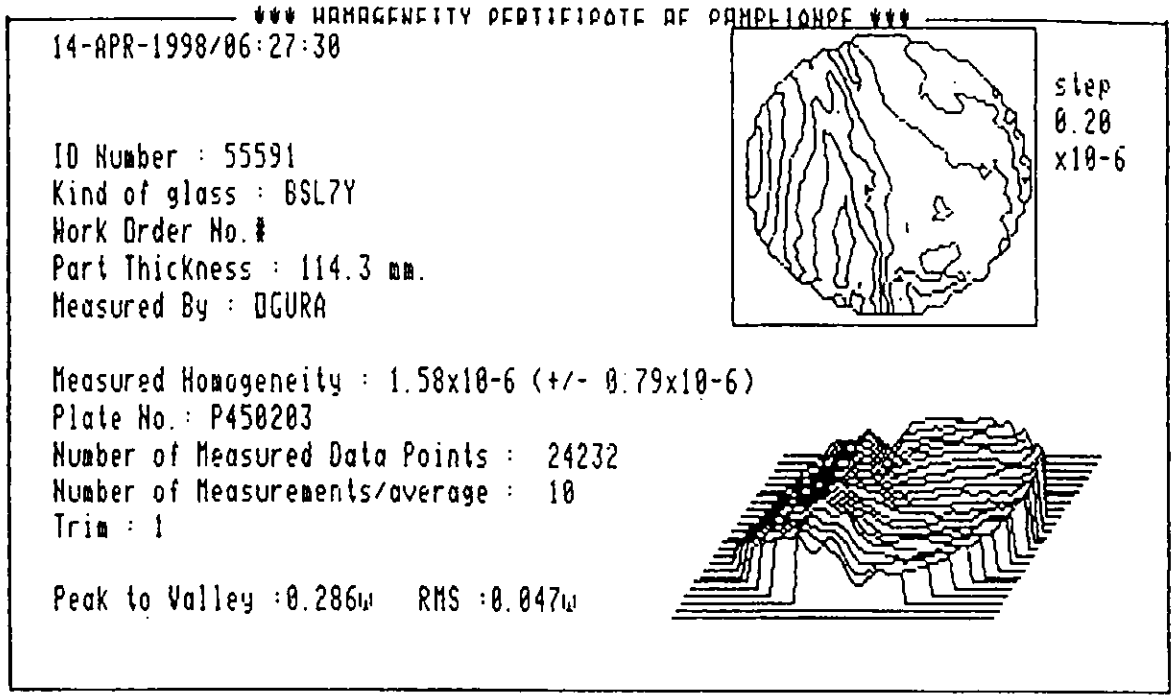

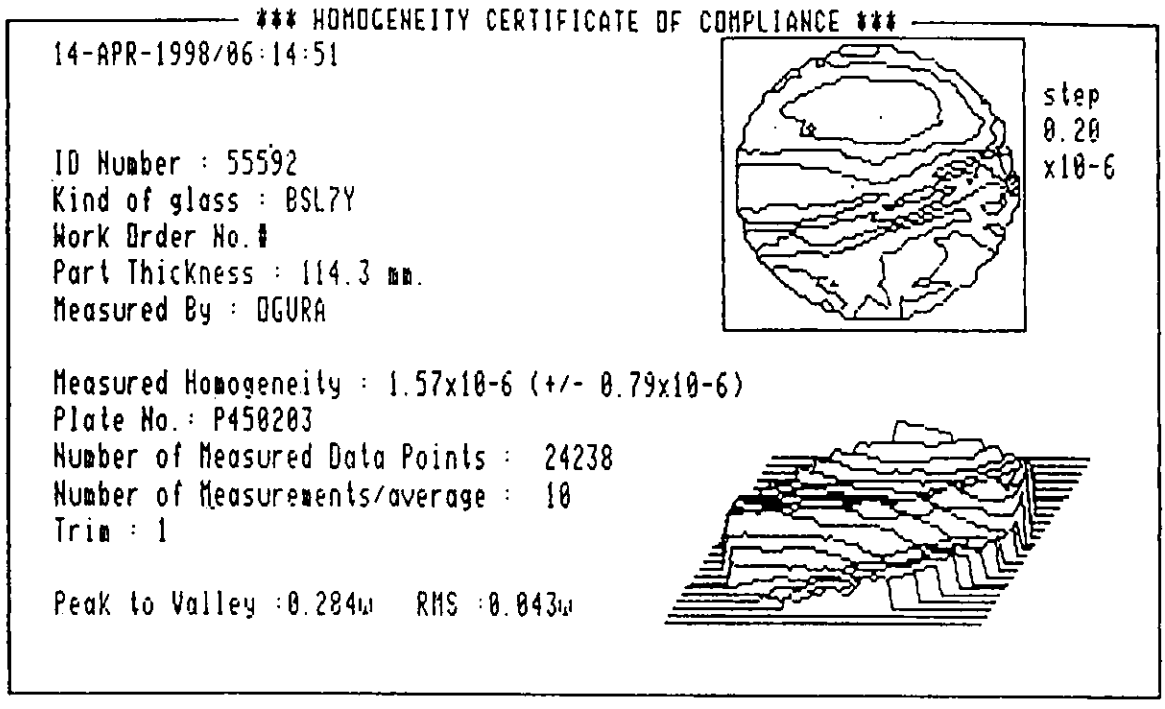

Figure 6-2. The test results of homogeneity of disc shaped glass material for the first lens after having polished both surfaces (2)

Polishing of spherical surfaces was done using the standard spherical surfaces. At the final stage, we checked the surfaces using Zygo interferometer if it was possible to do it. For a convex surface, it was not possible to see the entire surface at one time. So, we used the interferometer to see a part of it and repeated the process until we check the entire surface. The check of the first lens with the interferometer was made at the time of assembly when the lens was within the lens tube because it was difficult to hold the lens at the interferometer at the time of fabrication.

As examples, Figure 6-4 and 6-5 show the results of measurement of the concave surface of the first and the second lenses with the Zygo interferometer. Interferometer test was not done for the convex surface of the first and the third lenses, concave surface of the fourth lens, and aspheric surfaces.

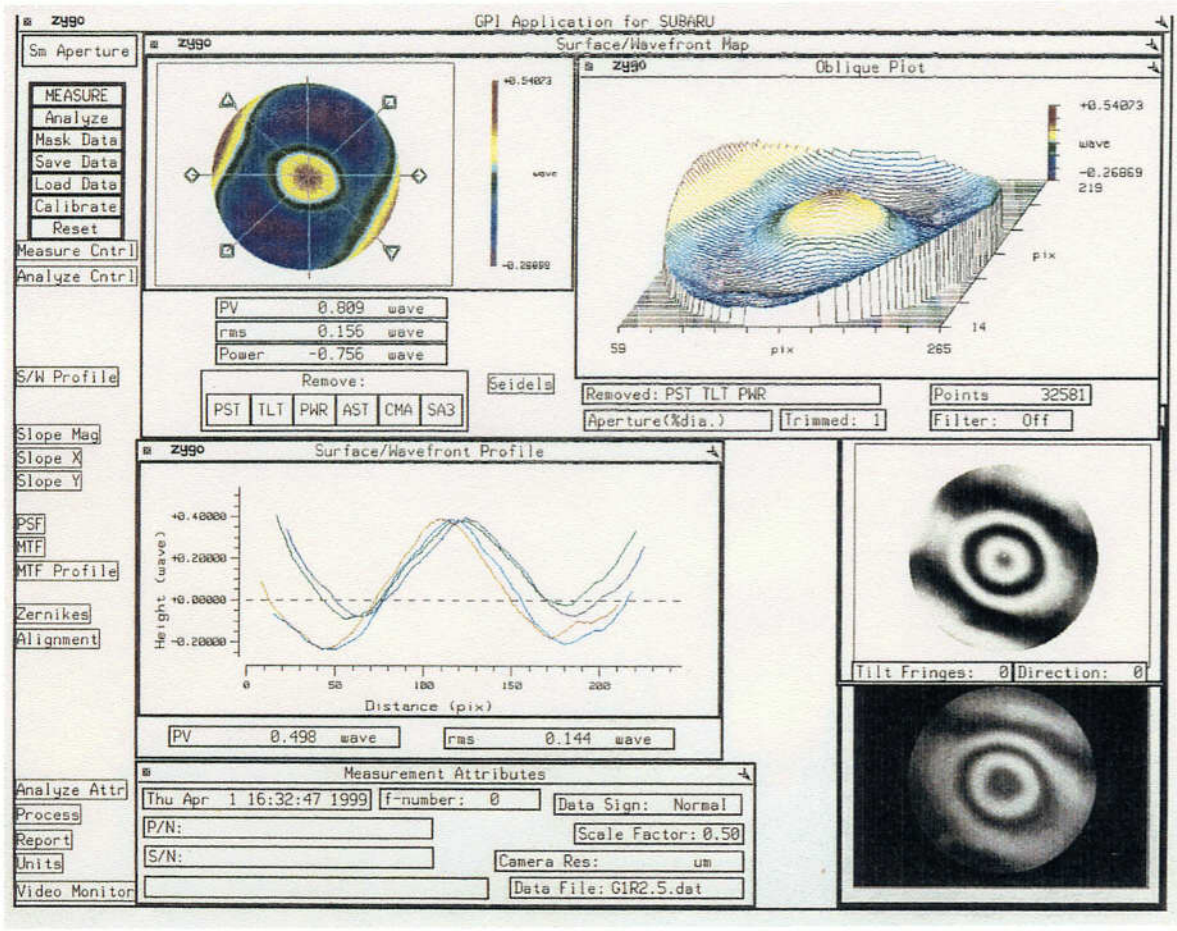

Figure 6-4. The results of measurement of the concave surface of the first lens with the Zygo interferometer

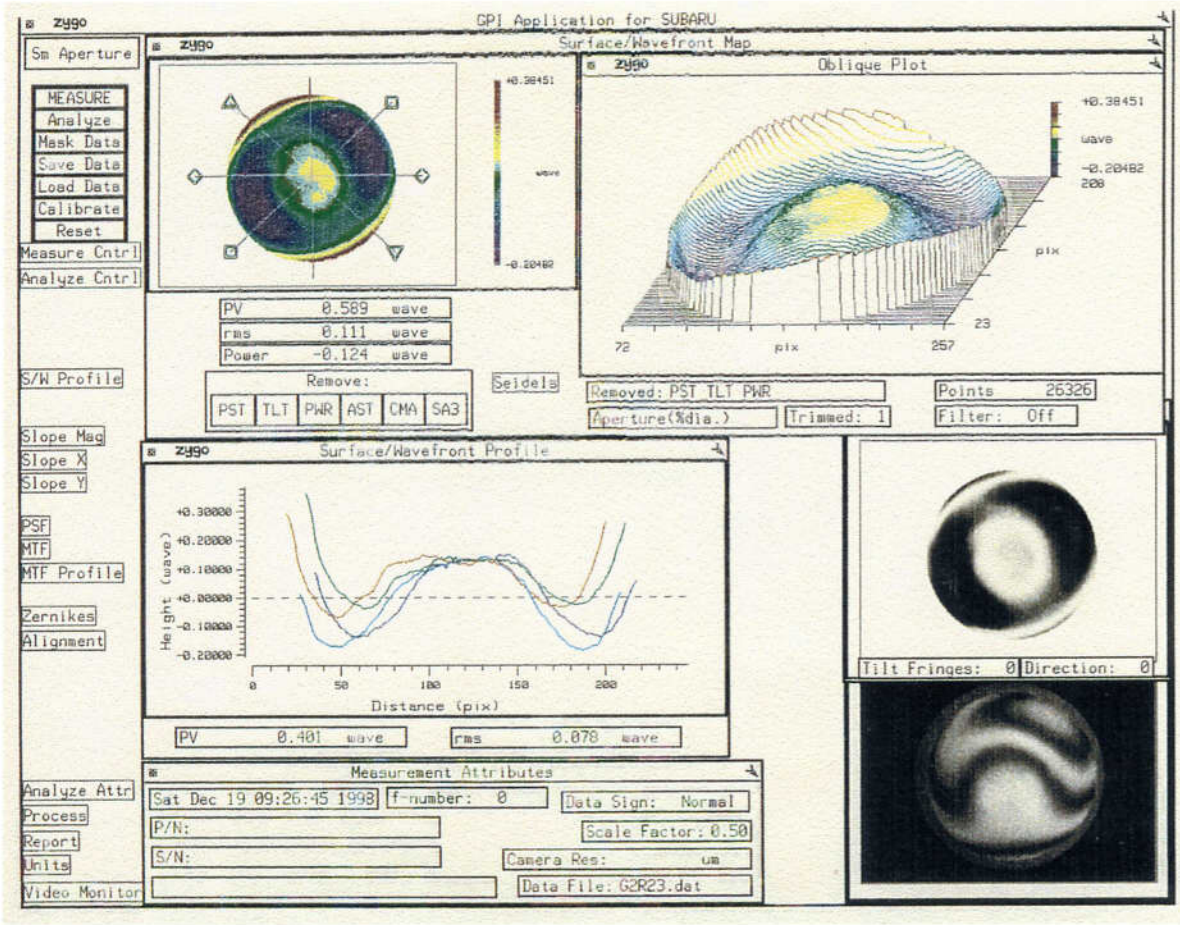

Figure 6-5. The results of measurement of the concave surface of the second lens with the Zygo interferometer

Fabrication and measurement of aspheric surface were done with CSSP(Canon Super-Smooth Polisher)(Ando 1992, Negishi 1994) that was developed within Canon, inc. Specification was 2 arc second and 3 arc second by slope error for the first surface of second lens and the second surface of the sixth lens, respectively. We stopped fabrication when we achieved the specification for 96% and 97% by area. Figure 6-6 shows a photo and a schematic of CSSP. Figures 6-7 and 6-8 show the results of measurement with CSSP for the aspheric surfaces of the second and the sixth lens, respectively.

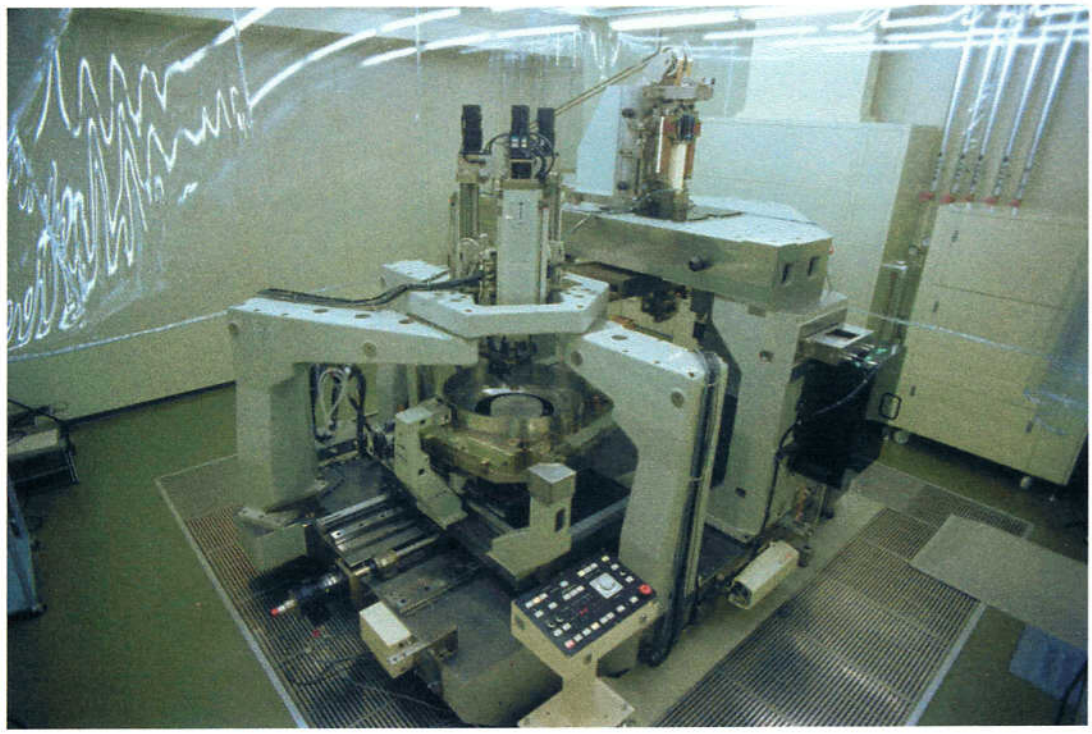

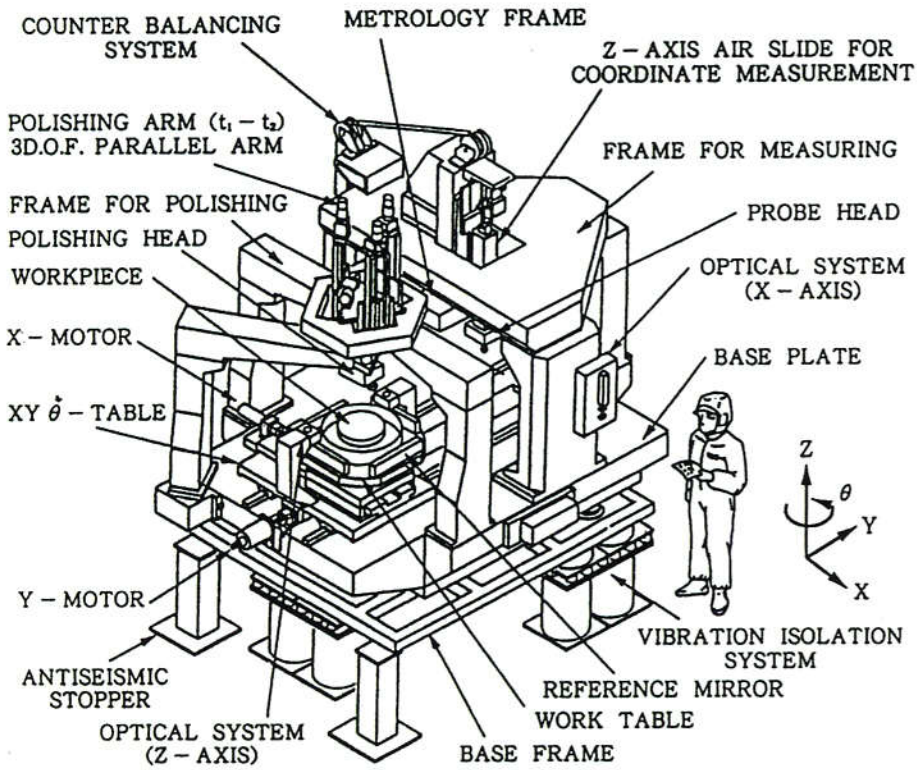

Figure 6-6. A photo and a schematic of the CSSP (Canon Super-Smooth Polisher) (Ando et al. 1992)

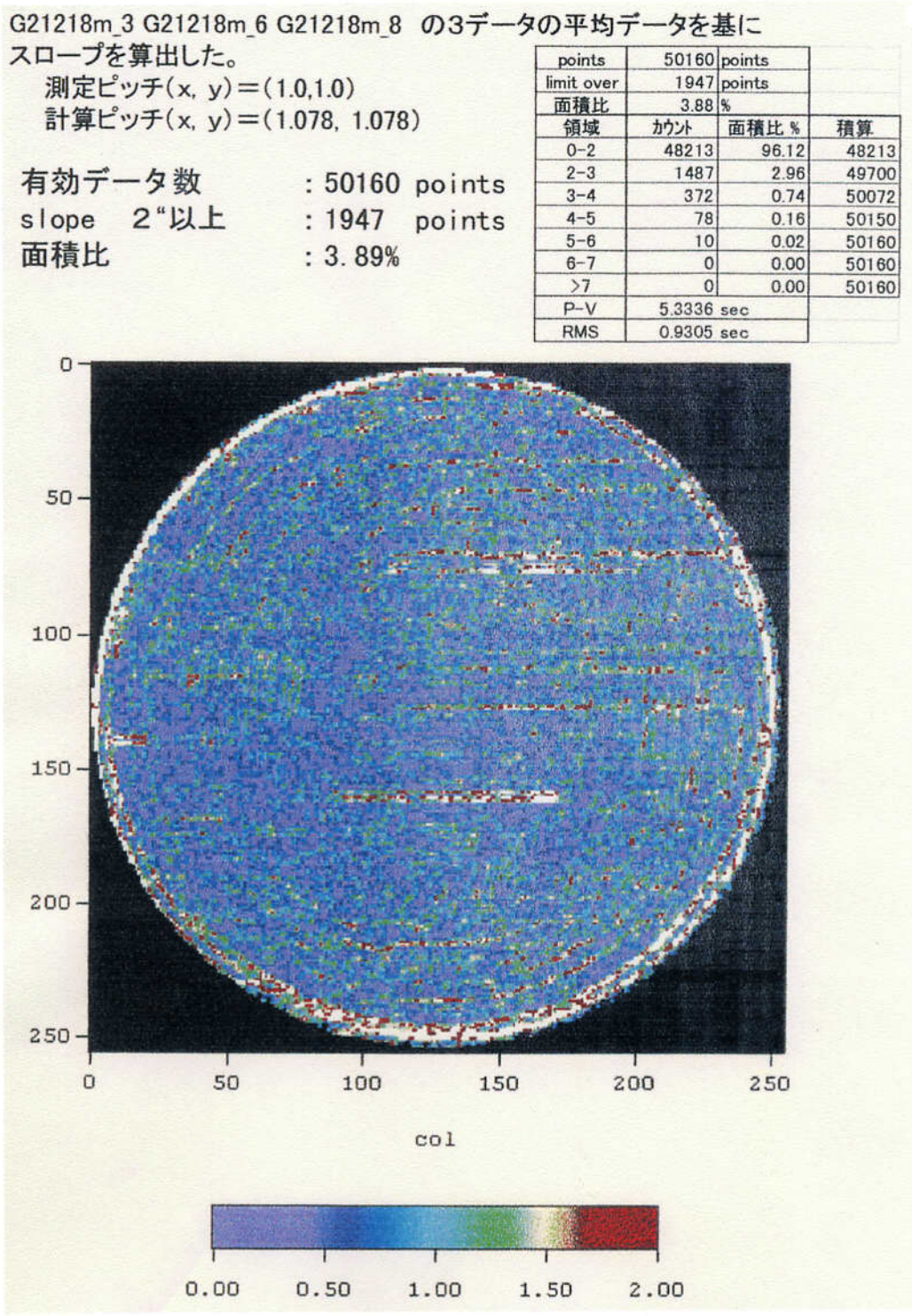

Figure 6-7. The results of measurement with CSSP for the aspheric surfaces of the second lens

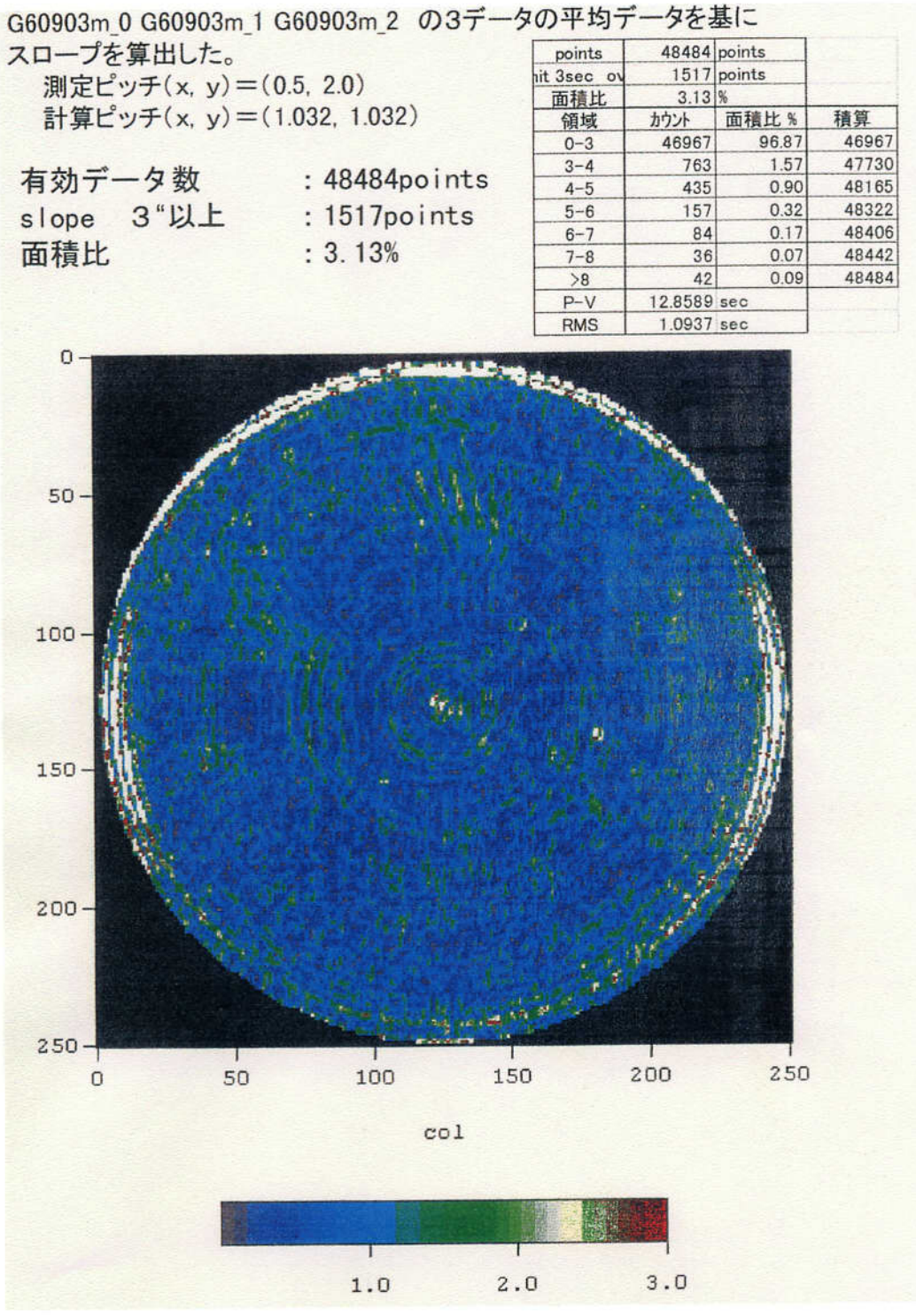

Figure 6-8. The results of measurement with CSSP for the aspheric surfaces of the sixth lens

Table 6-3 shows the thickness and its allowance in the fabrication drawing and the finished thickness. All the finished values are within the allowances, but it was judged to make adjustment of the distance between lenses.

Lens no.	Thickness in drawing	Allowance	Finished thickness
1	56	±0.1	55.94
2	16	±0.3	15.856
3	26	±0.2	25.77
4	14	±0.2	13.962
5	15	±0.1	14.99
6	30.29	±0.2	30.451
7	48.02	±0.2	48.083

Table 6-3. The thickness and its allowance in the fabrication drawing and the finished thickness

As the material for the lens tube, titanium material Ti-6Al-4V was used because its thermal expansion coefficient is close to glass and because it allows precise processing. It is alloy of titanium containing 6% of aluminum and 4% of vanadium by mass and is used in many ways. Figure 6-9 shows cross section of lens in the lens tube.

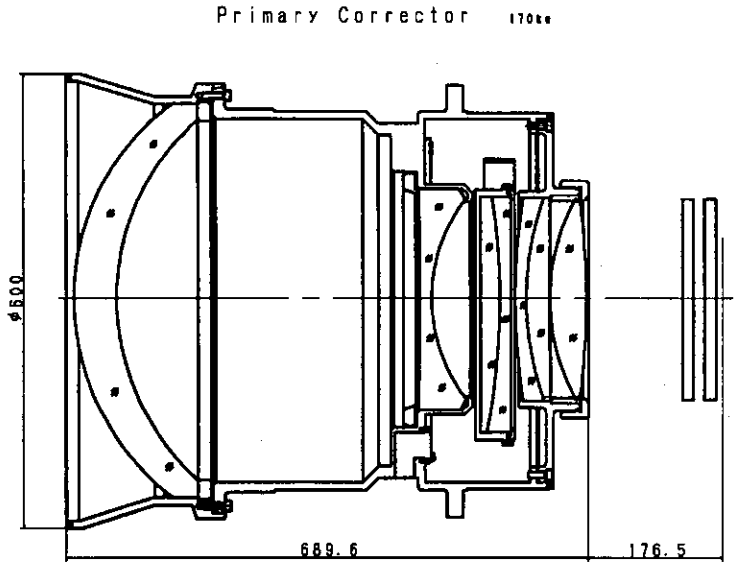

Figure 6-9. Cross section of lens in the lens tube

The inner diameter of the part of the lens tube where a lens fits in and the part that fixes the distance between lenses were based on the outer diameter and thickness of the finished lens and melt-data. As the assembly is done at the room temperature but the lens is used at lower temperature, clearance between lens and tube was set to be between 40 and 50 μm. The parts that decided distances between lenses were fabricated so that the effects on the aberrations due to differences between the design values and the final values are corrected.

When assembling lenses into the tube, we put stopper rings watching the lens surface through Zygo interferometer so that distortion of surface is minimum and then fixed them with bonding agent. Distance between lenses were measured and checked during assembly work. Table 6-4 shows the fabrication optical data of the primary corrector with melt-data and distances between lenses measured during assembly.

k	ea	r	d	Glass	n_e	$n_{(0.4)}$	$n_{(1.0)}$
1	8200	*30000	14207.88		1	1	1
2	506.8	326.76	55.94	(BSL7Y)	1.518880	1.53097	1.50770
3	467	319.65	398.5995		1	1	1
4	275	*-4475.19983	15.856	(BSL7Y)	1.51854	1.53062	1.50736
5	251.4	213.36	65.111		1	1	1
6	(337)	0	25.77	(PBM5)	1.60743	1.63341	1.58775
7	(337)	-897.65	13.962	(BSM51Y)	1.605811	1.62094	1.59239
8	(337)	0	5.4995		1	1	1
9	258.6	825.93	14.99	(PBM2Y)	1.624213	1.65236	1.60319
10	257.2	391.195	30.451	(BSL7Y)	1.518550	1.53062	1.50736
11	257.2	*5355.97529	0.836		1	1	1
12	257.3	268.24	48.083	(S-FPL51)	1.498524	1.50774	1.49027
13	254.5	-1098.3	125.50955		1	1	1
14	filter	0	15	SiO_2	1.460280	1.47032	1.45056
15		0	14.5		1	1	1
16	window	0	15	SiO_2	1.460280	1.47032	1.45056
17		0	10		1	1	1
18	image	0					

Aspheric constant

k	r	e^2	B	C	D	D'	E
1	30000	1.00835					
4	-4475.19983		3.38267E-9	-8.36303E-14	2.03782E-18	-1.33838E-20	3.49307E-23
11	5355.97529		1.30769E-9	-5.38888E-14	-6.67037E-18	6.94170E-20	-2.28747E-22

$$x = \frac{h^2/r}{1+\sqrt{1-(1-e^2)(h/r)^2}} + Bh^4 + Ch^6 + Dh^8 + D'h^9 + Eh^{10}, \quad h = \sqrt{y^2+z^2}$$

$EFL_{(c)}$ = 15317.899

Table 6-4. The fabrication optical data of the primary corrector for Subaru telescope with melt-data and distances between lenses measured during assembly

Figure 6-10 shows the aberration diagram, Figure 6-11 through 6-13 the spot diagram, and Figure 6-14 through 6-19 the radial energy based on the fabrication data.

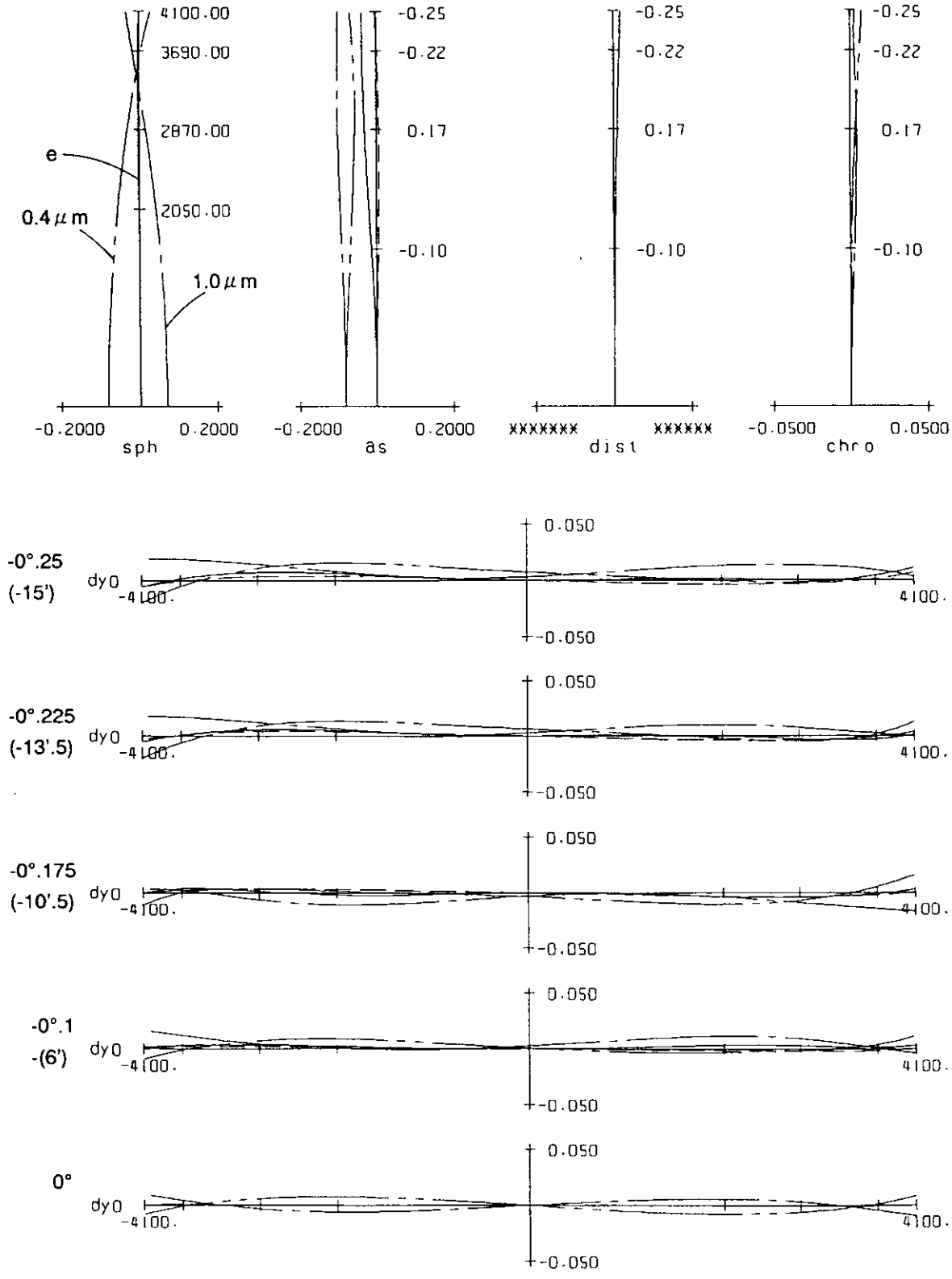

Figure 6-10. The aberration diagram based on the fabrication data, zenith distance 0º

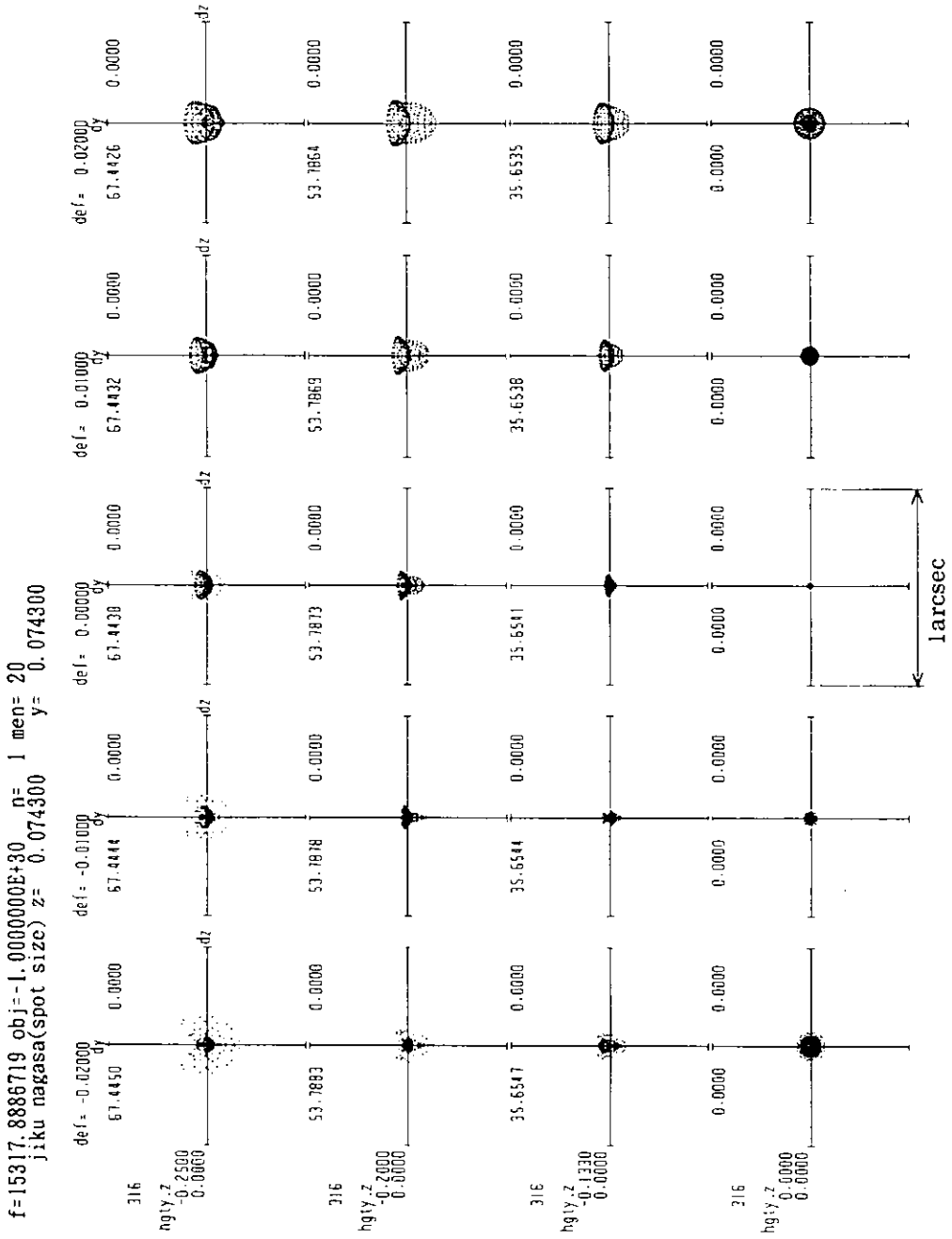

Figure6-11. The spot diagram based on the fabrication data, zenith distance 0º, wavelength 0.5461 μm

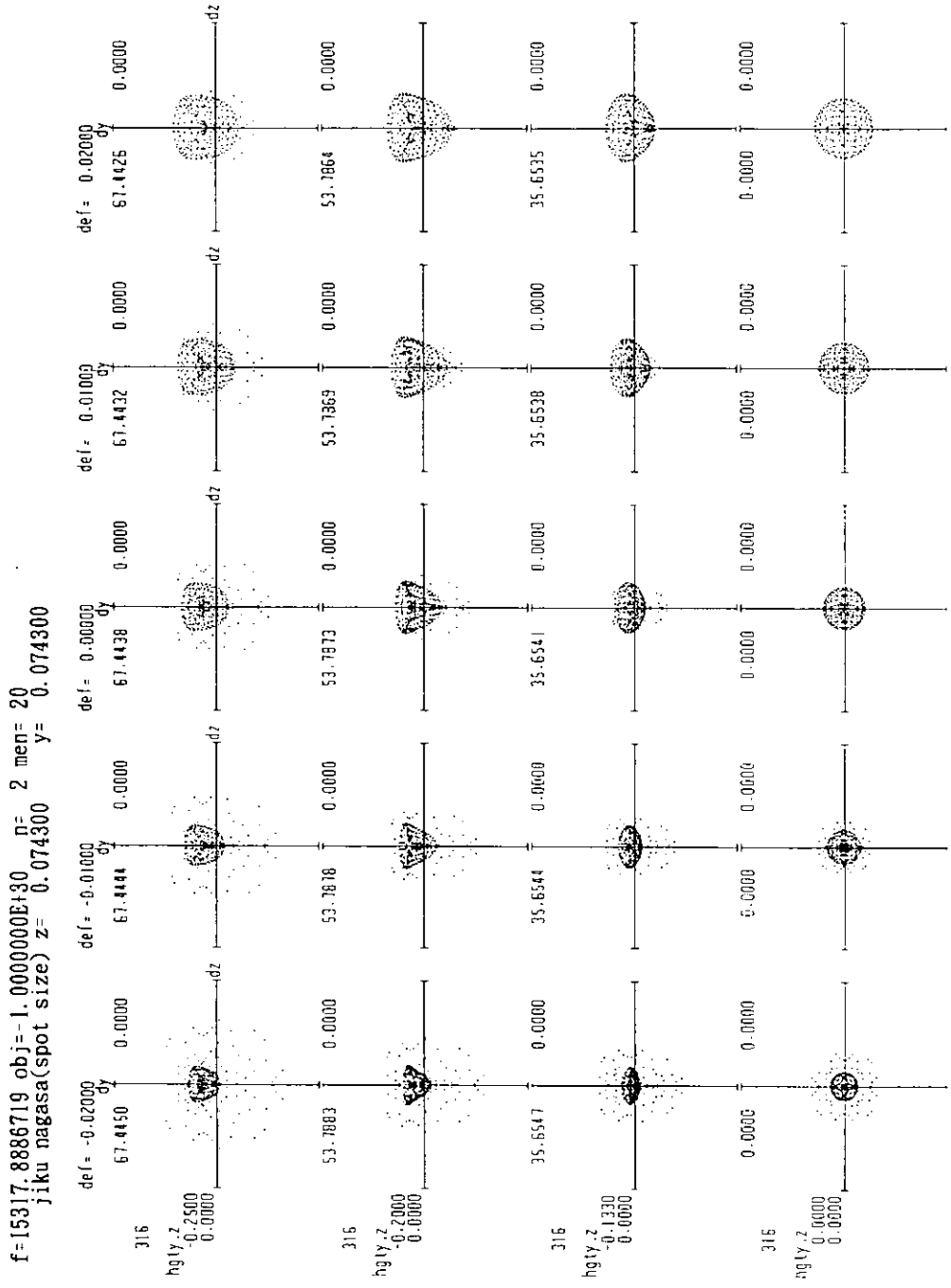

Figure 6-12. The spot diagram based on the fabrication data, zenith distance 0º, wavelength 0.4 μ m

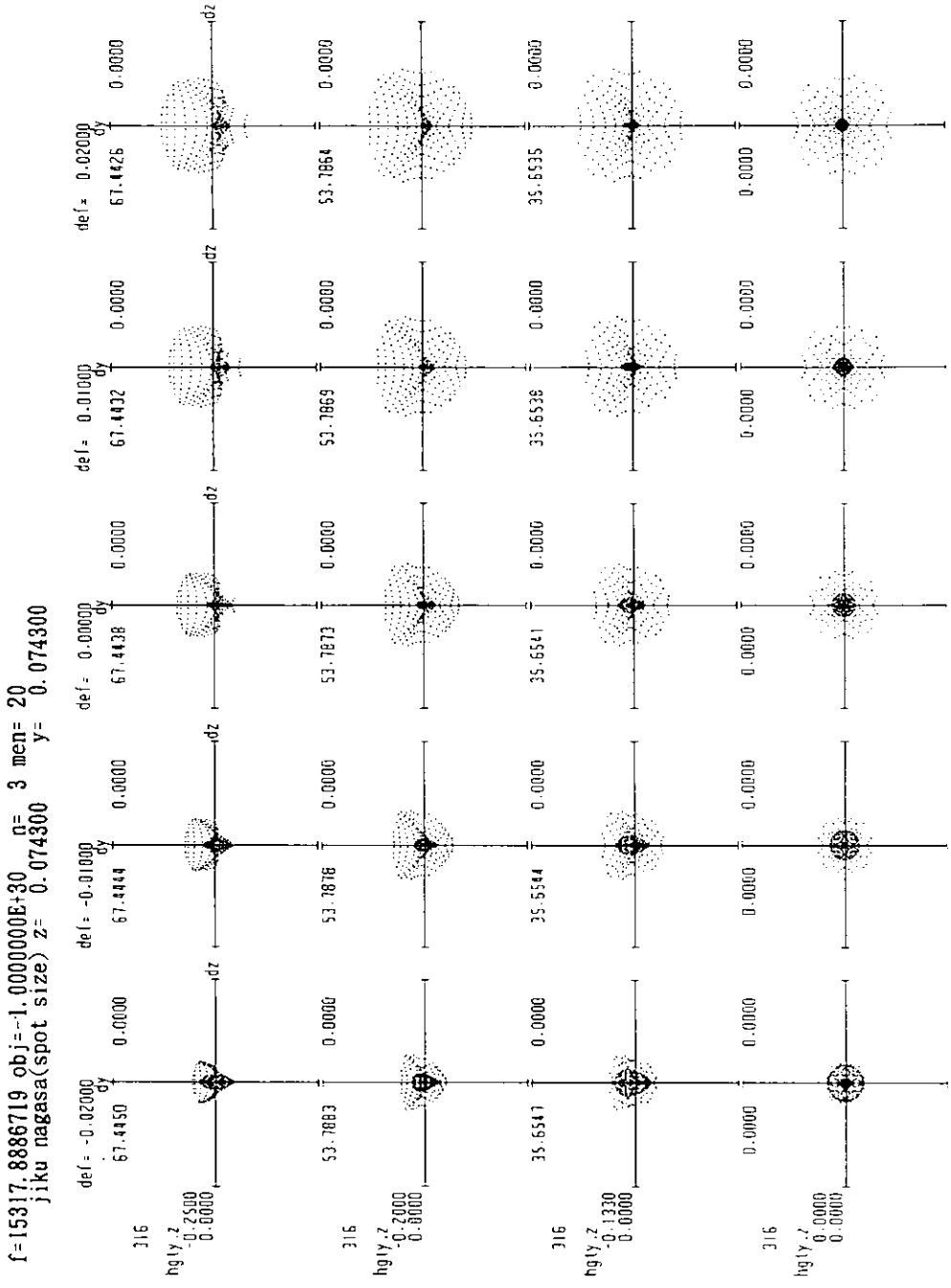

Figure 6-13. The spot diagram based on the fabrication data, zenith distance 0º, wavelength 1.0 μm

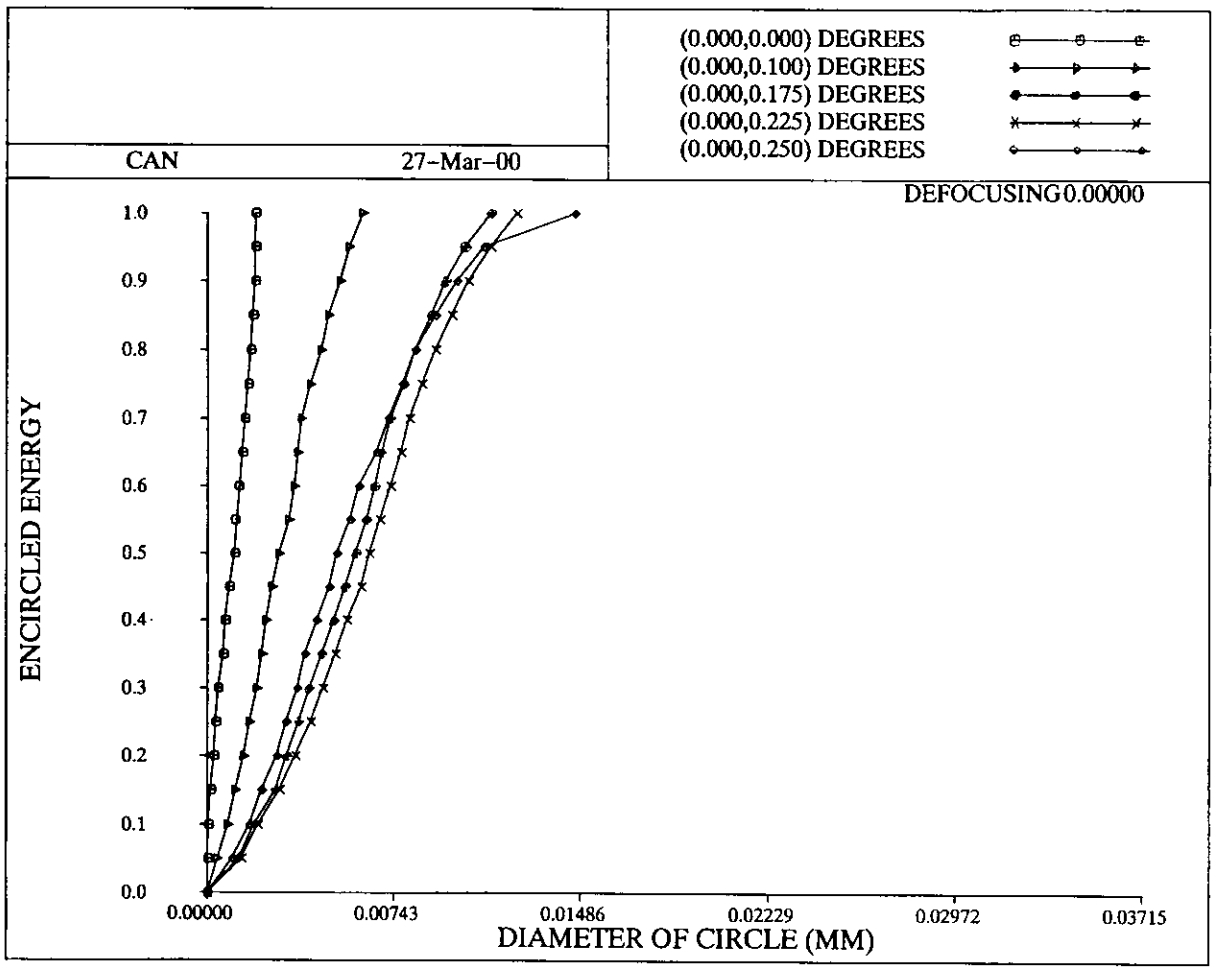

Figure 6-14. The radial energy based on the fabrication data, zenith distance 0º, wavelength 0.5461 μm

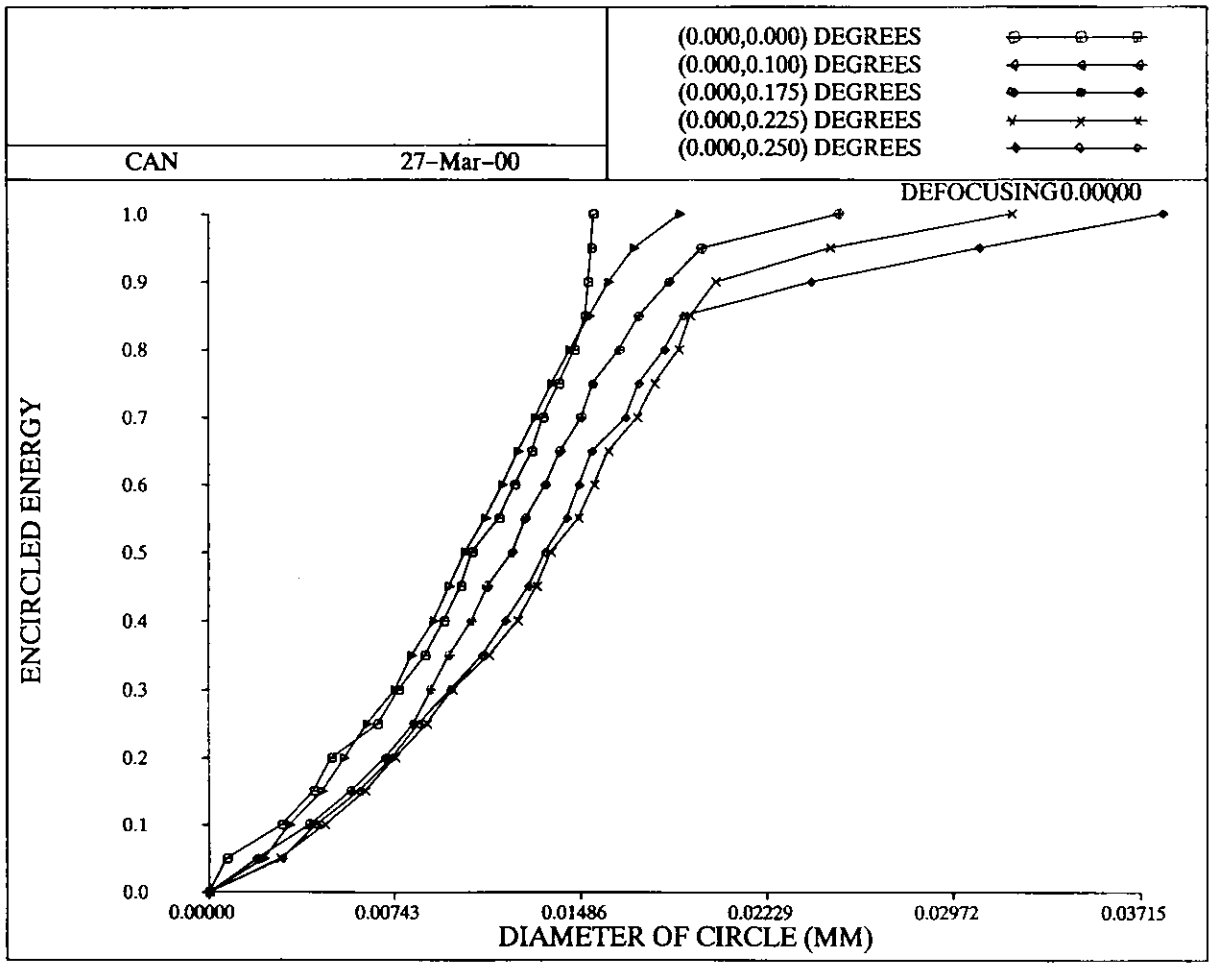

Figure 6-15. The radial energy based on the fabrication data, zenith distance 0°, wavelength 0.4 μm

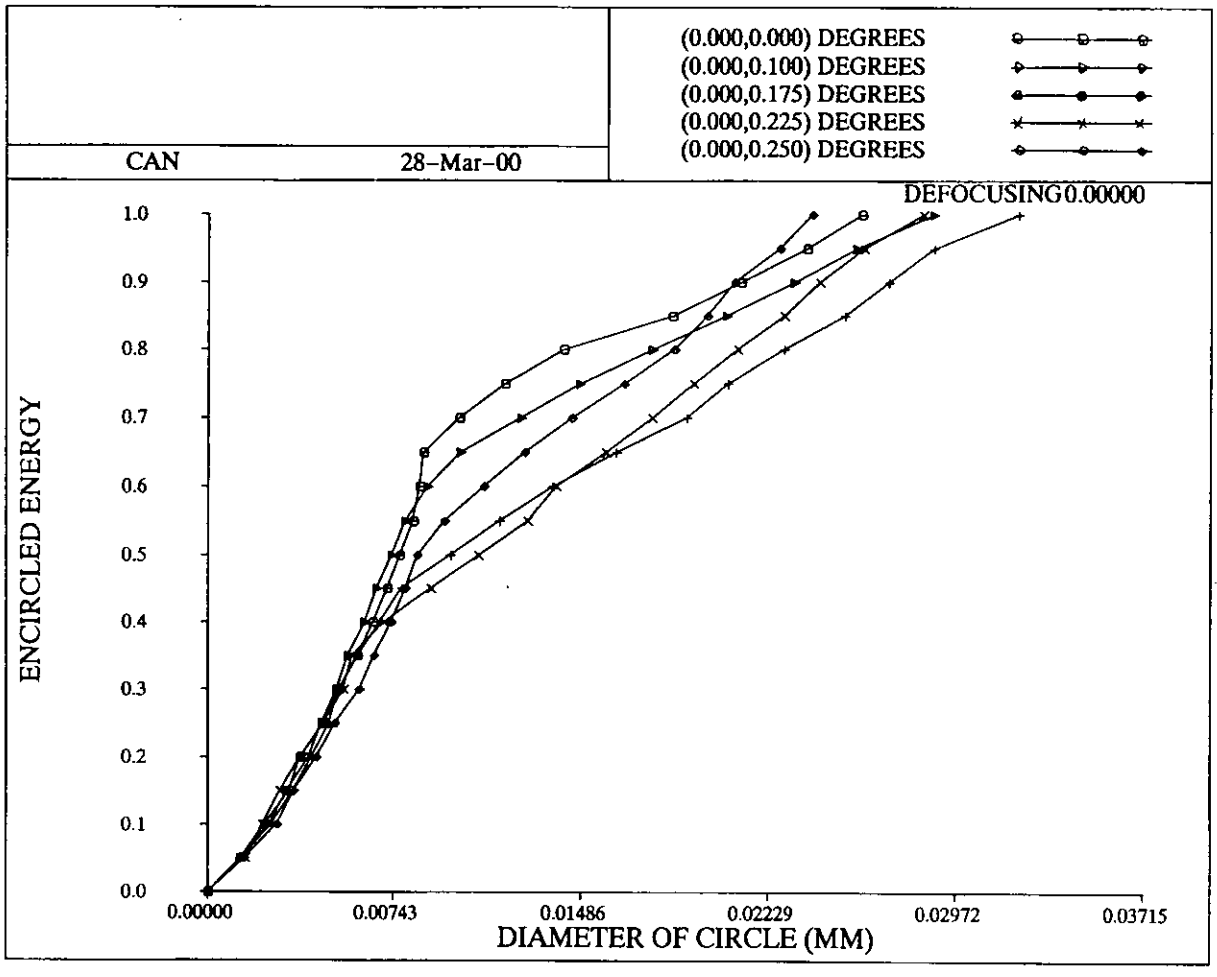

Figure 6-16. The radial energy based on the fabrication data, zenith distance 0º, wavelength 1.0 μm

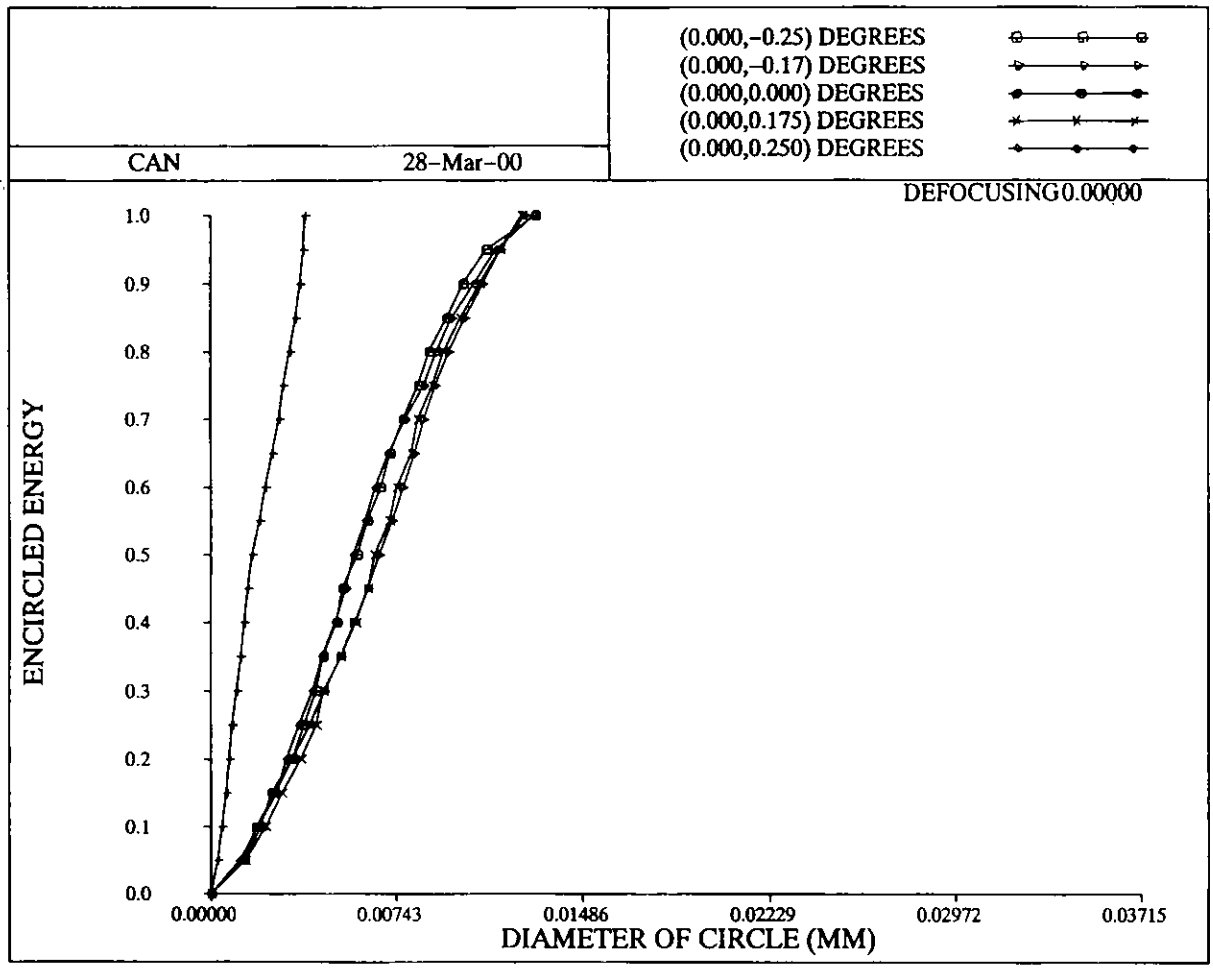

Figure 6-17. The radial energy based on the fabrication data zenith distance 60º, wavelength 0.5461 μm

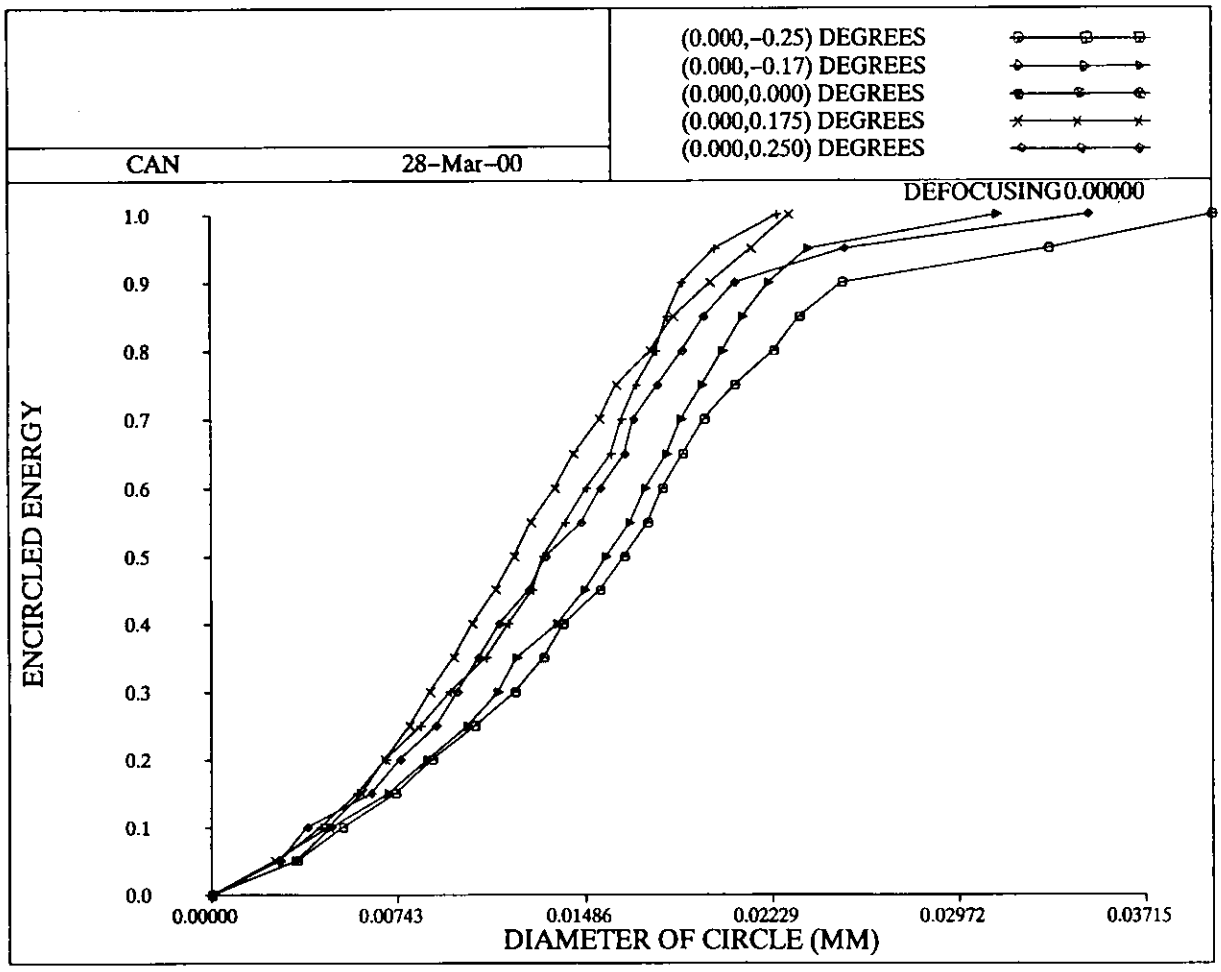

Figure 6-18. The radial energy based on the fabrication data zenith distance 60º, wavelength 0.4 μm

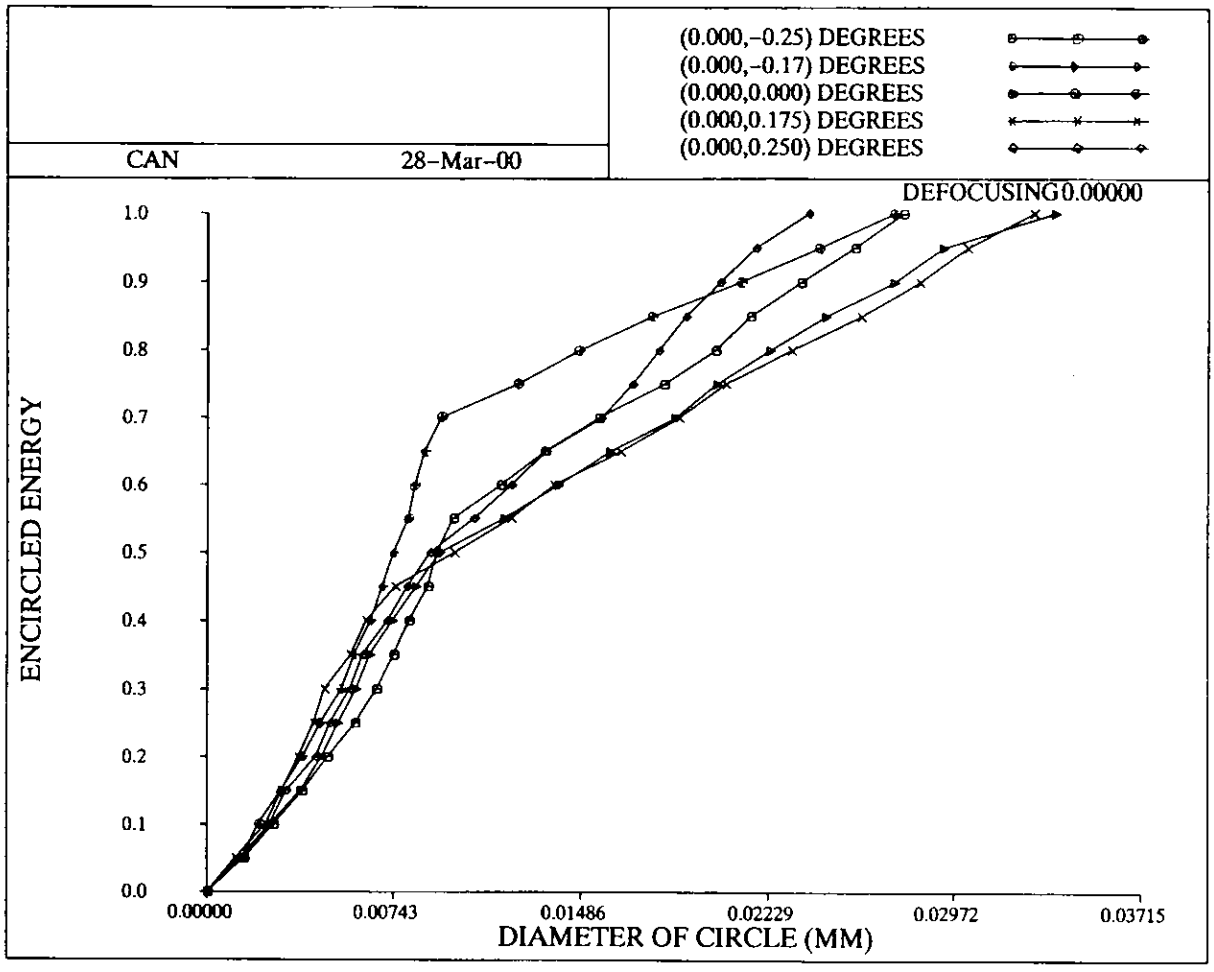

Figure 6-19. The radial energy based on the fabrication data zenith distance 60º, wavelength 1.0 μm

7. Null Lens Test

It is difficult to test the imaging performance of the assembled primary corrector because it is not an imaging system by itself. Its final evaluation will be done only after it is installed into the telescope and works with the primary mirror. As the manufacturer of the corrector, we used a concave spherical mirror and a null lens to make two tests. In the first test, we tested the imaging performance of the central part of the image field. In the second test, we checked the entire lens system.

The null lens for the test of the central part of the imaging field was designed in the following way. A point light source is placed at the position of the focal point of the corrector when used with the main mirror. On the other side of the corrector, we put a concave spherical mirror that reflects light back into the corrector. The position of the concave mirror is so determined that the paraxial position of the light source and the image coincide. This procedure puts the center of curvature of the concave mirror at the focus of the telescope mirror only. If the corrector is one for a parabolic main mirror, this procedure gives aberration free image on the optical axis. As the corrector is made for a hyperbolic mirror, the on-axis image has spherical aberration. Its amount is double the spherical aberration of the hyperbolic main mirror because the light in this test passes the corrector twice. We put a null lens between the light source and the corrector in order to remove this aberration. The null lens was composed of a concave lens and a convex lens and was placed that the pupil of the entire optical system falls at the position of the reference sphere of the interferometer. Figure 7-1 shows ray paths and residual wave aberration of the designed null lens for the central part of the imaging field.

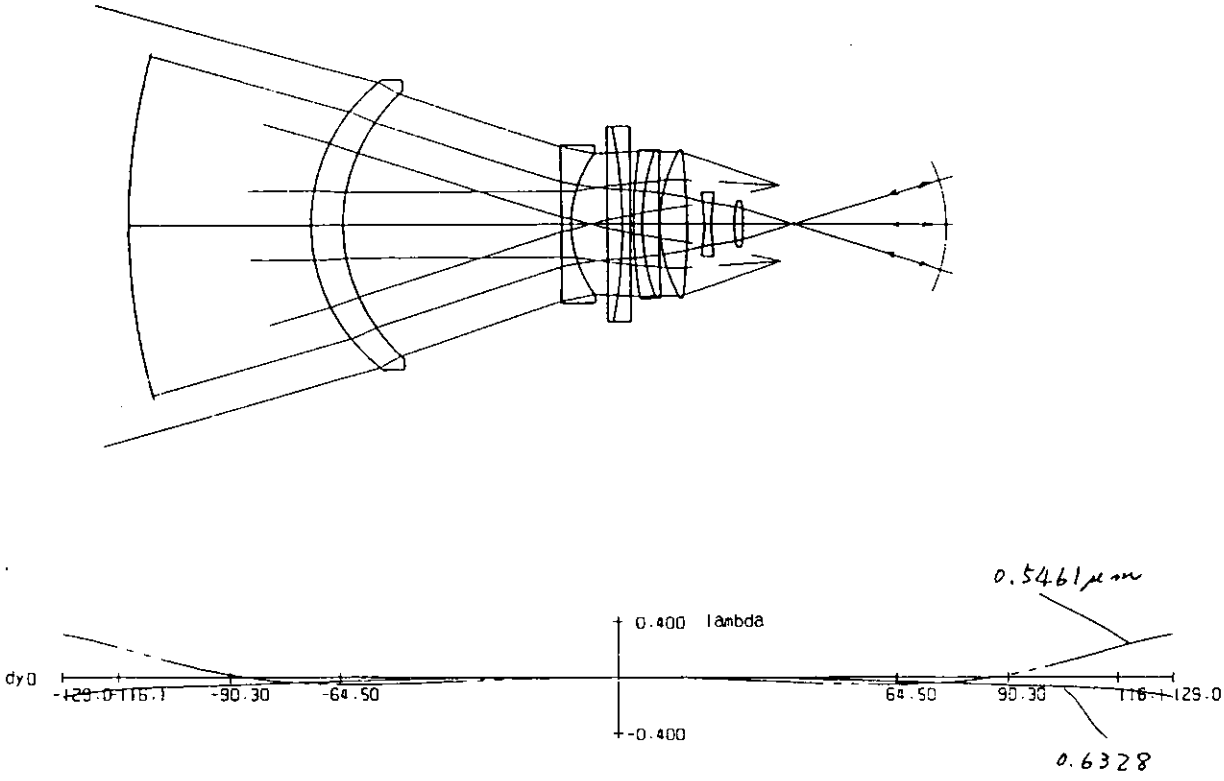

Figure 7-1. Ray paths and residual wave aberration of the designed null lens for the central part of the imaging field

The null lens for the entire lens system was designed in the following way. We choose the outermost ray among the rays that make an image at the edge of the field. A point light source was placed at a point where the two such outermost rays cross. The concave spherical mirror is placed so that the image falls at the same position as the light source. Then, a null lens was placed between the light source and the corrector as in the first test. In this test, we use rays that are quite different from the actual imaging rays. But this test allowed us to check the entire corrector system with the interferometer. Figure 7-2 shows ray paths and residual wave aberration of the designed null lens for the entire lens system.

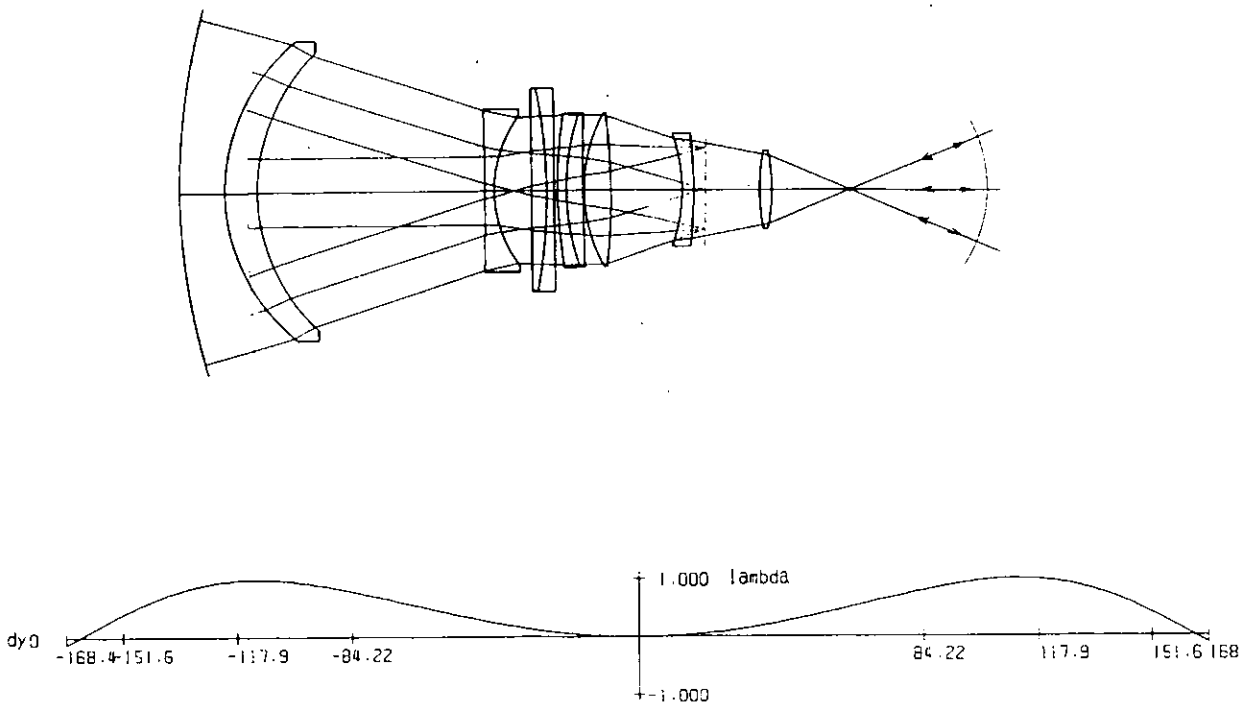

Figure 7-2. Ray paths and residual wave aberration of the designed null lens for the entire lens system

We used the melt data of the glass material and the thickness of processed lenses to modify the distance between the null lens and the primary focus corrector and the distance between two lenses in the null lens, then, the null lens was assembled. The diameter and the radius of curvature of the concave spherical mirror was determined to be 650 mm and 1123.7 mm, respectively, as the mirror was to be used in the both tests. Its thickness at the center was 95 mm. Figure 7-3 shows the result of measurement of the concave spherical mirror with the Zygo interferometer.

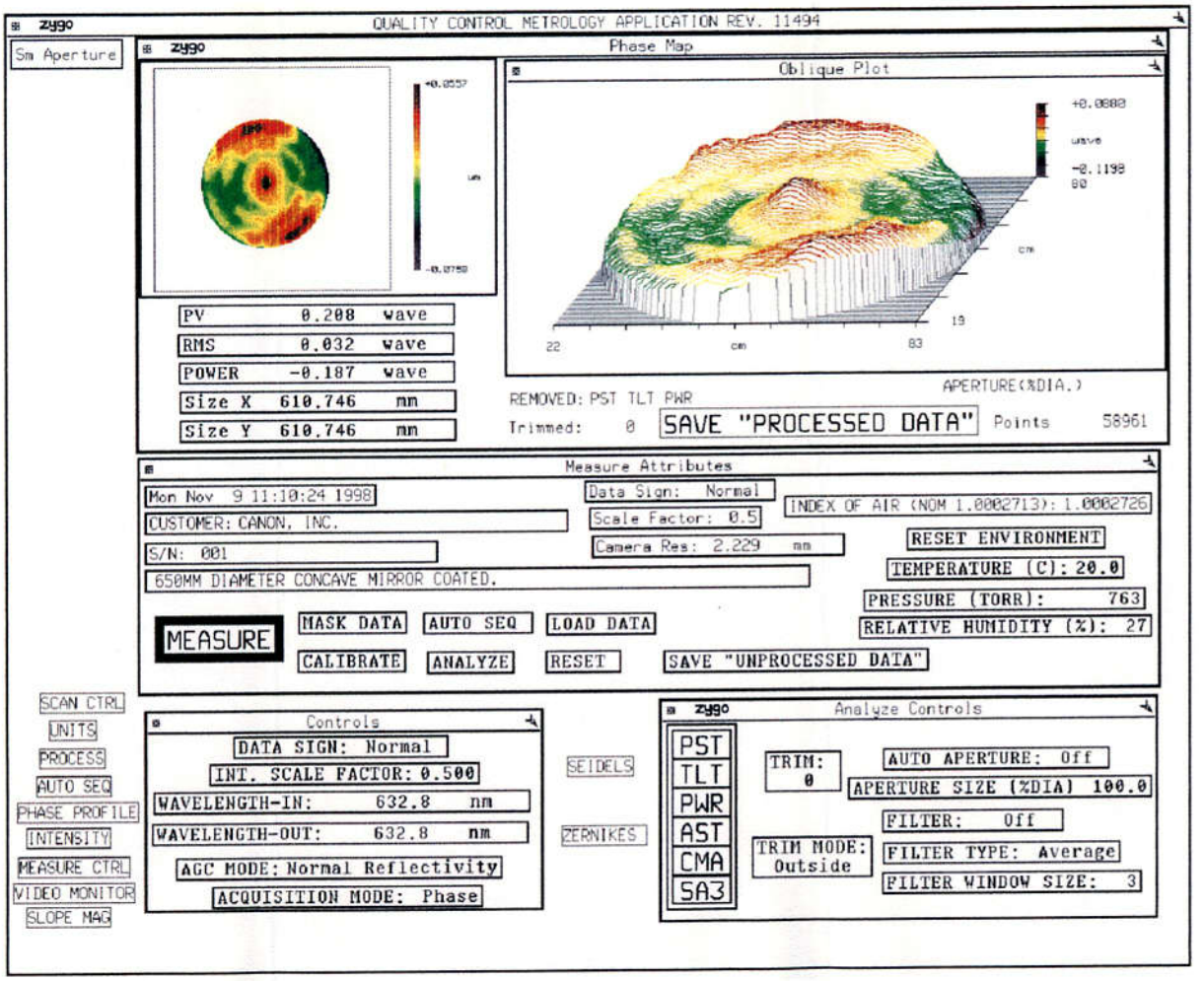

Figure 7-3. The result of measurement of the concave spherical mirror with the Zygo interferometer

A tool with a pinhole of 1.5 mm ϕ that places the pinhole at the imaging point of the primary focus corrector was made and was fixed to the corrector. A microscope with an on-axis lighting device was then put on a stage and was set so that its focal point coincides with the center of the pinhole of the tool. Then, the concave mirror was set so that it is at the right relative position with respect to the corrector. After these procedures, the concave mirror and the pinhole are placed at the correct positions relative to the corrector. We replaced the microscope with the Zygo interferometer to make measurements of the wave front. 0.6328 μ m line of He-Ne laser was used. Figure 7-4 shows the results of the measurements for the central part of the field. PV (Peak to Valley) was 0.825 wave and rms (root mean square) was 0.145 wave. The radius corresponding to 80 percent encircled energy calculated with the software that is a art of the Zygo interferometer was 3.05 μ m. This corresponds to 0.082 second of arc at the primary focus of the telescope.

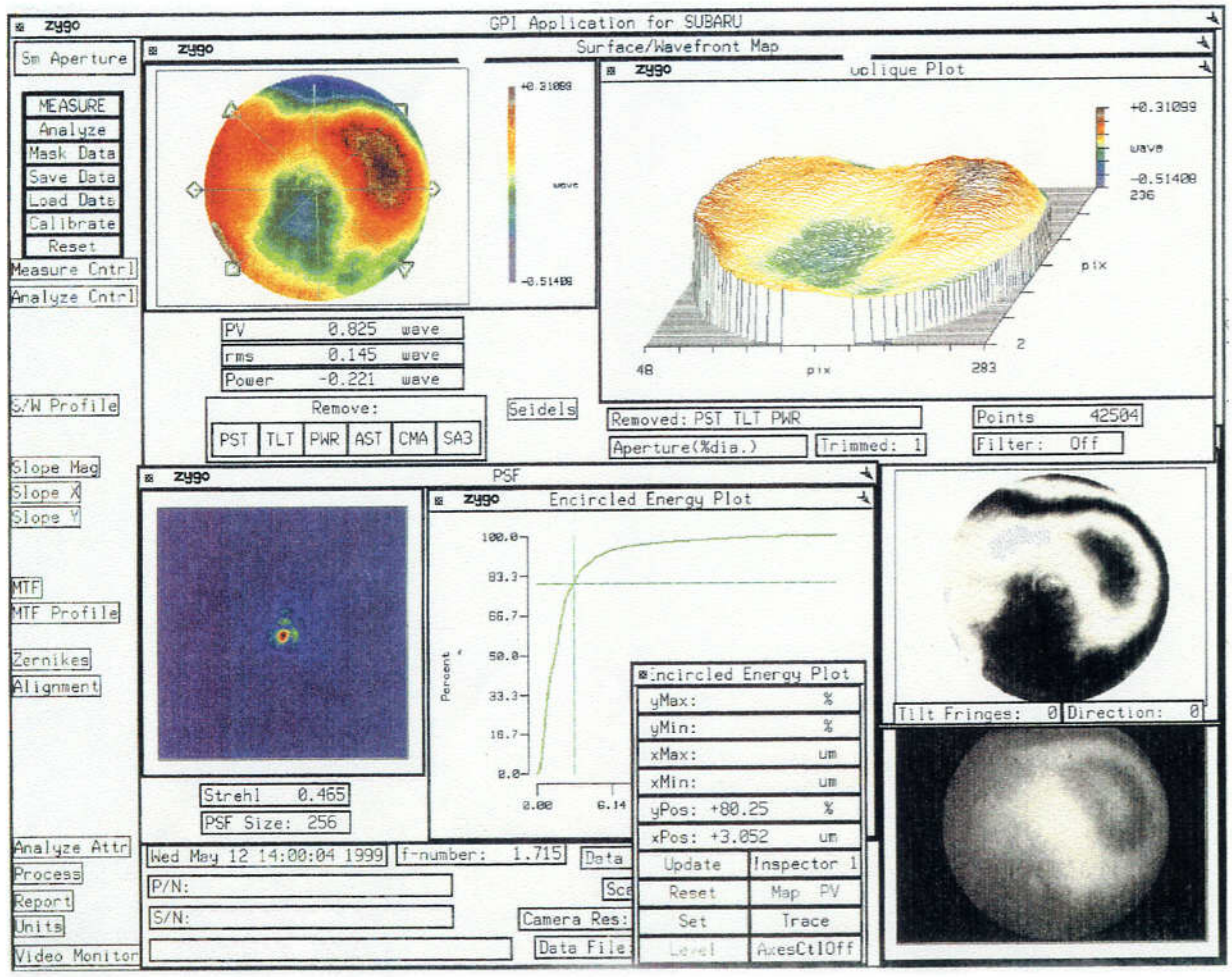

Figure 7-4. The results of the measurements for the central part of the field

PV (Peak to Valley) was 0.825 wave and rms (root mean square) was 0.145 wave. The radius corresponding to 80 percent encircled energy calculated with the software that is a art of the Zygo interferometer was 3.05 μm. This corresponds to 0.082 second of arc at the primary focus of the telescope.

We measured the wave front aberration with the ADC at positions corresponding to the altitudes 30 degrees and 43.5 degrees, but no conspicuous differences were perceived.

Figure 7-5 shows the results of the measurements to check the entire lens system with the Zygo interferometer. PV (Peak to Valley) was 1.689 wave and rms (root mean square) was 0.293 wave.

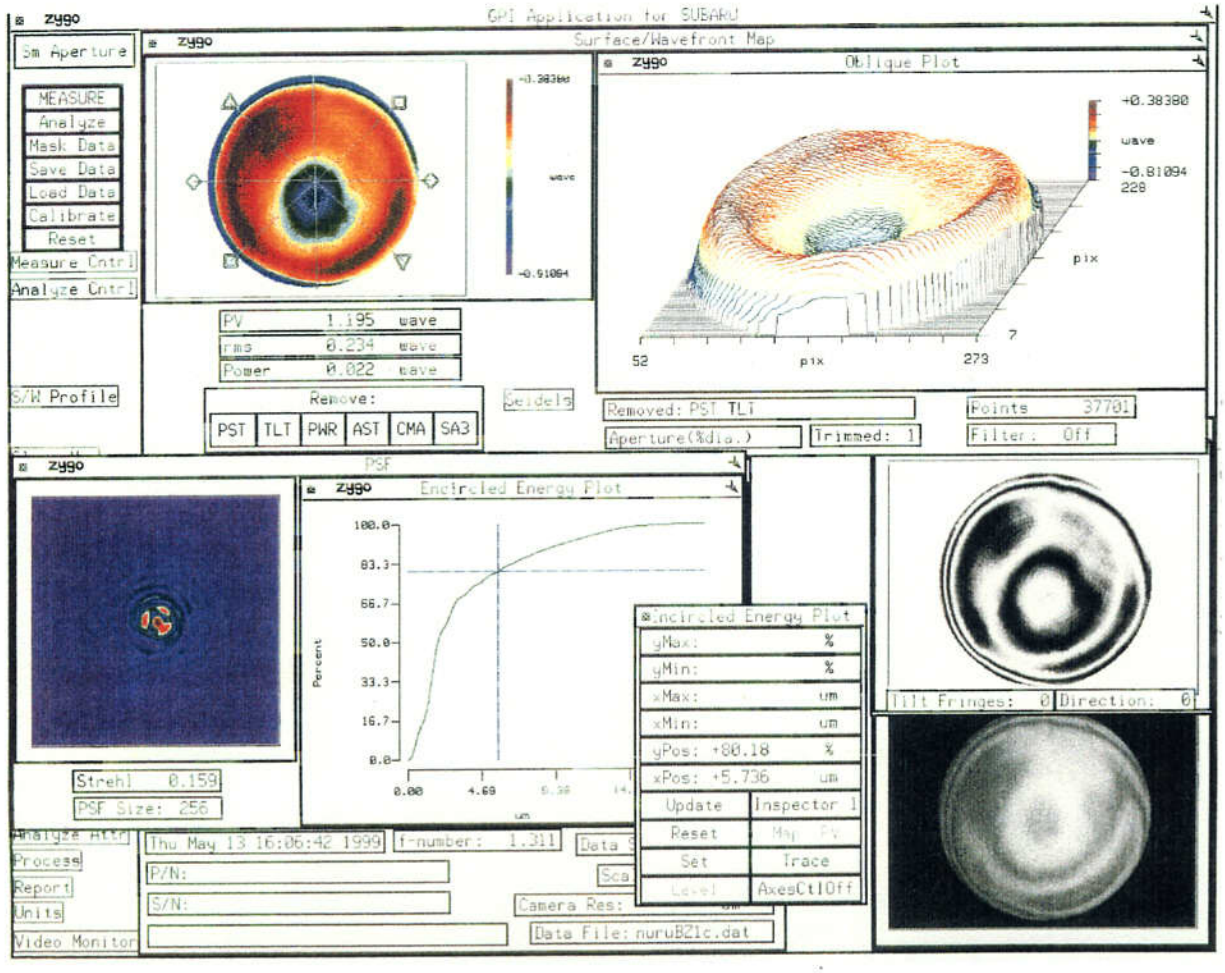

Figure 7-5. The results of the measurements to check the entire lens system with the Zygo interferometer. PV (Peak to Valley) was 1.689 wave and rms (root mean square) was 0.293 wave.

We expected that the latter results would have been a little bit smaller, but we judged that the performance of the entire corrector system was well within the given specification.

8. Performance Test

The first light test observation of the Suprime-Cam was done on July 31, 1999. Extensive tests to align the primary corrector with respect to the primary mirror was carried out in a couple of runs scheduled in 2000. Figure 8-1 shows the defocused images that indicates slightly remaining astigmatism.

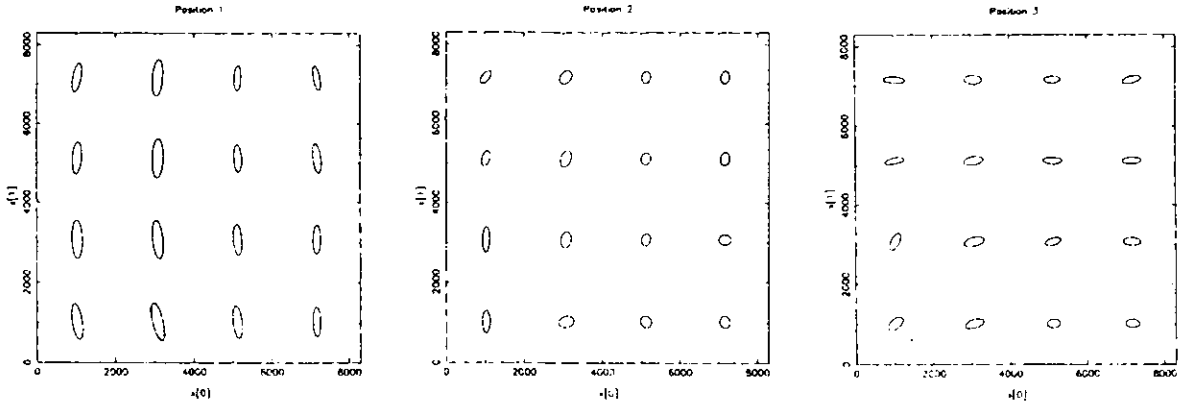

Figure 8-1. Defocused images are shown for three focusing positions with intervals of 0.05 mm. The abscissa and ordinates are the pixel numbers (0-8000). Images are drawn with magnification factor of 200. It is easily seen that these images (prolonged in the vertical direction in the left diagram and prolonged in the horizontal direction in the right diagram) are caused by astigmatism. (Private communication, Miyazaki 1999)

Although the alignment is not yet performed completely, the obtained image of the Suprime-Cam became impressive. Miyazaki(1999) reported, as is shown in Figure 8-2, that the FWHM of stellar image taken under a best seeing was 0.3 arc second at the field center and was better than 0.4 arcsec at the field periphery. Note that these values include the blurring of images by natural seeing. Defocused image (Figure 8-2) show astigmatism. This can be corrected by adjusting the supporting forces of the main mirror.

Photo 3 shows a breathtaking image of a spiral galaxy M63 taken with the Suprime-Cam in June 2000. The final alignment test is scheduled in August 2000. It is important to stress that the optical imaging performance of Suprime-Cam is shown to meet the severe specification.

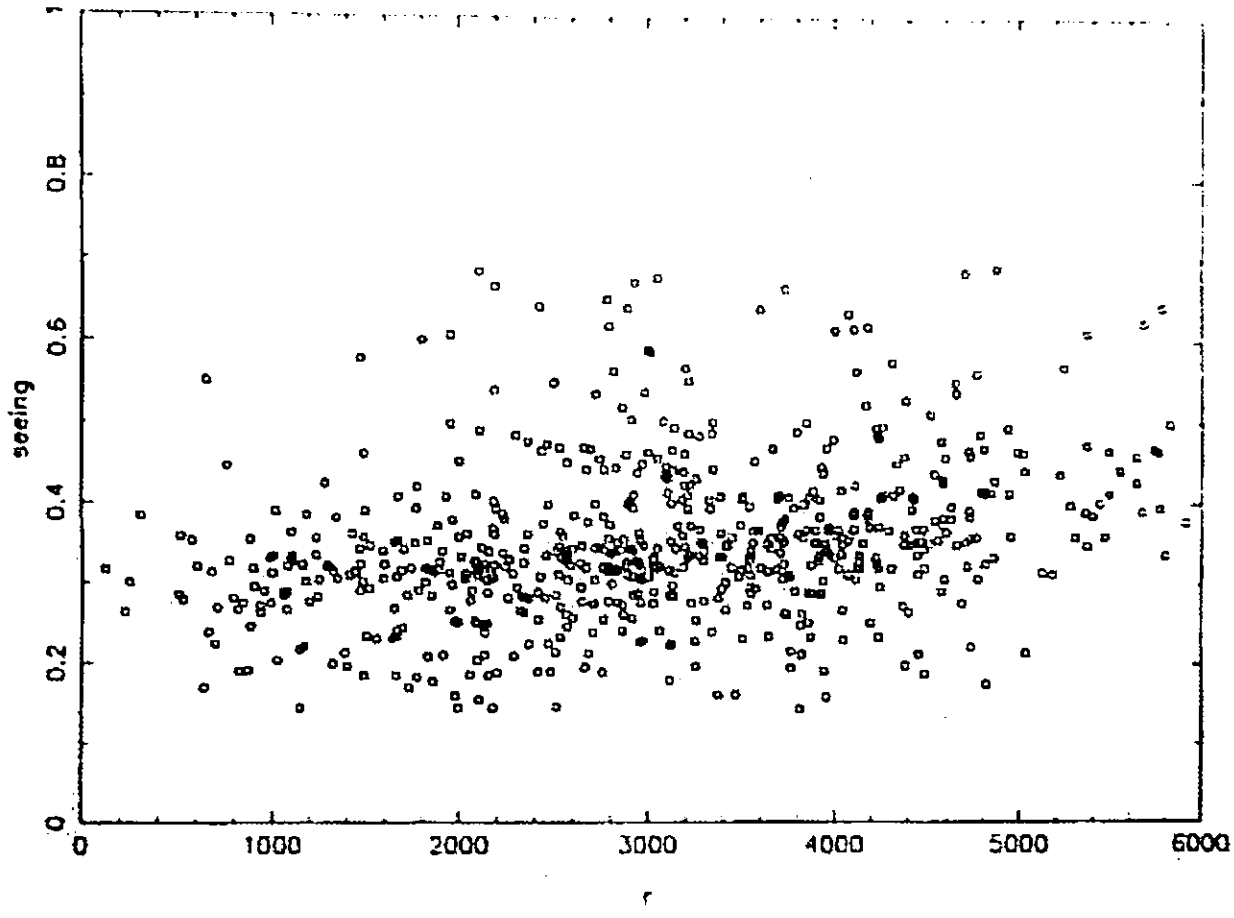

Figure 8-2. FWHM size of stellar images. The abscissa is the pixel number (0-6000) and the ordinate is the seeing size in arcsec. (Private communication, Miyazaki 2000)

9. Summary

Modern eight-meter class large telescopes use large mirrors but require to keep their enclosures that house the telescope as small as possible by keeping the focal length of the main mirror short. Therefore, the aperture ratio of the main mirror of such a telescope is smaller than that of a classical telescope. For example, the F-ratio of the Hale telescope is F/3.3 while that of Subaru telescope is F/1.83. This fact makes it difficult to design a high performance wide field primary corrector. Among the ten new generation telescopes of 8-10m primary mirrors, Subaru was the only exception that took a decision to implement the wide field primary focus.

In the present thesis, we report the successful designing and manufacturing of an unique primary corrector for the 8.2m Subaru Telescope. There are several new features introduced in designing and manufacturing this Primary Corrector.

(1) Usage of ultra-low dispersion glass material FPL51 to compensate chromatic differences of aberrations.

(2) Usage of two aspheric surfaces in the corrector made it possible to assure high imaging performances. Recently developed computer controlled polishing machine enabled polishing complicated aspheric surfaces accurately.

(3) Replacement of two direct vision prisms to a pair of compound lenses to accomplish better optical performance in correcting the atmospheric dispersion and the chromatic difference of aberrations.

(4) Invention of an original method to realize the atmospheric dispersion correction. By the introduction of a pair of compound lenses, it became possible to compensate the atmospheric dispersion by driving a pair of compound lens laterally with respect to the optical axis. This new method made the structure and the driving mechanism simpler than those used in the classical method where a pair of direct vision prisms were employed. Since the dispersion due to the atmospheric diffraction is in the altitude direction, and the Subaru Telescope uses the alt-azimuth mounting, only the shift of the compensating element of the corrector in the altitude direction was necessary.

(5) All the above new features incorporated made the design and the manufacturing of Subaru Primary Corrector with ADC possible.

The Subaru Primary Corrector manufactured based on the optical design reported in the present thesis was installed at the prime focus of the 8.2m Subaru Telescope and it was shown that this Primary Corrector performs perfectly to enable wide field

imaging observation over the wavelength region of 0.4μ-1.0μ at zenith distance 0-60 degrees. The FWHM image size obtained under a good seeing was 0.3 arcsec at its field center and better than 0.4 arcsec at the edge of the field.

10. Acknowledgments

At first, I was quite unfamiliar with astronomy and astronomical observing instruments. I started to study the optical design of primary corrector because of my idea of ADC described in this paper that led to fabrication and test of the entire corrector. My hearty thanks are due to Professor Kyoji Nariai who kindly taught me about the references and gave me design data of his previous studies. He also suggested me to write this paper and encouraged me during the entire period of writing. My thanks are also due to Professor Masanori Iye who taught me about observing instruments, and encouraged me to write this paper, to Dr. Satoshi Miyazaki who made the test observation of the corrector with the Subaru telescope and furnished me with the results that was quite satisfying for the fabricating team, to Ichiro Habe of OHARA INC. who provided us with glass material, Osamu Sakakibara, Noboru Ito, Izumi Mikami, Shinya Kawahara, Tadashi Matsushita, Yutaka Ezaki of MITSUBISHI ELECTRIC CORP. for their help during the fabrication of the primary corrector. In CANON INC, my thanks are first due to late Tetsuya Ara who was my first boss, to Dr. Yoshiya Matsui for teaching me optical design, to Koichi Ogawa, Mikichi Ban, Toru Aruga for suggesting and encouraging me to write this paper, to Hideo Yokota, Shouzou Moriya, for their assistance in this project, to Tadayuki Iwai, Yoshiki Kino for their effort in the mechanical design work, to Yuji Adachi, Tsuneo Otsuka, Yosimasa Katori, Naoyuki Miyauchi, Yoshio Matsui, Akihiro Fujinuma, Kanji Hatanaka, Shun-ichi Abe, Yoshihiko Sunahara, Toshikazu Shimadu, Tadahiro Shimasaki, Hiroshi Kumayama, Mitsuharu Ichinose, Yoshinari Furuya, Hiroaki Konya and many persons in the factory for their effort of processing, assembling and testing the primary corrector.

imaging observation over the wavelength region of 0.4μ-1.0μ at zenith distance 0-60 degrees. The FWHM image size obtained under a good seeing was 0.3 arcsec at its field center and better than 0.4 arcsec at the edge of the field.

10. Acknowledgments

At first, I was quite unfamiliar with astronomy and astronomical observing instruments. I started to study the optical design of primary corrector because of my idea of ADC described in this paper that led to fabrication and test of the entire corrector. My hearty thanks are due to Professor Kyoji Nariai who kindly taught me about the references and gave me design data of his previous studies. He also suggested me to write this paper and encouraged me during the entire period of writing. My thanks are also due to Professor Masanori Iye who taught me about observing instruments, and encouraged me to write this paper, to Dr. Satoshi Miyazaki who made the test observation of the corrector with the Subaru telescope and furnished me with the results that was quite satisfying for the fabricating team, to Ichiro Habe of OHARA INC. who provided us with glass material, Osamu Sakakibara, Noboru Ito, Izumi Mikami, Shinya Kawahara, Tadashi Matsushita, Yutaka Ezaki of MITSUBISHI ELECTRIC CORP. for their help during the fabrication of the primary corrector. In CANON INC, my thanks are first due to late Tetsuya Ara who was my first boss, to Dr. Yoshiya Matsui for teaching me optical design, to Koichi Ogawa, Mikichi Ban, Toru Aruga for suggesting and encouraging me to write this paper, to Hideo Yokota, Shouzou Moriya, for their assistance in this project, to Tadayuki Iwai, Yoshiki Kino for their effort in the mechanical design work, to Yuji Adachi, Tsuneo Otsuka, Yosimasa Katori, Naoyuki Miyauchi, Yoshio Matsui, Akihiro Fujinuma, Kanji Hatanaka, Shun-ichi Abe, Yoshihiko Sunahara, Toshikazu Shimadu, Tadahiro Shimasaki, Hiroshi Kumayama, Mitsuharu Ichinose, Yoshinari Furuya, Hiroaki Konya and many persons in the factory for their effort of processing, assembling and testing the primary corrector.

11. References

Ando, M., Negishi, M., Takimoto, M., Deguchi, A., Nakamura, N., Higonuma, M., Yamamoto, H.: 1992, *SPIE* 1720, 22

Avila, G.,Rupprecht, G., Beckers, J.M.: 1997, *Proc. SPIE* 2871, 1135

Epps, H.W., Angel, J.R.P., Anderson, E.: 1984, in *Very Large Telescopes, their Instrumentation and Programs,* eds. M.-H. Ulrich, K. Kjär, *Proc. IAU Coll.* 79, p.519

Gunn, J. E., Carr, M., Rockosi, C., Sekiguchi, M., Berry, K., Elms, B., Haas, E. de, Ivezi, Ž., Knappć, G., Lupton, R., Pauls, G., Simcoe, R., Hirsch, R., Sanford, D., Wang, S., York, D., Harris, F., Annis, J., Bartozek, L., Boroski, W., Bakken, J., Haldeman, M., Kent, S., Holm, S., Holmgren, D., Petravick, D., Prosapio, A., Rechenmcher, R., Doi, M., Fukugita, M., Smasaku, K., Okada, N., Hull, C., Siegmund, W., Mannery, E., Blouke, M., Heidtman, D., Schneider, D., Lucinio, R., Brinkman, J.: 1998, *Astron. Journal,* 116, 3040

Miyazaki, S.: 1999, *NAOJ/ATC REPORT* Oct. 8

Nariai, K., Yamashita, Y., Nakagiri, M.: 1985, *Ann. Tokyo Astron. Obs.*, 2nd Series, 20, 431

Nariai, K., Takeshi, K.: 1994, *SPIE* 2199, 532

Negishi, M., Ando, M., Deguchi, A., Takimoto, M., Narumi, H., Nakamura, N., Yamamoto, H.: 1994, *Proc. SICE '94,* 941

Ross, F. E.: 1935, *Astrophys. J.* 81, 156-172

Su Ding-qiang: 1986, *Astron. Astrophys.* 156, 381

Takeshi, K., Matsui, Y., Nariai, K., Ban, M.: 1994, *Japanese Laid Open Patent Application* No. 6-230274

Tanaka, W.: 1991, *Subaru Telescope Technical Report* 7

Wang Ya-nan, Su Ding-qian: 1990, *Astron. Astrophys.* 232, 589

Wynne, C. G.: 1965, *Appl. Opt.* 4, 1185

Appendix

A. Primary Corrector with Concentric type ADC

Flat Surfaces in the ADC described in 5.2(c) can be replaced with two concentric spherical surfaces. In this case, the ADC unit is moved around the center of curvature of the concentric spheres. Optical data of a design of primary corrector with a flat boundary surface is given in Table A-1 and its cross section is shown in Figure A-1. Aberration diagrams are shown in Figure A-2. In fact, the lateral type ADC can be interpreted as the concentric type whose radius of curvature of the concentric surfaces is infinitely large. In order to facilitate to understand how the concentric type ADC works, the boundary surface in this ADC is made flat.

B. Temporary model of the Primary Corrector with Lateral shift type ADC

In 5.2(c), we obtained a temporary model with lateral type ADC and its cross section is shown there. As the model underwent another modification (see 5.2(d)) before it became final, optical data, aberration diagrams, and spot diagrams are shown here in Table B-1 and Figures B-1 thru B-8.

C. Primary Corrector with an FOV of 42 minutes

Primary corrector design of FOV of 42 minutes is shown here. Optical performance of this corrector is satisfactory. Figure C-1 shows the cross section of the design with a field of view of forty-two minutes of arc. Table C-1 shows its optical data, and Figures C-2, C-3, C-4, C-5, C-6, C-7, C-8, and C-9 are its aberration diagrams and spot diagrams. As the size of the prime focus unit decided by the structural design of the Subaru telescope did not allow forty-two minutes of arc deign, the thirty minutes design was selected for fabrication.

k	ea	r	d	glass	maker	n_d	ν_d
1*	8200.046	30000.00000	14127.00000				
2	553.534	388.46602	56.00000	bsl7	ohara	1.516330	64.15
3	516.410	390.02138	428.40000			1.	
4	297.841	1158.43358	16.00000	bsl7	ohara	1.516330	64.15
5*	274.173	251.27130	144.30000			1.	
6	324.000	-956.00000	14.00000	pbl26	ohara	1.567322	42.83
7	324.000	0.00000	30.00000	gfk70	sumita	1.569070	71.30
8	324.000	-1000.00000	10.00000			1.	
9*	255.443	331.43254	41.00000	bsl7	ohara	1.516330	64.15
10	251.259	-1890.05289	156.00000			1.	
11	250.000	0.00000	15.00000	bsl7	ohara	1.516330	64.15
12	250.000	0.00000	10.00007				

Aspheric constant

k	r	e^2	B	C	D	E
1	30000	1.00835				
5	251.2713		-1.08572E-9	-2.75136E-15	8.57271E-20	-4.52537E-24
9	331.43254		-2.07230E-9	-2.09783E-16	-5.15656E-19	3.66462E-24

$$x = \frac{h^2/r}{1+\sqrt{1-(1-e^2)(h/r)^2}} + Bh^4 + Ch^6 + Dh^8 + Eh^{10}, \quad h = \sqrt{y^2+z^2}$$

f_e = 15602.479

Table A-1. Optical data of Primary Corrector with Concentric type ADC

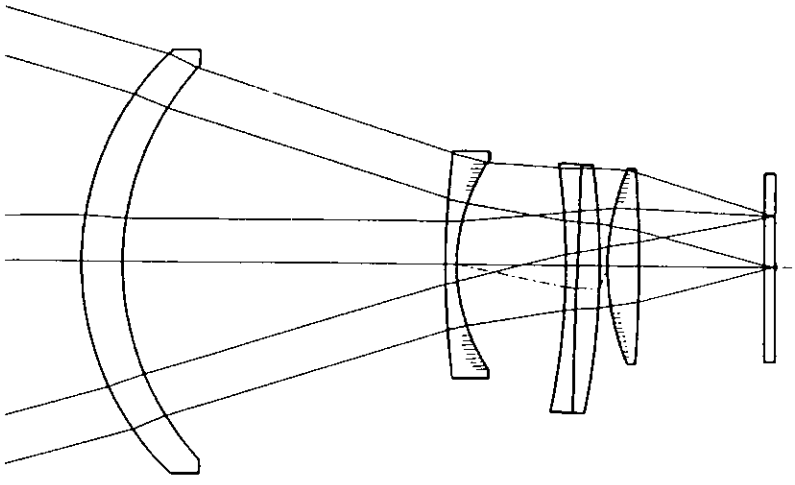

EFL=15.602m, Fno.=1.90, FOV=30 arcmin

Figure A-1. Primary Corrector with Concentric type ADC

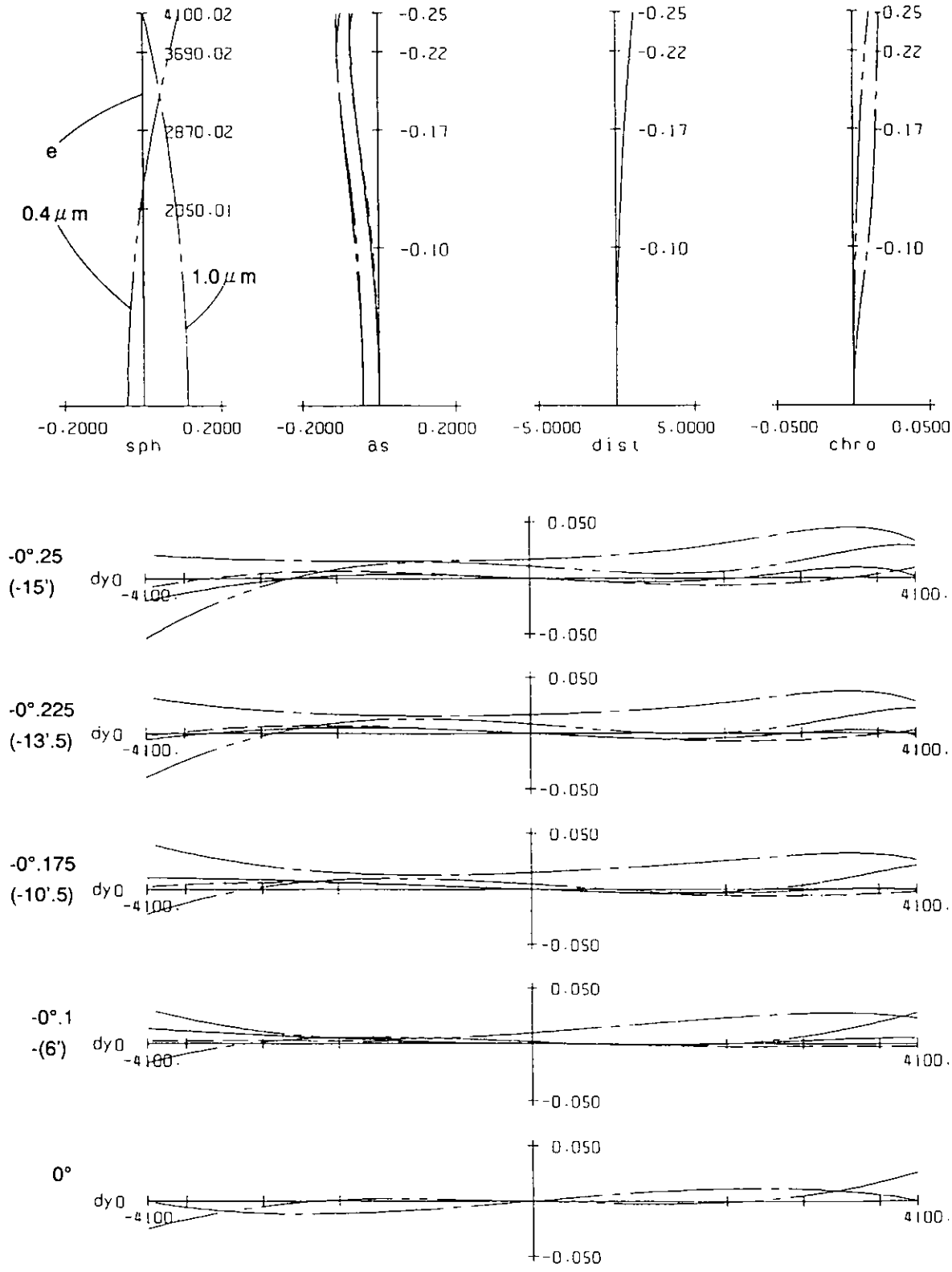

Figure A-2. Aberration diagrams of Primary Corrector with Concentric type ADC

k	ea	r	d	glass	maker	n_d	ν_d
1*	8200.000	30000.00000	14211.98754				
2	504.652	325.03089	56.00000	bsl7	ohara	1.516330	64.15
3	465.144	318.86167	381.51365			1.	
4	281.148	13552.38382	16.00000	bsl7	ohara	1.516330	64.15
5*	257.223	221.89367	68.26377			1.	
6	322.000	0.00000	30.00000	pbm5	ohara	1.603420	38.01
7	322.000	-900.00000	14.00000	bsm14	ohara	1.603112	60.70
8	322.000	0.00000	9.65481			1.	
9	261.211	1202.74976	15.00000	pbm2	ohara	1.620041	36.26
10	259.875	454.94325	30.07215	bsl7	ohara	1.516330	64.15
11	259.760	-5719.60207	1.00000			1.	
12*	258.412	297.48663	46.46515	fpl51	ohara	1.496999	81.61
13	254.923	-1235.65592	155.44315			1.	
14	250.000	0.00000	15.00000	bsl7	ohara	1.516330	64.15
15	250.000	0.00000	10.00000			1.	

Aspheric constant

k	r	e^2	B	C	D	E
1	30000	1.00835				
5	221.89367		-9.24310E-10	1.03340E-14	1.65364E-19	2.83288E-23
12	297.48663		5.75144E-10	3.34561E-14	9.72165E-19	1.34052E-23

$$x = \frac{h^2/r}{1+\sqrt{1-(1-e^2)(h/r)^2}} + Bh^4 + Ch^6 + Dh^8 + Eh^{10}, \quad h = \sqrt{y^2+z^2}$$

f_e = 15312.981

Table B-1. Optical data of Temporary model of the Primary Corrector with Lateral shift type ADC

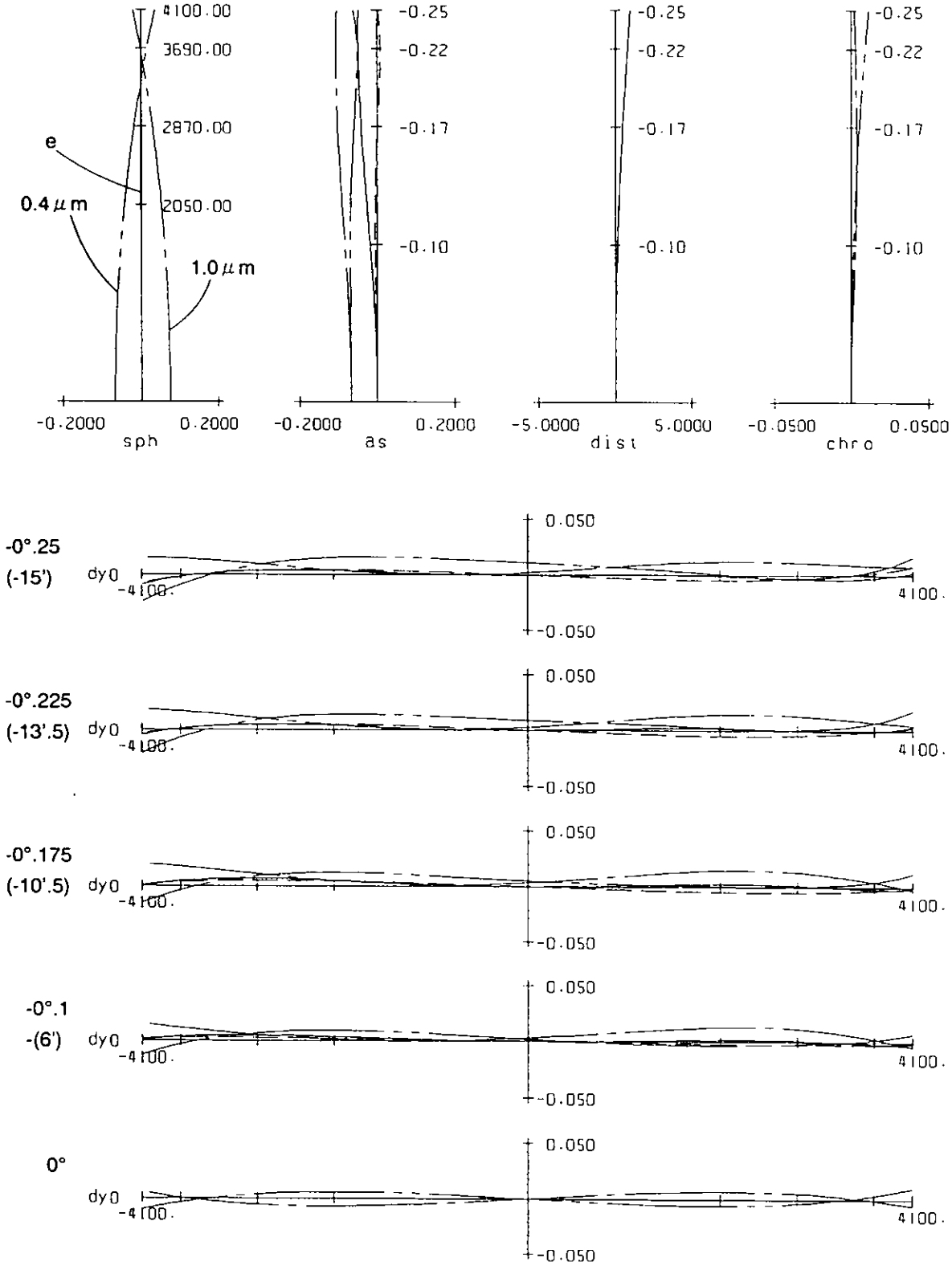

Figure B-1. Aberration diagrams of Temporary model of the Primary Corrector with Lateral shift type ADC, zenith distance 0°

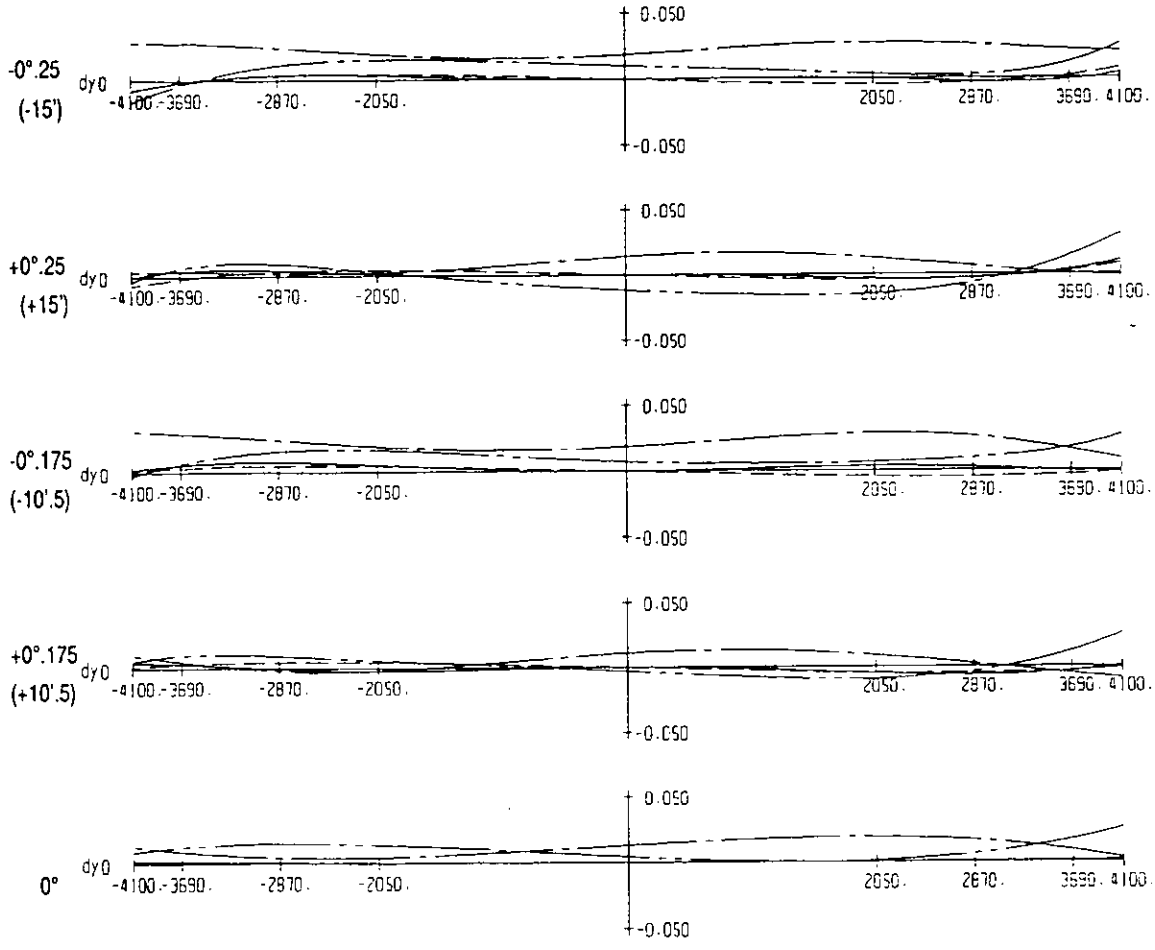

Figure B-2. Aberration diagrams of Temporary model of the Primary Corrector with Lateral shift type ADC, zenith distance 60°

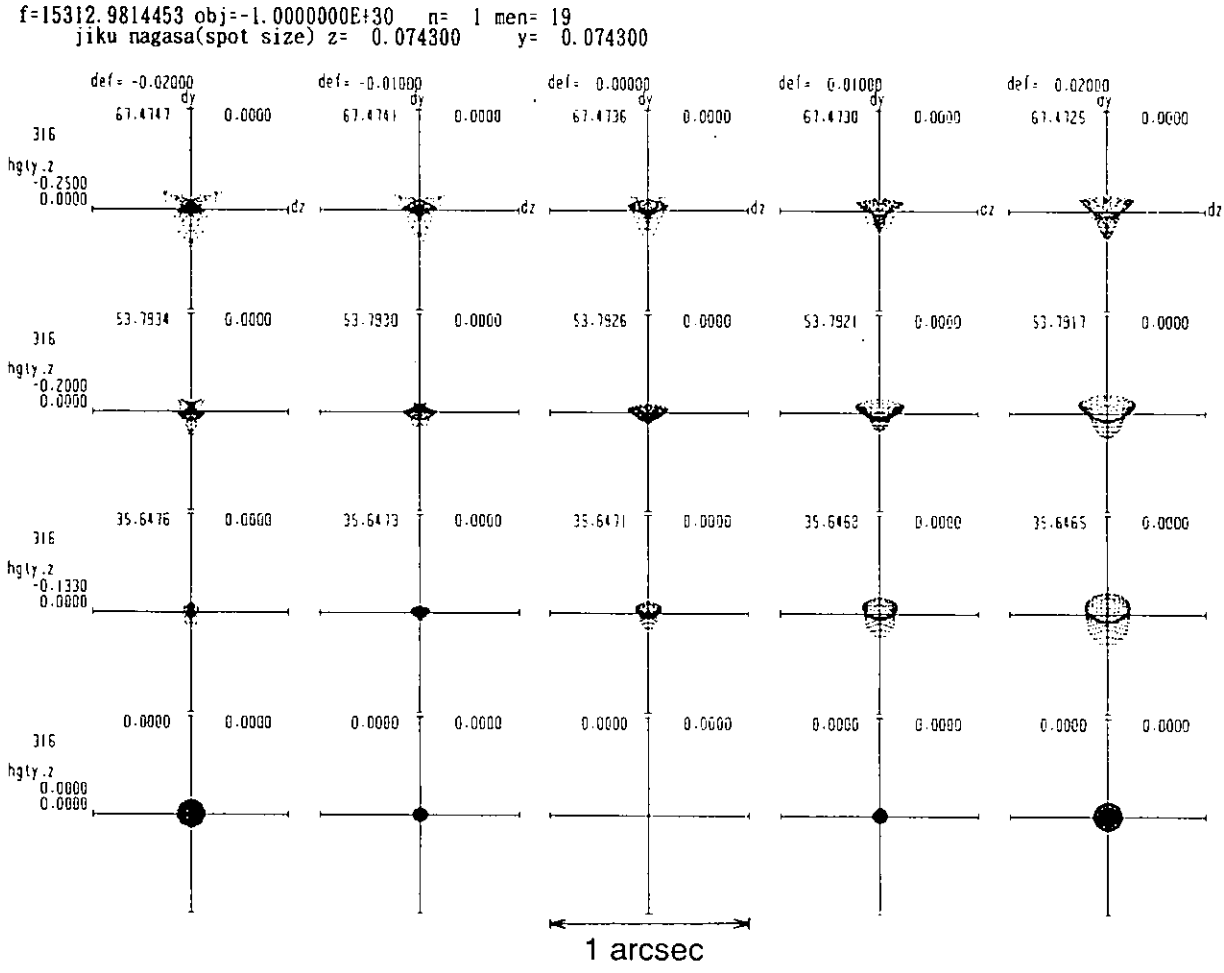

Figure B-3. Spot diagrams of Temporary model of the Primary Corrector with Lateral shift type ADC, zenith distance 0°, λ = 0.5461 μm

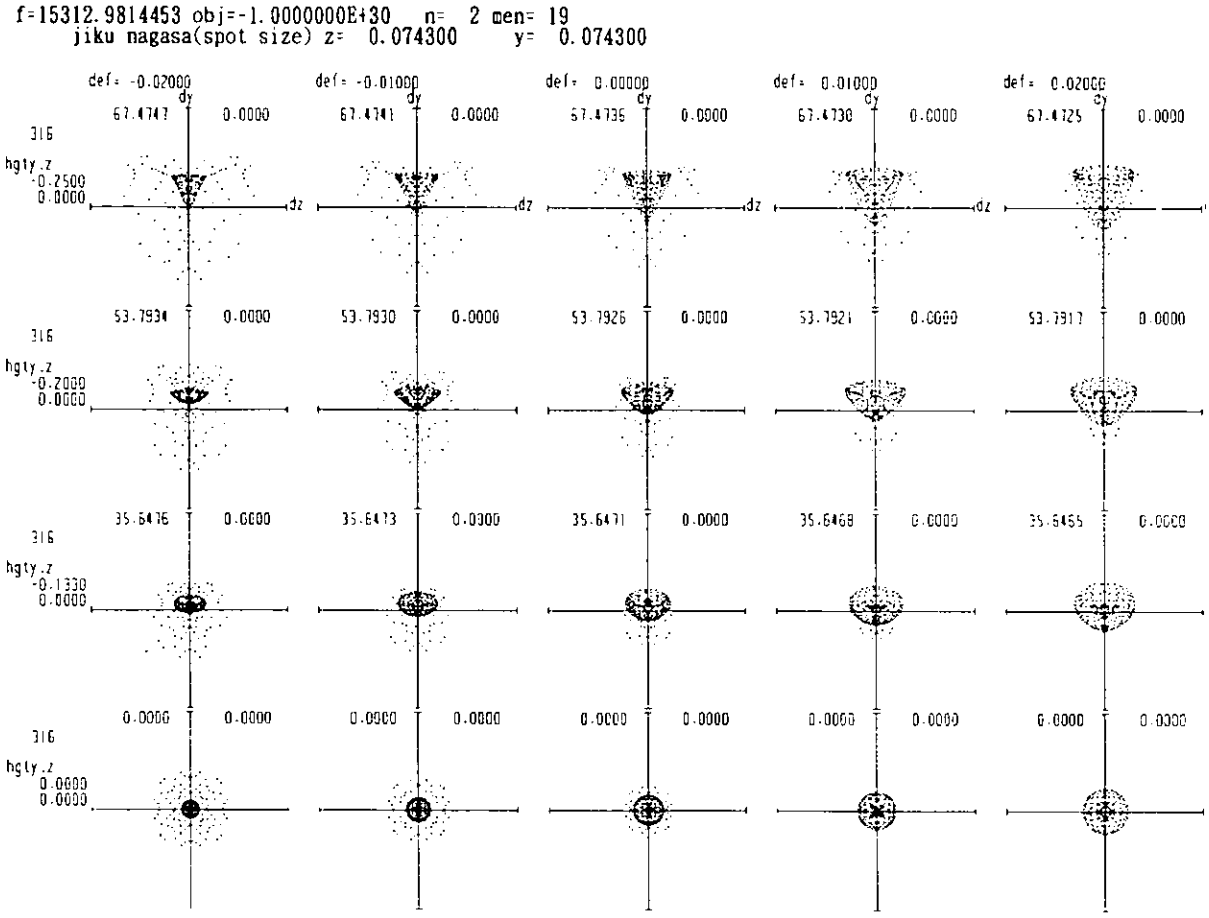

Figure B-4. Spot diagrams of Temporary model of the Primary Corrector with Lateral shift type ADC, zenith distance 0°, λ = 0.4 μ m

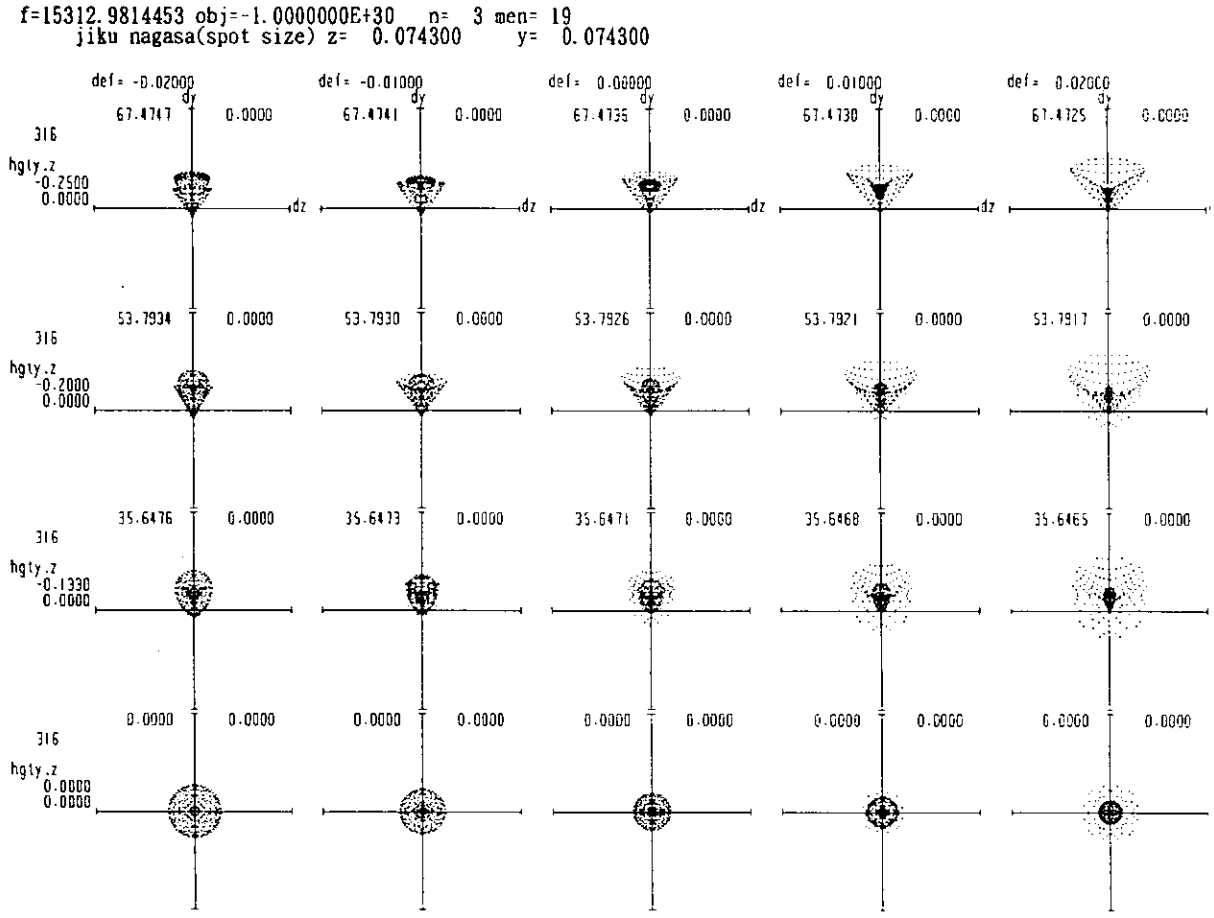

Figure B-5. Spot diagrams of Temporary model of the Primary Corrector with Lateral shift type ADC, zenith distance 0°, λ = 1.0 μ m

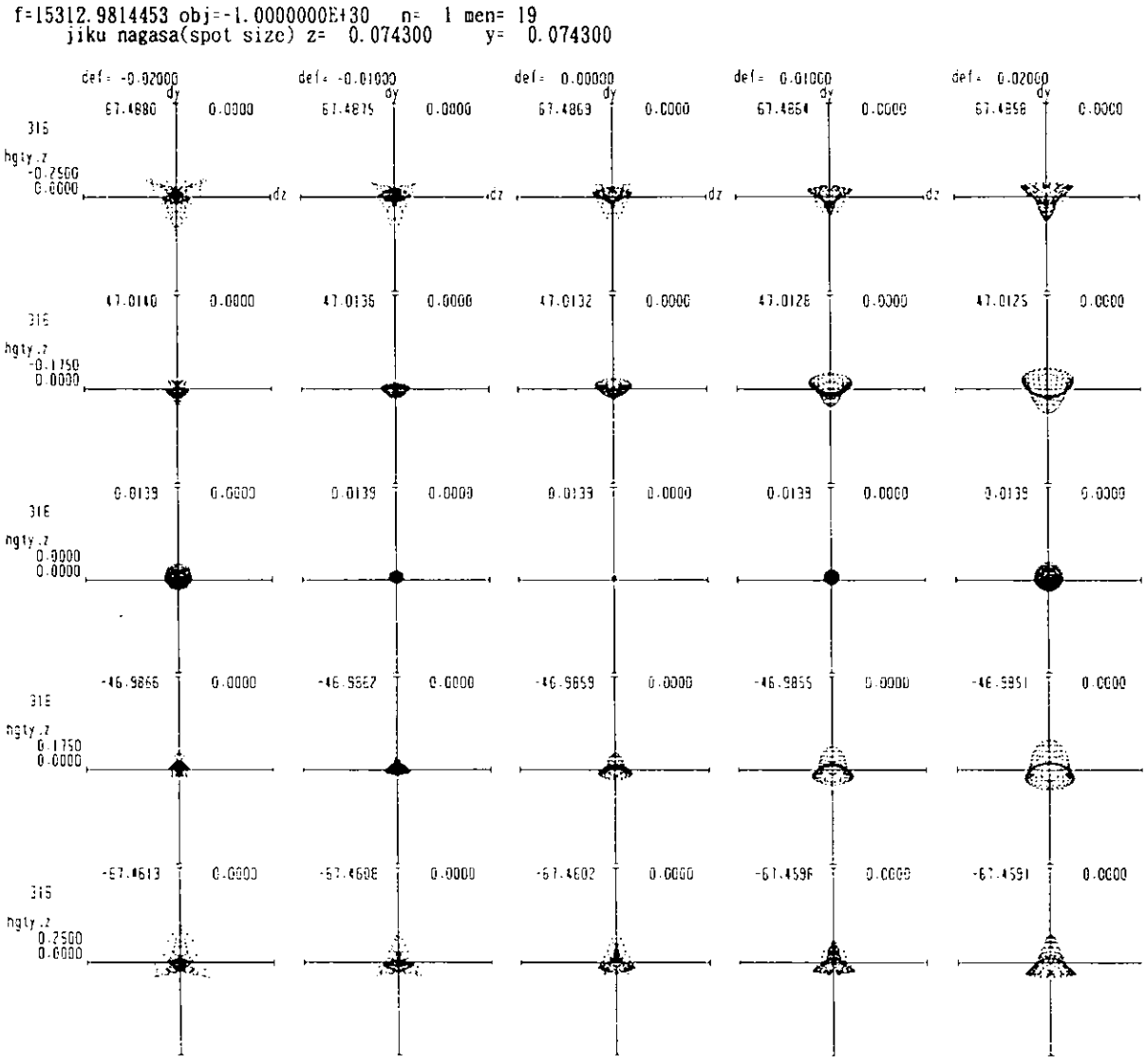

Figure B-6. Spot diagrams of Temporary model of the Primary Corrector with Lateral shift type ADC, zenith distance 60°, λ = 0.5461 μm

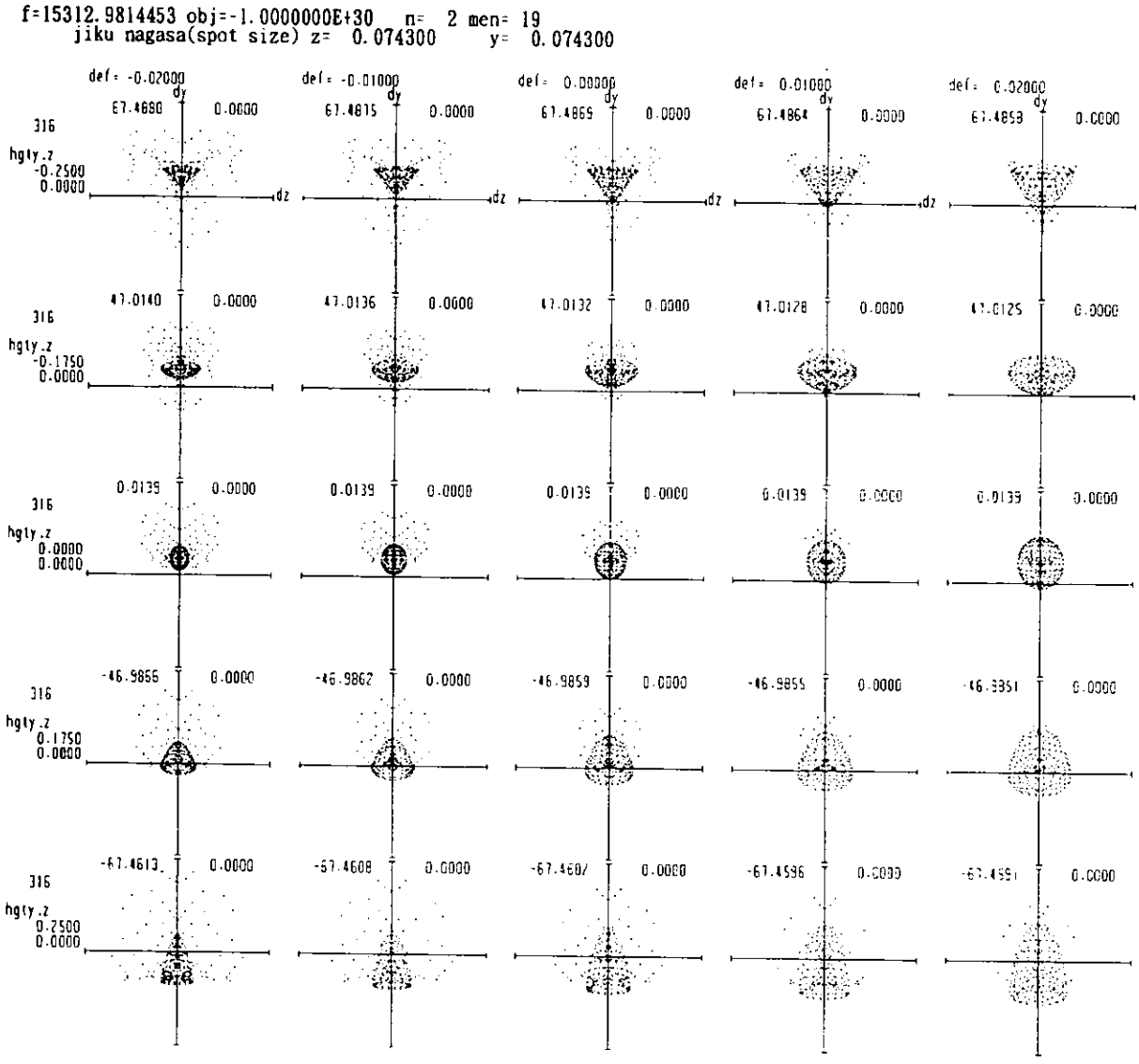

Figure B-7. Spot diagrams of Temporary model of the Primary Corrector with Lateral shift type ADC, zenith distance 60°, $\lambda = 0.4\,\mu$m

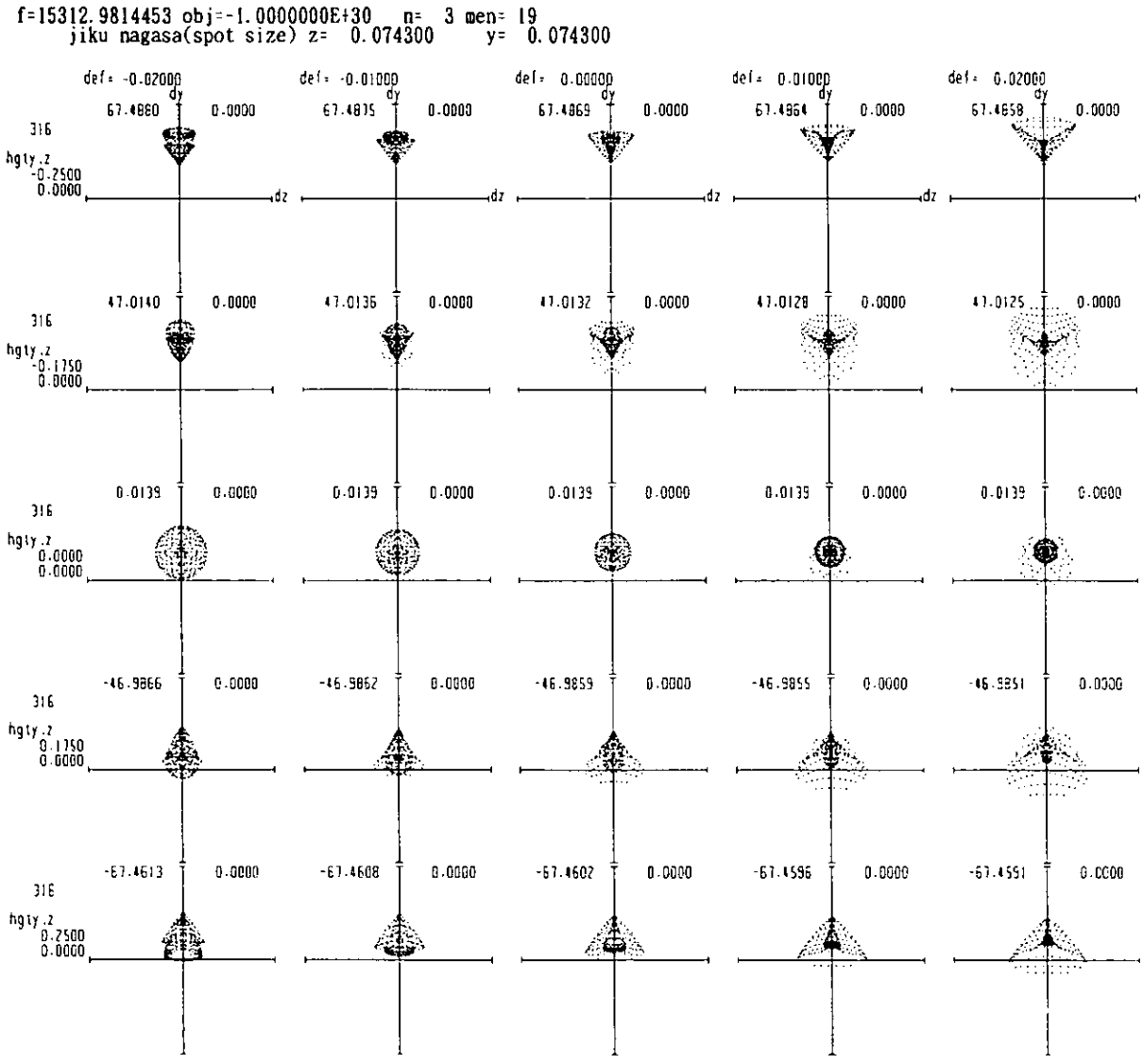

Figure B-8. Spot diagrams of Temporary model of the Primary Corrector with Lateral shift type ADC, zenith distance 60°, $\lambda = 1.0\,\mu$m

k	ea	r	d	glass	maker	n_d	ν_d
1*	8200.064	30000.00000	14095.16071				
2	603.405	374.97597	60.00000	bsl7	ohara	1.516330	64.15
3	563.554	374.91774	424.11089			1.	
4	361.424	5197.61211	16.00000	bsl7	ohara	1.516330	64.15
5*	329.386	265.04813	87.34037			1.	
6	332.245	4671.30401	28.69563	pbl1	ohara	1.548141	45.78
7	332.571	-927.33937	14.00000	bsl7	ohara	1.516330	64.15
8	333.061	-1744.73722	39.92055			1.	
9	383.000	0.00000	14.00000	pbm5	ohara	1.603420	38.01
10	383.000	800.00000	36.00000	bsm14	ohara	1.603112	60.70
11	383.000	0.00000	5.00000			1.	
12*	324.929	336.66710	55.98708	fpl51	ohara	1.496999	81.61
13	320.690	-4826.87899	166.42380			1.	
14	400.000	0.00000	15.00000	bsl7	ohara	1.516330	64.15
15	400.000	0.00000	10.00000			1.	

Aspheric constant

k	r	e^2	B	C	D	D'	E
1	30000	1.00835					
5	265.04813		-2.86017E-10	2.28334E-15	-1.48293E-19	2.05554E-21	-3.33436E-24
12	336.6671		1.29674E-9	2.30773E-14	7.48361E-19	-3.64316E-21	1.26670E-23

$$x = \frac{h^2/r}{1+\sqrt{1-(1-e^2)(h/r)^2}} + Bh^4 + Ch^6 + Dh^8 + D'h^9 + Eh^{10}, \quad h = \sqrt{y^2+z^2}$$

$f_e = 15299.060$

Table C-1. Optical data of Primary Corrector with a FOV of 42 minutes

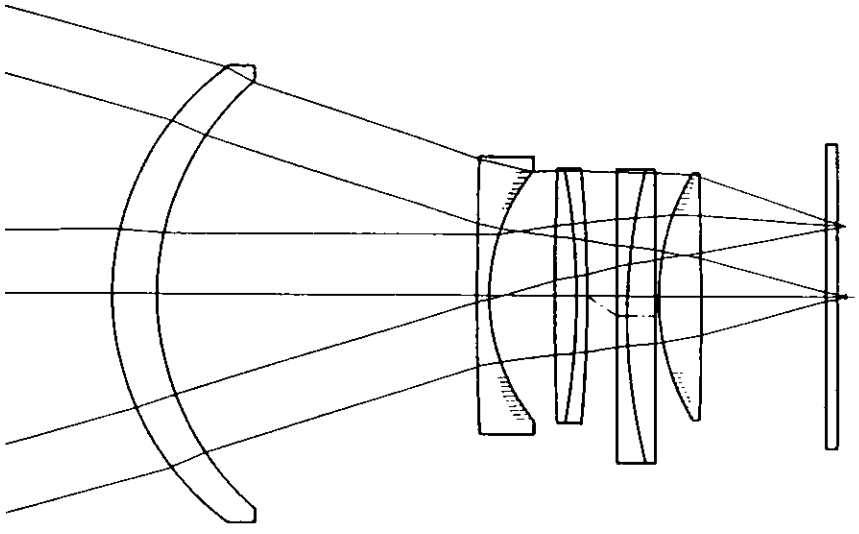

Figure C-1. Cross section of Primary Corrector with a FOV of 42 minutes

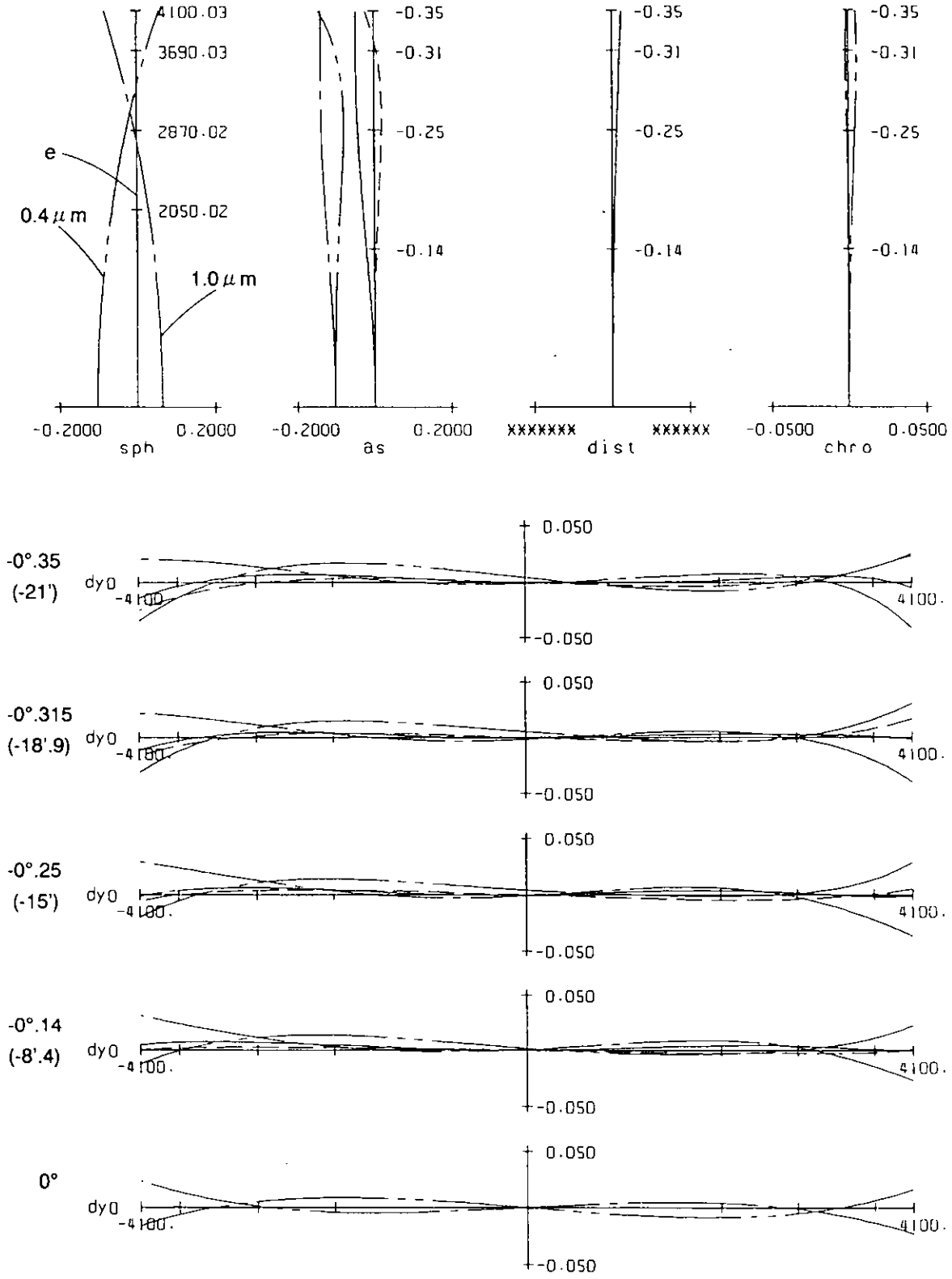

Figure C-2. Aberration diagrams of Primary Corrector with a FOV of 42 minutes, zenith distance 0°

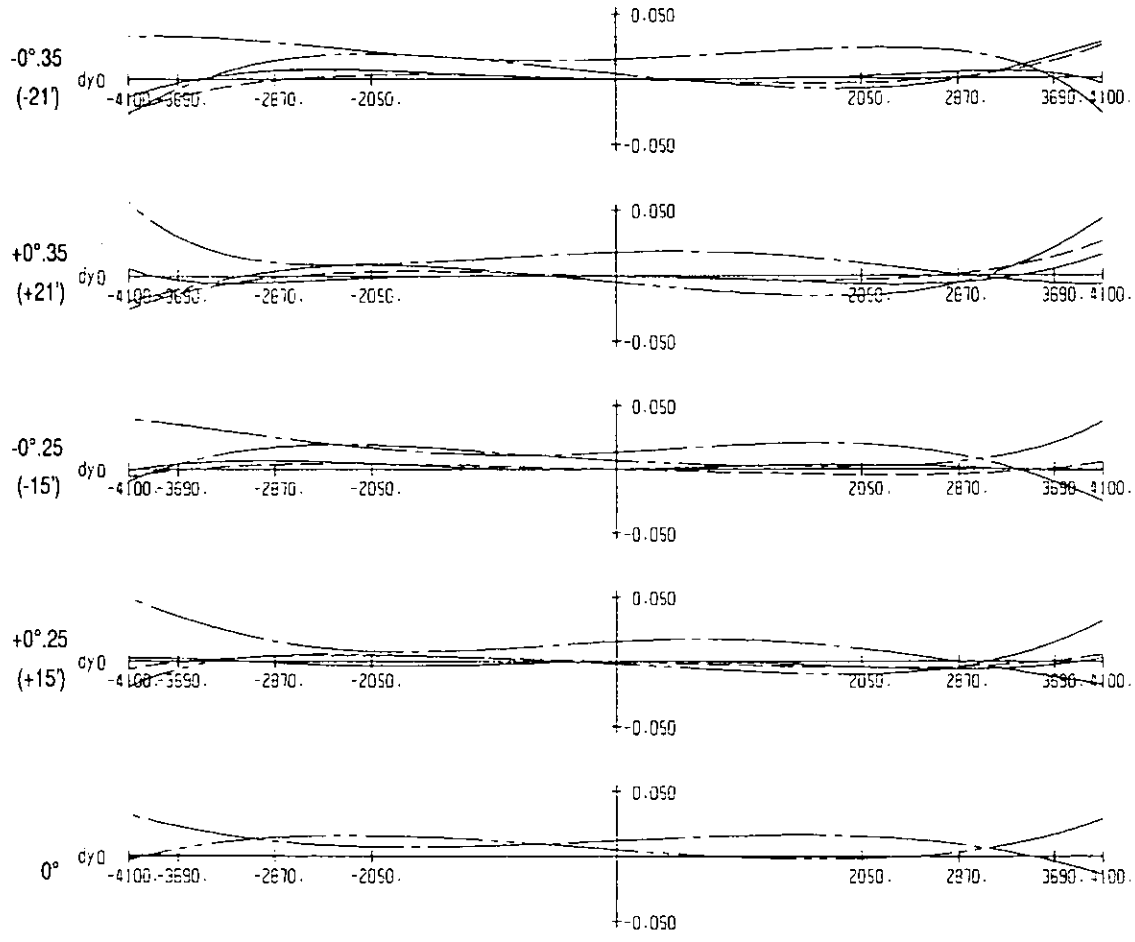

Figure C-3. Aberration diagrams of Primary Corrector with a FOV of 42 minutes, zenith distance 60°

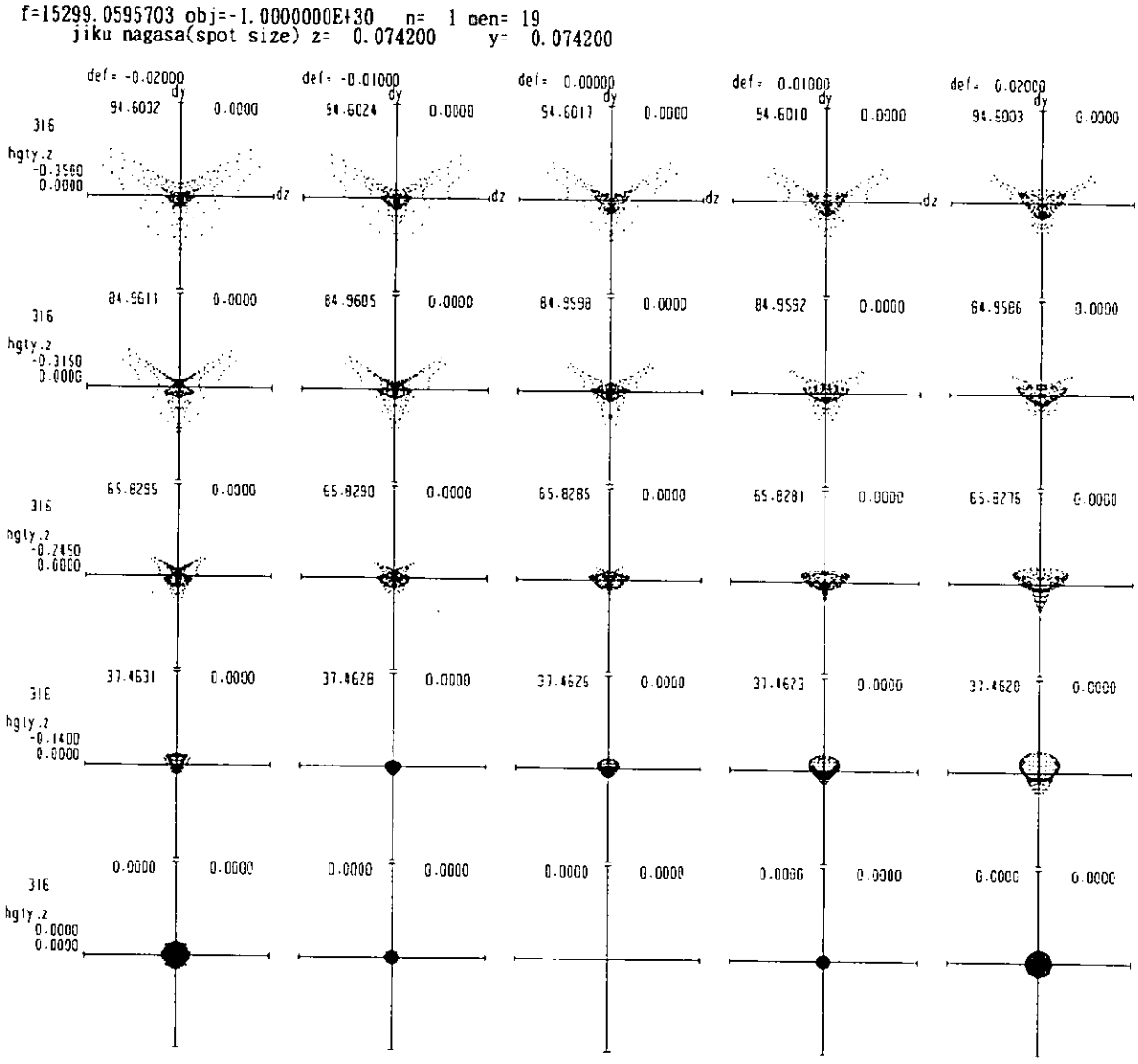

Figure C-4. Spot diagrams of Primary Corrector with a FOV of 42 minutes, zenith distance 0°, λ = 0.5461 μm

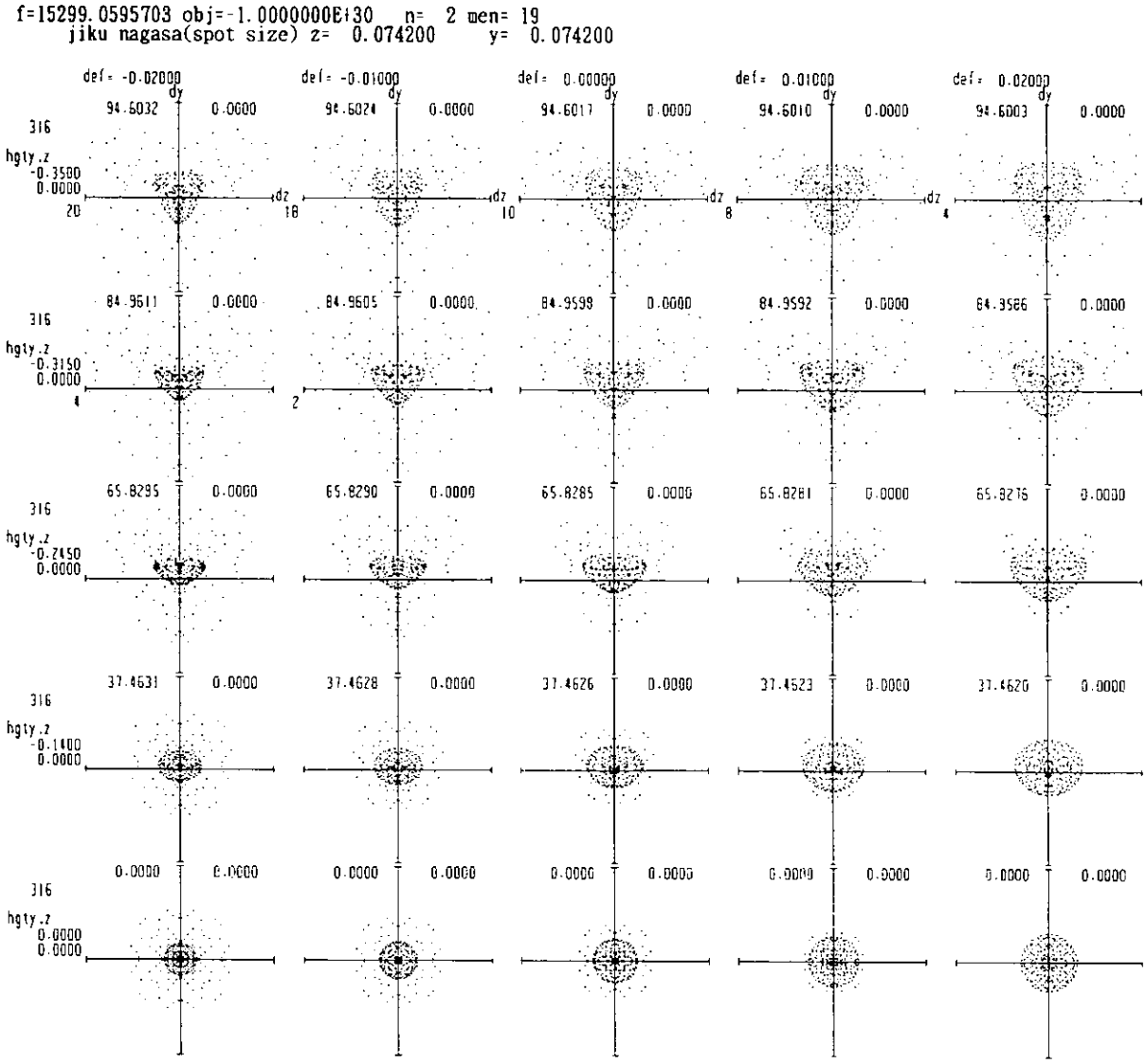

Figure C-5. Spot diagrams of Primary Corrector with a FOV of 42 minutes, zenith distance 0°, $\lambda = 0.4\,\mu$m

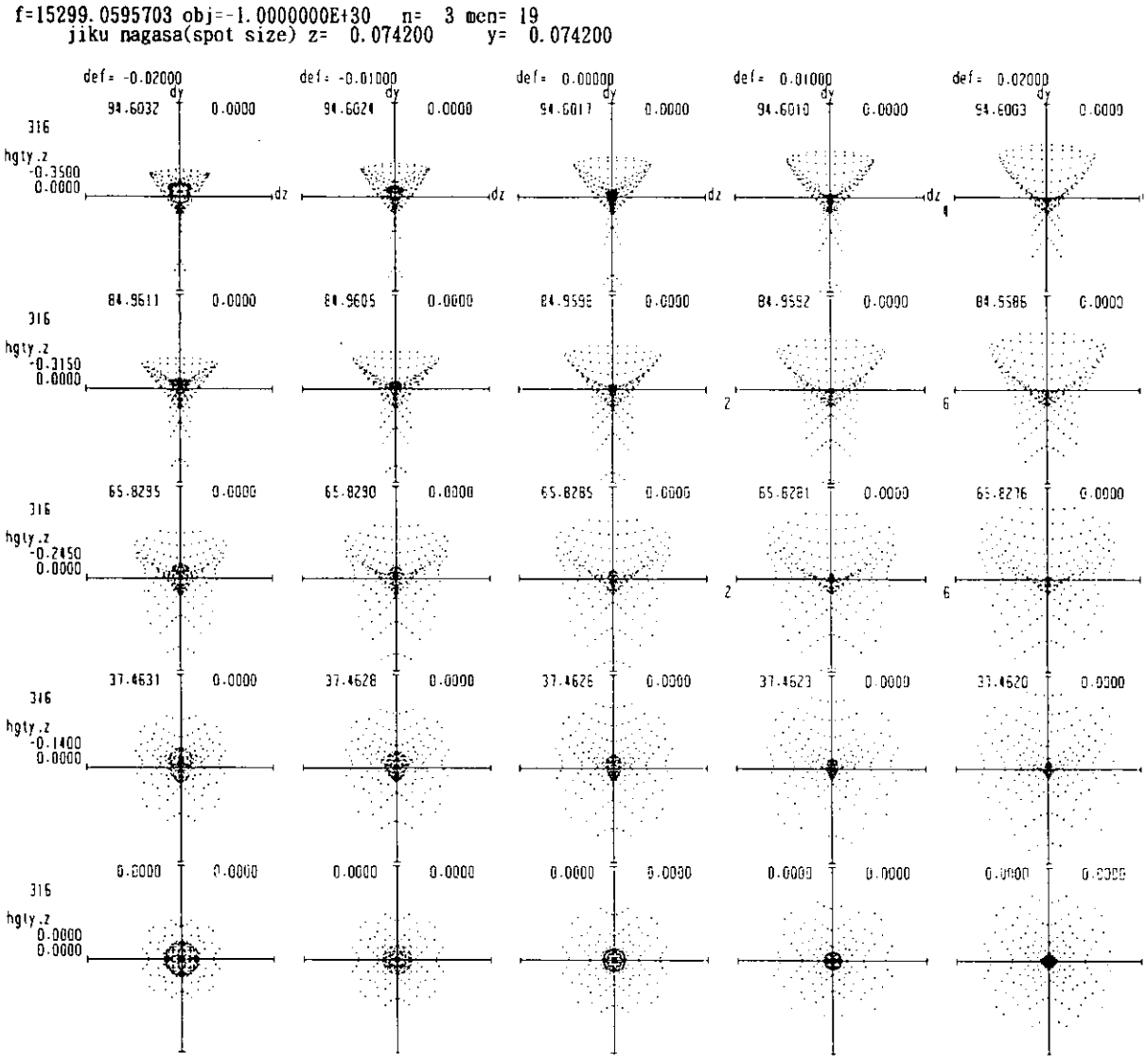

Figure C-6. Spot diagrams of Primary Corrector with a FOV of 42 minutes, zenith distance 0°, λ = 1.0 μ m

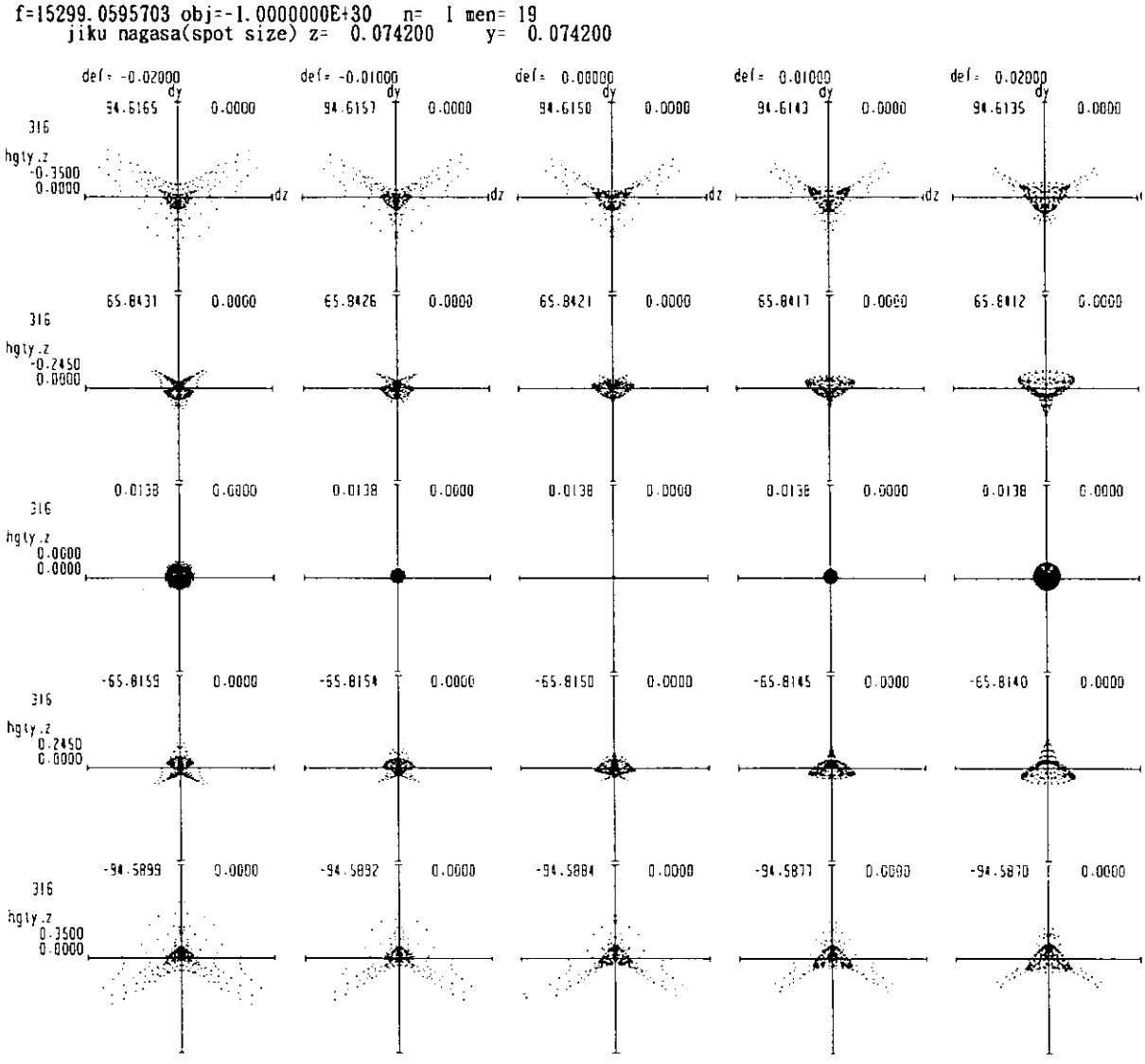

Figure C-7. Spot diagrams of Primary Corrector with a FOV of 42 minutes, zenith distance 60°, λ = 0.5461 μm

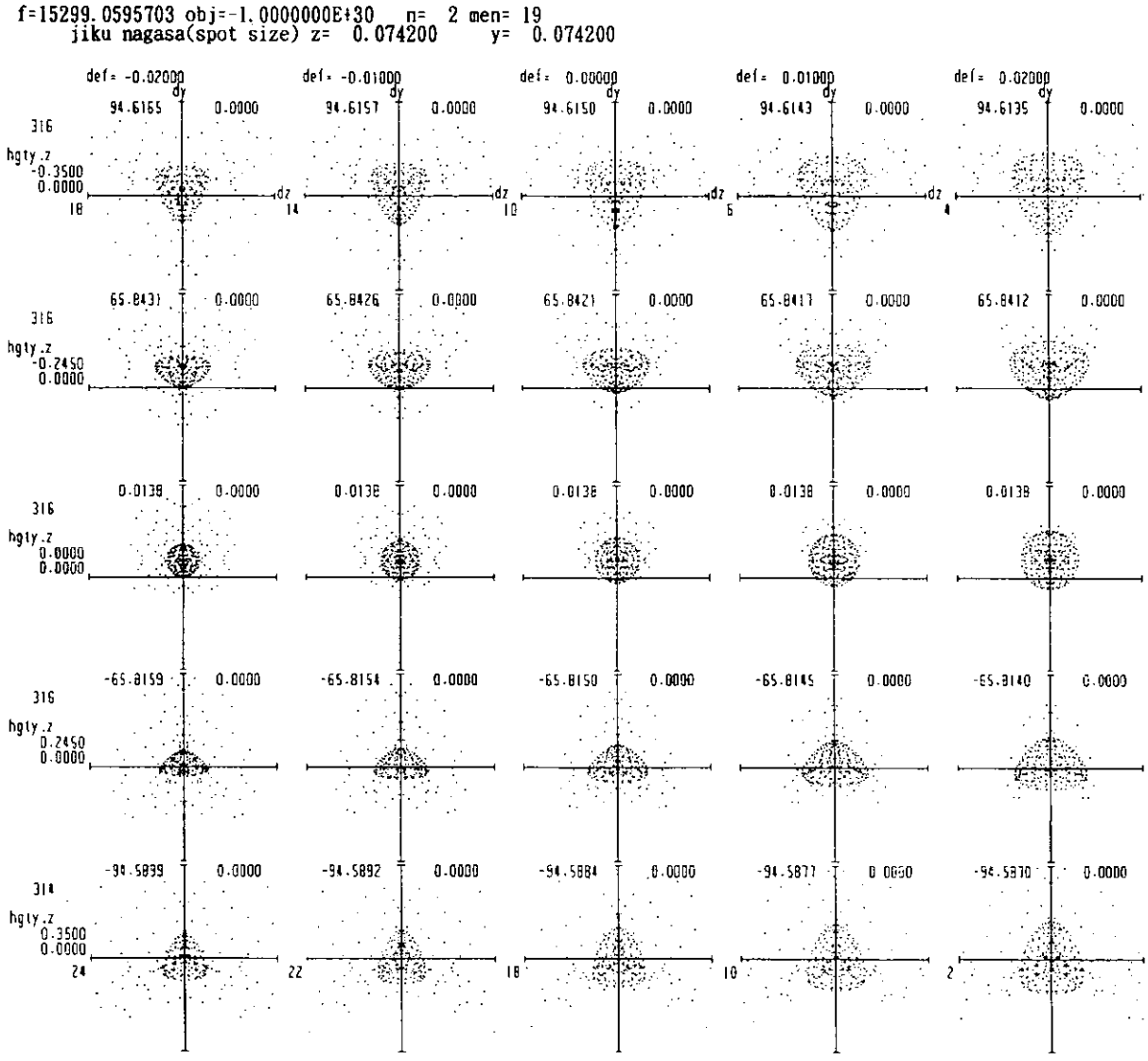

Figure C-8. Spot diagrams of Primary Corrector with a FOV of 42 minutes, zenith distance 60°, $\lambda = 0.4\,\mu$m

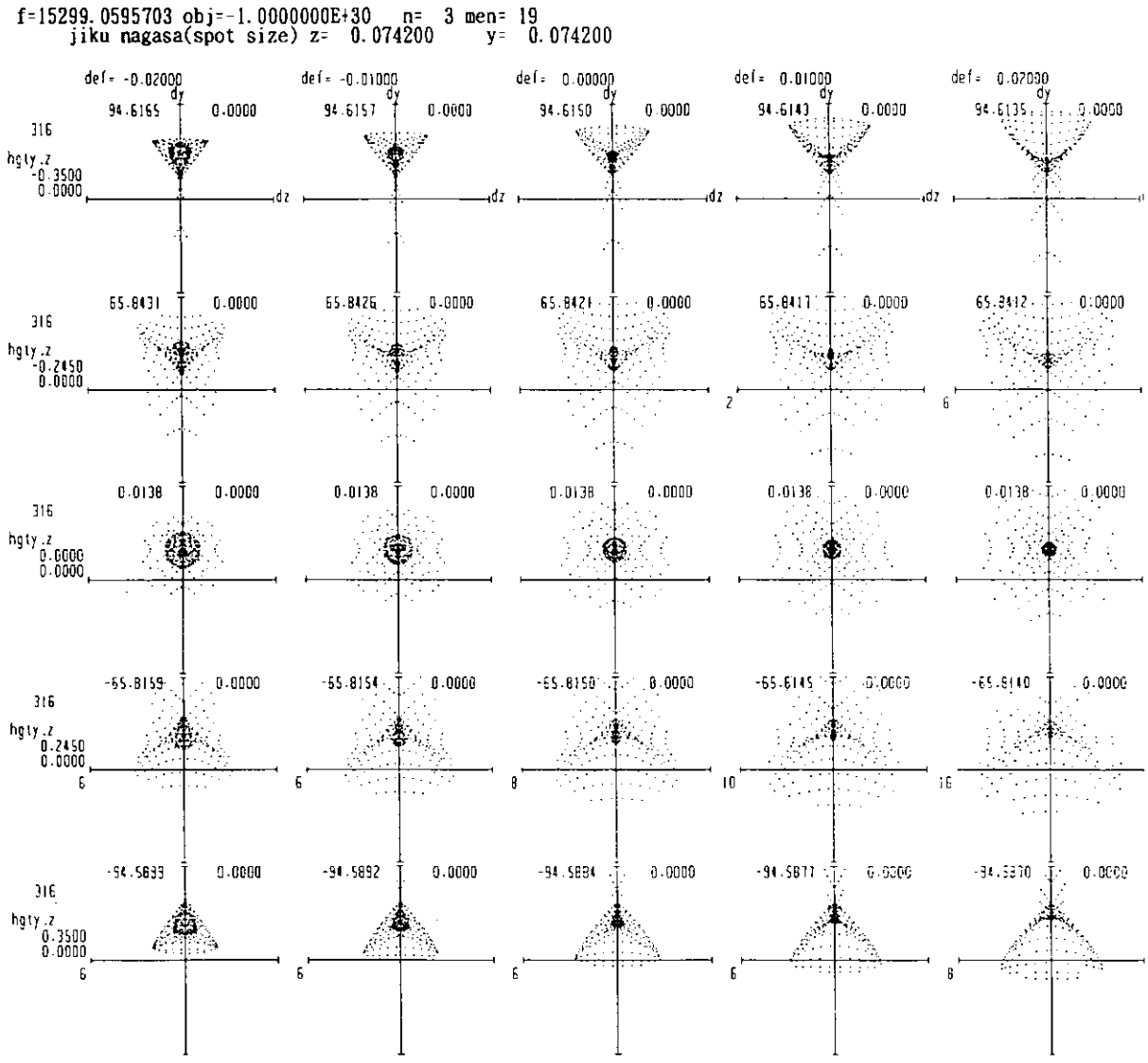

Figure C-9. Spot diagrams of Primary Corrector with a FOV of 42 minutes, zenith distance 60°, $\lambda = 1.0\,\mu$m